

POLITECNICO DI TORINO

**Corso di Laurea Magistrale in
Ingegneria Biomedica**



Tesi di Laurea Magistrale

Preparation and characterization of Ti-6Al-4V surfaces
functionalized with silver for antibacterial purposes: study
of ionic and nanoparticles release mechanism

Relatori:

Prof.ssa Silvia Maria Spriano

Ing. Sara Ferraris

Candidato:

Gianmaria Padoan

MARZO-APRILE 2018





Table of contents

1	INTRODUCTION	1
2	SILVER NANOPARTICLES AND SILVER IONS RELEASE	3
2.1	Silver uses over time	4
2.2	Silver nanoparticles applications	7
2.2.1	Food.....	7
2.2.2	Consumer products.....	8
2.2.3	Medical devices.....	9
2.3	Silver nanoparticles release.....	10
2.4	Silver ions release.....	13
2.4.1	Release kinetics	14
2.4.2	Aggregation mechanism.....	17
2.4.3	Controlled silver ions release	18
3	SILVER NANOPARTICLES ANTIBACTERIAL ACTIVITY	22
3.1	Orthopedic implants infections.....	22
3.1.1	Micro-organisms responsible for infections.....	22
3.1.2	Biofilm formation mechanism	24
3.2	Silver nanoparticles antimicrobial activity.....	26
3.2.1	Connection to the cell membrane	27
3.2.2	Interaction with the respiratory chain.....	31
3.2.3	Generation of reactive oxygen species (ROS)	33
3.2.4	Biofilm resistance	37
3.3	Enhanced cytocompatibility	38
4	PROTEIN ADSORPTION ON BIOMATERIALS	40
4.1	Kinetics of protein absorption	40
4.1.1	Surface properties.....	42
4.1.2	Protein properties	44
4.2	Instrumental analysis for evaluating adsorbed proteins	46
4.2.1	Optical techniques.....	46
4.2.2	Spectroscopic techniques.....	47
4.2.3	Microscopic techniques.....	48
4.2.4	Spectrometric techniques	49
4.3	Influence of adsorbed proteins.....	50



5	MATERIALS AND METHODS	54
5.1	Samples preparation	54
5.2	Surface treatments.....	57
5.3	Samples carachterization.....	59
5.4	Exposure plan.....	61
5.5	Simulated physiological fluids.....	63
5.6	UV Digestion	64
5.7	Photon cross-correlation spectroscopy (PCCS).....	65
5.8	Grafite furnace Atomic Absorption spectroscopy	66
5.9	X-ray photoelectron spectroscopy (XPS)	67
5.10	In vitro bioactivity.....	68
5.11	Zeta potential measurements	69
6	RESULTS AND DISCUSSION.....	72
6.1	Scanning electron microscopy (SEM)	72
6.1.1	Ti6Al4V-MP.....	72
6.1.2	Ti6Al4V-CT.....	73
6.1.3	Ti6Al4V-CT + Ag (0.001m)	74
6.1.4	Ti6Al4V-CT + Ag (0.005m)	75
6.2	Photon cross-correlation spectroscopy (PCCS).....	78
6.3	Total metal release	80
6.3.1	Other works.....	87
6.4	X-ray photoelectron spectroscopy (XPS)	90
6.5	In vitro bioactivity tests	94
6.5.1	Ti6Al4V-CT Ag (0.001M) 14 days in SBF.....	95
6.5.2	Ti6Al4V-CT Ag (0.001M) 28 days in SBF.....	98
6.6	Zeta potential measurements	101
7	CONCLUSIONS.....	103
8	REFERENCES.....	105
9	AKNOWLEDGMENTS	112



1 INTRODUCTION

Titanium and its alloys are materials commonly used in the field of orthopedic and dental prosthetics because of the good mechanical properties and corrosion resistance which make them biocompatible.

The objectives of the prosthetic surgery are to obtain an implant able to interact with biological systems and have a good mechanical resistance adequate to the stress to which it is subjected in order to obtain stable anchorage, restitution of the mobility, bone integration and regeneration of healthy bone tissue at the implant site treating or replacing any organ, tissue and function.

For bone integration, the low Young's modulus of titanium and its alloys (around 110 GPa) is considered as a mechanical advantage because the high flexibility can result in a limited stress shielding compared to other implant materials, inducing healthier and faster bone regeneration.

Despite this, the inactivity of the material can result in the growth of a fibrotic capsule that negatively affects the healing of the implant.

For this reason, over the years, in literature numerous studies have proposed surface modifications (machined, blasted, etched surfaces, plasma spray, sintering and electrochemical deposition) able to increase the adhesion between implant and bone which depends on various factors such as roughness, chemical composition and surface oxide, allowing excellent primary and secondary stability ¹.

Bacterial infections are another critical factor since surfaces of internal fixation implants may represent preferential sites for bacterial adhesion.



Consequences of implant-associated infections include failure of the prosthesis, prolonged hospitalization, systemic antibiotic therapy, several revision procedures, possible amputation, and even death.

The events of bacterial infections are quite contained, it is estimated a rate of about 2-5% for hip and knee prosthesis ² but, due to the high number of prosthetic implant operations, it is a fact to keep in consideration.

Normally, bacterial infections are treated by local and systemic administration of antibiotics, but they are still a problem given the development of bacterial strains with good antibiotic resistance.

Therefore, the interest in the search for alternative antibacterial agents is born, among which silver is considered a promising solution given that it has long been known and studied for its antibacterial properties.

The present thesis project was carried out on samples of Ti6Al4V alloy. The disks were treated superficially by a chemical method introducing a nanotexture on the surface and enriching it with hydroxyl groups essential for inorganic bioactivity.

Some samples have been enriched into the outer surface oxide with silver during a controlled oxidation process.

The treated samples were subjected to surface characterization, release tests, bioactivity tests and measurements of the zeta potential with the aim of assessing the goodness of the treatments carried out to obtain a titanium surface suitable for orthopedic implants able to promote bone integration and avoid bacterial colonization.



2 SILVER NANOPARTICLES AND SILVER IONS RELEASE

In recent years, a new and fast emerging field was that of nanotechnologies. Nanotechnology refers to the sciences, engineers, technologies that involves the manipulation of matter to create new structures, materials and devices controlling shape and size at the nanometer scale (1nm-100nm) ³.

Nanomaterials have specific characteristics that influence physical, chemical and biological properties. It is this small size, combined with the chemical composition and surface structure, that gives nanoparticles (NPs) its unique features which is why they represent an area of great potential for new technological and environmental applications ³.

Due to new properties attributed to engineered nanoparticles many new consumer products including NPs are gaining in commercial use. Nanoscale materials can be now found in electronic, cosmetics, appliances, automotive, food and beverage, health and fitness fields. According to the nanotechnology consumer product inventory ^{4,5}, since 2007 the Health and Fitness category includes the largest listing of products in the CPI and silver is one of the most used elements in form on nanomaterial and mentioned in products description (Fig. 1).

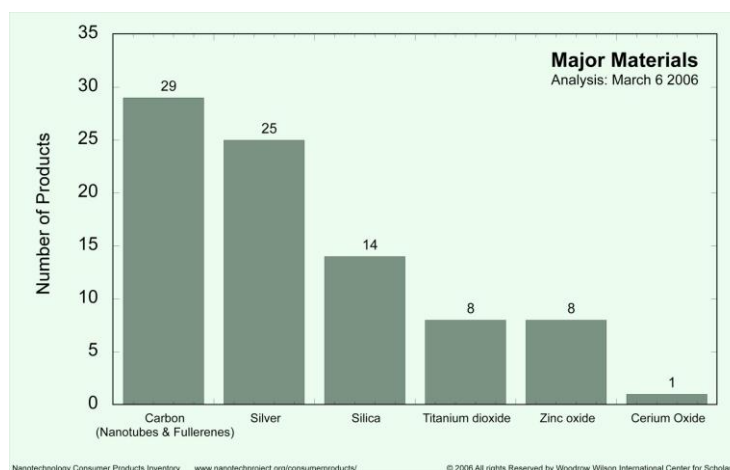


Fig. 1. Numbers of products containing nanotechnology associated with specific materials. ⁴



This success at the industrial and market level is not actually a novelty, if we consider its properties, such as the well-documented antibacterial properties ⁶.

2.1 Silver uses over time

Silver has been known since ancient times as an antibacterial agent and has been used in the past for jewelry, utensils, monetary currency, dental alloys, photography, explosives, buckets and containers for storing and transporting food ^{7,8}.

Until the introduction of antibiotics, silver and silver compounds were originally used as an effective antimicrobial agent, specifically in the management of open wounds and burns ^{9,10}.

The colloidal solutions used for the treatment of wounds and infections were one of the most common silver-based release system in which silver particles of different shape, size and concentrations are held in suspension by small electrical currents ^{9,11}.

With the advent of the World War II and with the invention of modern antibiotics, the interest in the antibacterial properties of silver fades slowly ^{10,12}.

The great use of antibiotics, however, immediately leads to the formation of resistant bacterial strains and so, in the following years, silver-based products came back to market as alternative medicine ^{13,14}. Silver began to be used again for the management of burned patients in the 1960s, in the form of 0.5% AgNO₃ solution. In 1968, silver sulfadiazine was introduced by Fox, obtained by combining silver nitrate (AgNO₃) with a newly discovered sulphonamide antibiotic. It is still marketed in the form of cream for the treatment of burned patients ^{6,9}.



At the end of the 90's, many silver-based dressings were introduced into the market. They are generally made up of polymeric structures within which silver is incorporated in the form of salts or nanoparticles.

To generate silver nanoparticles several chemical, physical and biological methods are used ¹⁵ (Fig. 2).

The most common method is chemical reduction from silver salts (AgNO_3 generally) using organic and inorganic reducing agents such as sodium borohydride (NaBH_4), citrate, glucose; stronger reducing agents lead to smaller monodisperse nanoparticles ¹⁶.

Since reducing agents are often retained to cause contamination, preparation by green synthesis approaches have been introduced utilizing environmentally benign reducing agents. They include mixed-valence polyoxometallates, polysaccharide, Tollens, irradiation, and biological methods¹⁷.

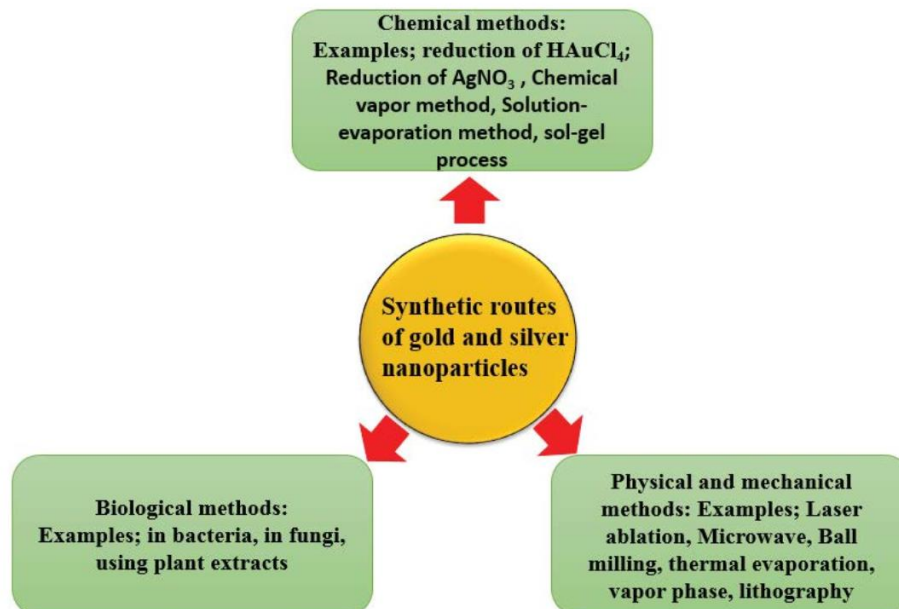


Fig. 2. Different synthesis methods of silver nanoparticles. ¹⁵



The major issues to be addressed in the synthesis processes are the control of sizes, shapes, size distribution, stability and aggregation of the nanoparticles (Fig. 3).

The stability of silver nanoparticles within the solution is one of the main objectives so that they can exert their maximum and longer biological action¹⁶.

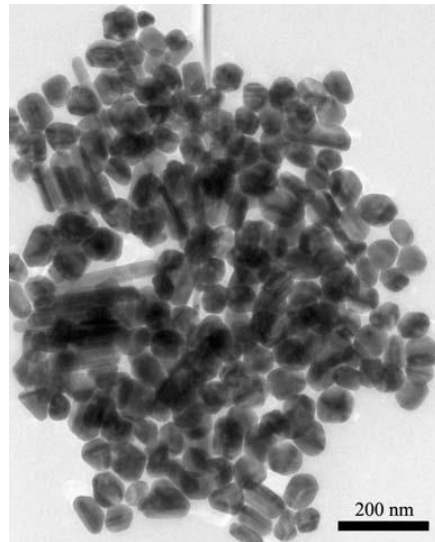


Fig. 3 TEM image of silver nanoparticles. ¹³

Silver, in metallic form or in combination with other compounds, has been widely employed at industrial level and its uses are considered a possible source of silver in the environment.

Silver bioaccumulation and effects in water, air, soil and organisms have been determined over time, but, the accumulation of silver ions, considered the major causes of toxicity, only in rare cases (more sensitive organisms) reached levels responsible for adverse effects due to the low bioavailability ^{12,18,19}.

Although silver can't be considered harmful to human health and environment, the development of nanotechnologies, with the introduction of nano-silver, has raised growing concerns about the toxic effects and environmental impacts ¹⁸⁻²⁰.

2.2 Silver nanoparticles applications

Silver nanoparticles are popular consumer product additives, although their potential beneficial effects are generally well described, the potential adverse effects and impacts of NPs have received attention.

The comparison between nano-scale materials and their macrometric version has led to interesting results. Nanoparticles, in this case nano-silver, show at the nanometric level different chemical, physical and optical properties.

This behavior is mainly due to the greater surface area which allows an increased dissolution with relative higher availability of silver ions.

In addition, greater interaction with microorganisms, biomolecules and biological receptors was found ^{12,13,21}.

The growing introduction of NPs-based consumer products urges the need to generate a better understanding about the potential negative impacts on environment and humans.

Three major product categories including silver nanoparticles are food, consumer products and medical products ^{12,13}.

In all these applications, the use of NPs is mainly focused on the remarkable bacterial growth inhibition abilities.

2.2.1 Food

In the food sector, the use of nano-silver includes the processing, conservation and consumption phase of the food production chain.

In the production phase, the nanomaterials are used for the purification of water and soil, in the machinery in the form of coatings (for antibacterial purposes), in food packaging with the aim of guaranteeing longer storage time and freshness and as additives in food (supplements) ^{22,23} (Table 1).



NPs in food may appear in suspension or emulsion and are known to have different structures and shapes.

Chain phase	Application	Nanotechnology	Function
Processing of food	Food preparation equipment	Incorporated nanosized silver particles	Anti-bacterial coating of food handling devices
Conservation	Refrigerators Storage containers	Incorporated nanosized silver particles	Anti-bacterial coating of storage devices
	Food products	Nanosized silver sprays	Antibacterial action
	Packaging materials	Incorporation of active nano-silver particles	Oxygen scavenging, prevention of growth of bacteria
Food consumption	Supplements	Colloidal metal nanoparticles	Claimed to enhance desirable uptake

Table 1. Summary of applications of nano-silver in the food production chain. ¹²

2.2.2 Consumer products

The product categories in which nano-silver is represented, are: electronics, filtration, purification, personal care and cosmetics, household products/home improvement, textile and shoes, medical devices ¹² (Table 2).

Fabrics functionalized with silver nanoparticles represent the most abundant part of products available on the market.

They include t-shirts, socks, shoes, and sportswear and are considered one of the main means of NPs release into the environment ¹².

The different methods of manufacturing and including NPs, incorporated between the fibers or directly linked to them, strongly influence the availability and release of NPs ²⁴⁻²⁶.

Categories	Subcategories	Examples
Personal care and cosmetics (30)	Skin care (14)	(Body) cream, hand sanitizer, hair care products, beauty soap, face masks
	Oral hygiene (6)	Tooth brush, teeth cleaner, toothpaste
	Hair care (3)	Hair brush, hair masks
	Cleaning (2)	Elimination wipes and spray
	Coating (2)	Make-up instrument, watch chain
	Baby care (2)	Pacifier, teeth developer
	Over the counter health products (1)	Foam condom
Textile and shoes (34)	Clothing (28)	Fabrics and fibers, socks, shirts, caps, jackets, gloves, underwear
	Other textiles (2)	Sheets, towels, shoe care, sleeves and braces
	Toys	Plush toys
Electronics (29)	Personal care (13)	Hair dryers, wavers, ions, shavers
	Household appliances (8)	Refrigerators, washing machines
	Computer hardware (6)	Notebooks, (laser) mouse, keyboards
	Mobile devices (2)	Mobile phones
Household products/home improvement (19)	Cleaning (9)	Cleaning products for bathroom, kitchen, toilets, detergents, fabric softener
	Coating (4)	Sprays, paint supplements
	Furnishing (3)	Pillows
	Furnishing/coating (3)	Showerheads, locks, water taps
Filtration, purification, neutralization, sanitization (13)	Filtration (8)	Air filters, ionic sticks
	Cleaning (6)	Disinfectant and aerosol sprays

Table 2. Examples of products containing nano-silver. ¹²



2.2.3 Medical devices

The silver nanoparticle applications in the medical area are largely therapeutic and include several products since its properties can be controlled and adapted for the wide variety of medical devices. Ag-NPs have been commonly incorporated into wound dressings in cases of burns or chronic wounds, such as leg ulcers, diabetic foot ulcers and pressure ulcers. A significant amount of products are on the market for these purposes (e.g., Anticoat) ²⁷, and, compared with other silver compounds, Ag-NPs seemed to promote healing and achieve better cosmetics.

Further, nano-silver containing materials have been used for the manufacture of catheters, vascular prostheses, surgical mesh, orthopedic and dental prostheses (Table 3) ¹³.

In particular, in the orthopedic field, sector in which high percentages of bacterial infections have been recorded, silver nanoparticle technology started to get remarkable interest. The antibacterial effects have been proved as regards tumor prostheses, external fixator pins and bone cement, applications which are prone to bacterial adhesion, colonization and biofilm formation leading to loss of fixation, failure and removal ²⁸.

Medical domains	Examples
Anesthesiology	Catheter for administration of local anesthetic (1)
Cardiology	Battery used in implantable cardioverter-defibrillator (1)
Nephrology	Hemodialysis catheter (2)
Urology	Urinary catheter (2) Battery used in implantable electrical pulse generator (1)
Wound care	Burn and wound dressing, professional use (15) Burn and wound dressing, over the counter (2) Burn glove (1) Burn sock (1) Tubular stretch knit (1) (Adhesive) strip, professional use (2) (Adhesive) strip, over the counter (2) Gel (1) Compress (2) IV/catheter dressings (2)

Table 3. Medical devices containing nano-silver. ¹²



2.3 Silver nanoparticles release

As products containing silver nanoparticles are widely used, the release of silver nanoparticles into the environment is a potentially serious issue.

The main routes of exposure to Ag-NPs are dermal contact, inhalation and ingestion, wound surface application and insertion or implantation of medical devices ¹² which bring Ag-NPs in contact with different fluids environments (Table 4).

The skin has been investigated as the primary route of exposure for nanomaterials from the use of consumer products which are meant to be applied on the skin (e.g., socks).

From other products investigated, Ag-NPs can possibly be inhaled during normal use (e.g., sprays, dust or fumes containing Ag-NPs) or may be ingested (e.g., supplements, water) ⁵.

Category	Sub category	Exposure route	Potential exposure*
Food and beverages	Cleaning	Inhalation/dermal	High
	Cooking utensils, coatings	Dermal	Low
	Storage	Dermal	Low
	Supplements	Oral	High
Personal care and cosmetics	Skin care	Dermal	High
	Oral hygiene	Oral	High
	Cleaning	Dermal	High
	Hair care	Dermal	Low?
	Baby care	Dermal	High?
	Over the counter products	Dermal?	High?
Textile and shoes	Clothing	Dermal	?
	Other textiles	Dermal	?
	Toys	Dermal/Oral	?
Electronics	Personal care	Dermal	Low
	Household appliances	Dermal	Low
	Computer hardware	Dermal	Low
	Mobile devices	Dermal	Low
Household products/home improvement	Cleaning	Inhalation/dermal	High
	Coating	Dermal	High??
	Furnishing	Dermal	Low
	Furnishing/coating	Dermal	Low
Filtration, purification, neutralization, sanitization	Filtration	Inhalation	?
Medical products	Cleaning	Inhalation/dermal	High
	Breathing mask	Inhalation	?
	Endotracheal tube	Inhalation	?
	Gastrointestinal tube	Oral	?
	Catheters	Intravascular/intrathecal/ intravesical/urethral	?
	Contact lens	Ophthalmic	?
	Incontinence material	Dermal	?
	Orthopedic implants	Intramedullary	?
	Orthopedic stockings	Dermal	?
	Pharmaceuticals	Oral/dermal	?
	Sling for reconstructive pelvic surgery	Intraperitoneal	?
	Surgical mask/textile	Inhalation/dermal	?
	Wound dressings	Dermal	High

Table 4. Ranking of the potential human exposure to nano-silver. ¹²



Several studies and researches ^{24–26,29,30} investigated the release of silver from different materials and products (socks, fabrics, paints, etc.).

They might be helpful to evaluate the possible human and environmental risks associated with the use of products containing silver nanoparticles.

Benn and Westerhoff, in their study ²⁴, determined silver release from six brands of commercially available socks into water to assess the environmental risks.

The study was performed in distilled water replicating a washing machine cycle.

The results showed the presence of silver released both in the form of nanoparticles and in the ionic form (greater dissolution of NPs by increasing the exposure time).

The socks contained up to 1360 µg/g of silver and, at the end, in 500 ml wash water, the silver content varied from 1.5 to 650 µg.

These results, comparing the silver leached from different socks, suggest a dependence of the release on the manufacturing process and on the type of medium used (distilled water and tap water) ²⁴.

Another study evaluated the release of Ag-NPs from fabrics placed in contact with artificial sweat ²⁵.

For this study, portions of tissues, both prepared in the laboratory and present on the market, have been used. They have been put in contact with different formulations of artificial sweat (different for pH) for 24h to 37 °C. After the incubation silver was released from different fabrics ranging from 0 to 322 mg/kg of fabric weight. In this case, similarly to the previous study, the quantity of silver released was found to be dependent on the initial amount of silver contained into the fabrics, on tissue quality and manufacture, and exposure media (pH).

Kaegi et al. ²⁹ investigated the release of metallic Ag-NPs from paints for outdoor applications, believed to be one of the most relevant sources of Ag-NPs released into the aquatic environment.



Facade panels were exposed to ambient weather conditions over a period of a year and the release from rain events was determined.

A high Ag-NPs leaching was observed during the initial runoff events with a maximum of 145 $\mu\text{g/L}$.

About 30% of the initial silver content in the facades was released at the end of the experiment and Ag-NPs were mostly found to be attached to an organic binder.

Given the use of silver nanoparticles in topical products or tissues in contact with skin, an increasing issue is the need to know the potential to penetrate the stratum corneum and to diffuse into underlying structures.

Larese et al.³¹ investigated, in their study, the in vitro skin penetration of Ag-NPs.

The research was performed using the Franz diffusion cell method, comparing the behavior of both intact and damaged full thickness human skin (epidermis and dermis).

They concluded that silver can pass through the intact skin with an average amount of 0.46 ng/cm^2 and, interestingly, was found a five time greater Ag-NPs penetration through the damaged skin (Fig. 4).

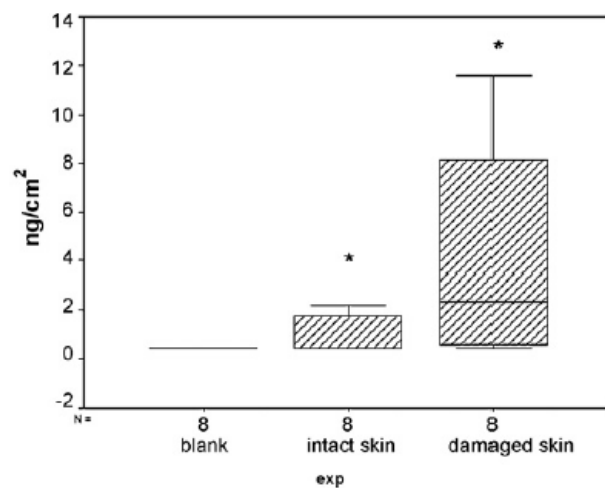


Fig. 4. Silver skin penetration at 24h.³¹



Last but not least, the release of silver nanoparticles can take place directly inside the body from medical products.

Roe et al.³² studied the Ag-NPs release from catheters coated with silver using AgNO₃. Silver release from the catheters was determined in vitro and in vivo using radioactive silver (^{110m}Ag⁺).

Experiments were performed with catheters (five strands, 2 cm long segments of each type, were studied) coated with two concentrations of silver: 600 µg/g of catheter (concentration similar to that used in the antimicrobial activity) and 1000 µg/g.

In 10 days the average amount of silver released daily from catheters was 45.1±1.1 ng/cm (catheters coated with 1000 µg/g silver) and 24.1±2.4 ng/cm (catheters coated with 600 µg/g silver).

Cumulative daily release data, examined to better understand release kinetics, showed a biphasic silver release during the ten days experiment, with a greater release on the first days.

In conclusion, the total amount of silver released from catheters with high silver content was 20% higher than the amount of silver released from the catheters coated with lower silver content.

2.4 Silver ions release

The widespread use of nano-silver into consumer and medical products as an antimicrobial agent inevitably leads to Ag-NPs release into the environmental or biological ambient.

When nanoparticles are exposed to a liquid environment, they can undergo chemical transformation which can affect transport, bioavailability, bioaccumulation and toxicity³³.

Given the increasing amount of surface area as particle size decreases, nanoparticles have high surface energies. Once in contact with biological or aqueous medium, silver can be oxidized and dissolved to



silver ions (Ag^+), which are believed to be the main active and reactive species of silver with inherent toxicity^{20,34}.

Then, nano-silver behaves similarly to a drug delivery system, which transport and release the active species, in this case Ag cations, to biological target sites.

Ions release is a relevant behavior of Ag -NPs and understanding Ag^+ release is important to evaluate their biological impact.

Several studies tried to understand the nanoparticles dissolution kinetics³⁵ and the different parameters affecting and controlling the silver ions release^{20,33,36–40}.

The ways silver nanoparticles behave in contact with water and more interestingly with biological media are currently under study and not completely understood.

Given the big amount of formulations of Ag -NPs, a proper analysis and comparison of the available data is very difficult.

The comprehension of ions release was obtained mainly in water studies to better understand mechanisms and kinetics. Regarding the evaluation of the dissolution rate and the transformations that nanoparticles can undergo in the human body, studies have been carried out in simulated physiological solutions.

All these transitions have been considered to be dependent on many factors including physical and chemical characteristics of nanoparticles such as size and surface coatings and on environmental conditions such as pH, ionic strength, presence of ligands, organic matter etc.

2.4.1 Release kinetics

According to Liu et al. research³⁵, ions release has been shown to be a synergistic oxidation process involving both dissolved dioxygen and protons.



In their study, citrate-stabilized nano-silver colloids were synthesized and time-dependent dissolution was evaluated by means of centrifugal ultrafiltration and atomic absorption spectroscopy (AAS).

They investigated the Ag^+ release from solid particles in both natural and deoxygenated water (Fig. 5) and by varying the pH.

The release in deoxygenated water was completely inhibited suggesting the important role of dissolved O_2 in the dissolution process.

Furthermore, the release of ionic silver was found to be strictly pH dependent (Fig. 6).

These results suggest the cooperative action of both protons and dissolved O_2 in the Ag-NPs dissolution process.

The reaction stoichiometry proposed is the following:

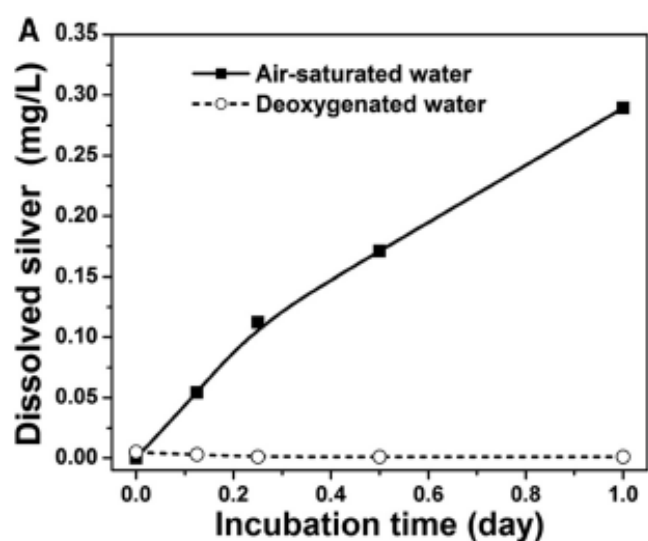
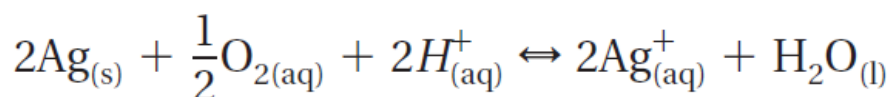


Fig. 5. Silver ion release dependent on dissolved O_2 .³⁵



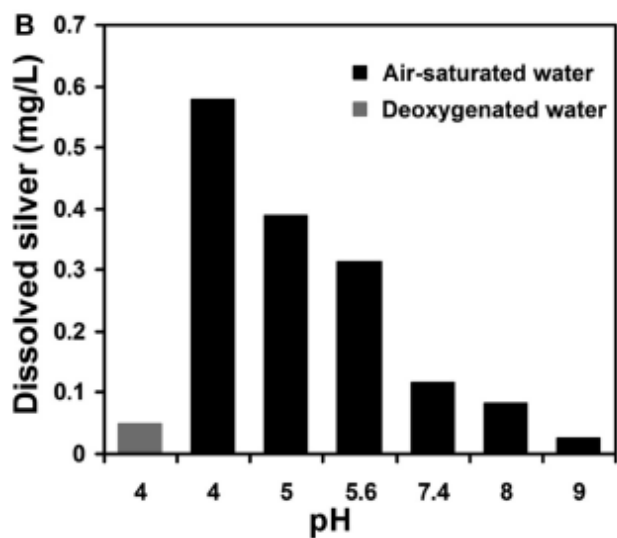


Fig. 6. Silver ion release dependent on pH. ³⁵

The oxidation process was found to be a simple redox reaction involving the production of peroxide intermediate (H_2O_2) which are responsible of an oxidant effect and an ulterior fast reaction:



The coupled release of reactive oxygen species (ROS), such as hydrogen peroxide, may explain the enhance toxicity of silver nanoparticles compared to the bulk silver, where the intermediates are further reduced to water ²⁰.

These nanoparticles dissolution studies were carried out in simple aqueous de-ionized media to avoid particle agglomeration facilitating thermodynamic analysis and quantitative kinetics.



2.4.2 Aggregation mechanism

Other experiments were obtained in natural environment^{35,36,40} or in solution simulated biological system^{33,37,38} to better comprehend Ag-NPs dissolution behavior in more complex media.

Stebounova et al.³⁸ investigated the behavior of two engineered silver nanoparticles (aggregation, sedimentation and dissolution) in two simulated biological media representing the fluids present in the lungs to understand nanoparticle fate once inhaled.

Nanoparticles, respectively uncoated and with thick polymer coating (polyacrylic acid polymer derivative) synthesized to prevent the nanoparticles from aggregating were studied.

Dissolution studies were carried out in Gamble's solution (pH 7.4, simulating interstitial fluid in the lungs) and in ALF solution (pH 4.5-5, simulating the composition of alveolar and interstitial macrophages) both prepared following the procedures described by Stopford et al.⁴¹.

The authors concluded that silver nanoparticles form aggregates and agglomerates when immersed in high ionic strength biological media and precipitate faster with the increasing solution ionic strength (Fig. 7), in an independent way from surface coatings.

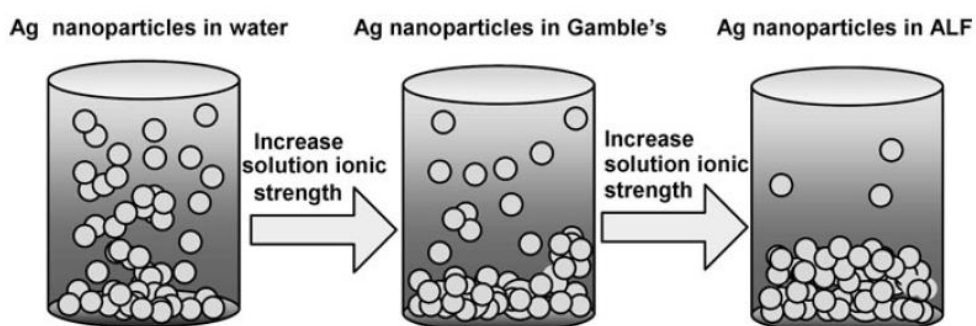


Fig. 7 Nanoparticle aggregation and precipitation increasing solution ionic strength. ³⁶

In this study the Ag-NPs dissolution and inherent Ag⁺ release is found to be negligible.

Inhibition of oxidation may be related to the aggregation process into high ionic strength solutions^{35,40}, which has been evaluated to be dependent on initial Ag-NPs concentration.

Firstly, the higher Ag-NPs concentration may limit the diffusivity of dissolved oxygen and protons in the solution to reaction sites, secondly it causes more rapid aggregation leading to less surface area available for oxidation reaction⁴⁰.

2.4.3 Controlled silver ions release

Silver ions release into the environment can be influenced by other important factors that can be varied to control the dissolution process and improve nano-silver technologies.

Liu et al.³⁷ focused their study on different approaches to control the release of biologically active silver optimizing methods for a better products performance and safety.

They determined different approaches to slow or accelerate the ions release.

Primarily, they demonstrated the mainly influence of the NPs size on silver ions release. Decreasing nanoparticles size bring to a higher surface area available for dissolved O₂ and protons in the solution to initiate their oxidation effect and consequently the ions release.

Another major effect is due to the surface modifications. Addition of citrate anions can lead to the occupation of the initial chemisorption sites for oxygen.

Treatment with Na₂S can sulfurize the silver to form Ag₂S which is insoluble and protective of the surface.

Several formulations including starch, gum Arabic and polymer coatings can also be used to protect the particle surface from oxygen access.



The media composition is essential in tailoring silver ions release. Antioxidants (e.g., SOD or catalase enzymes) and natural organic matter present in the media can decrease the Ag^+ rate into the solution causing the removal of reactive oxygen intermediates created during the oxidation reaction pathway.

Furthermore, compounds containing thiols, cysteine and glutathione have binding affinities with silver and can bind to the nanoparticles surface excluding oxygen from active sites.

The results obtained in this study are summarized in Fig. 8.

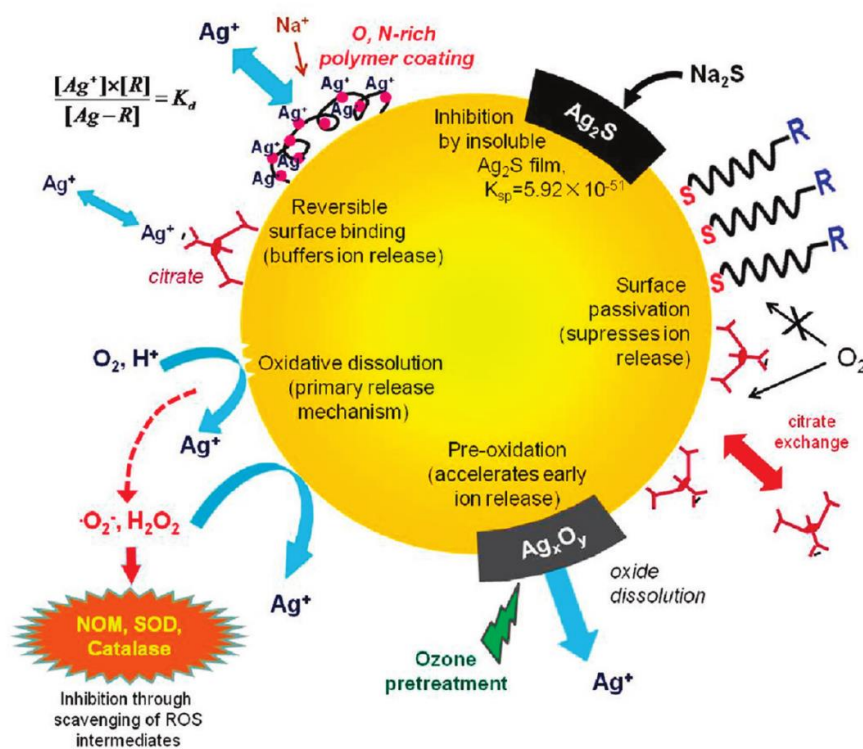


Fig. 8. Chemical approaches to tailor release of biologically active silver. ³⁷

In addition, a different release rate was found by Kittler et al.³⁴ for freshly prepared and aged nanoparticles.

They studied the dissolution from citrate-stabilized and polyvinylpyrrolidone (PVP) stabilized nanoparticles in water concluding that silver nanoparticles stored for several weeks in dispersion resulted to

be more toxic due to the augmented ions release, evidencing the relevance of nanoparticles manufacture and storage on the biological behavior.

The availability of Ag^+ released into the environment is dependent from media composition, which influence the speciation, mobility and bioactivity of silver.

Liu et al.³³ showed how Ag-NPs, after the dissolution process, can undergo a transformation pathway in contact with different biological environments in the human body.

Firstly, they showed an accelerate Ag-NPs dissolution in the stomach (pH 1.5 of gastric acid) compared to lysosome, inflammatory phase of wound and extracellular fluids, obtaining an ulterior prove of the relevant action of pH.

In biological media, free Ag^+ released by the oxidation process might complex and precipitate with Cl^- , reducing their concentration to a very low value.

Silver ions can also be bound by human serum albumin (HSA) and other proteins, due to the ability of Ag^+ to strongly bind thiol groups (-SH), transported in the circulatory system and distributed to other tissues and organs through ligand exchanges between thiol groups.

Thiols and chloride presence are reported to decrease the free Ag^+ concentration by complexation and precipitation influencing the potential biological activities.

In this study the authors focused on the Ag-NPs transformation leading to argyria (Fig. 9). Silver ions in near-skin regions could be photo-reduced to metallic immobile Ag-NPs and subsequent react with reduced selenium species forming argyria deposits.



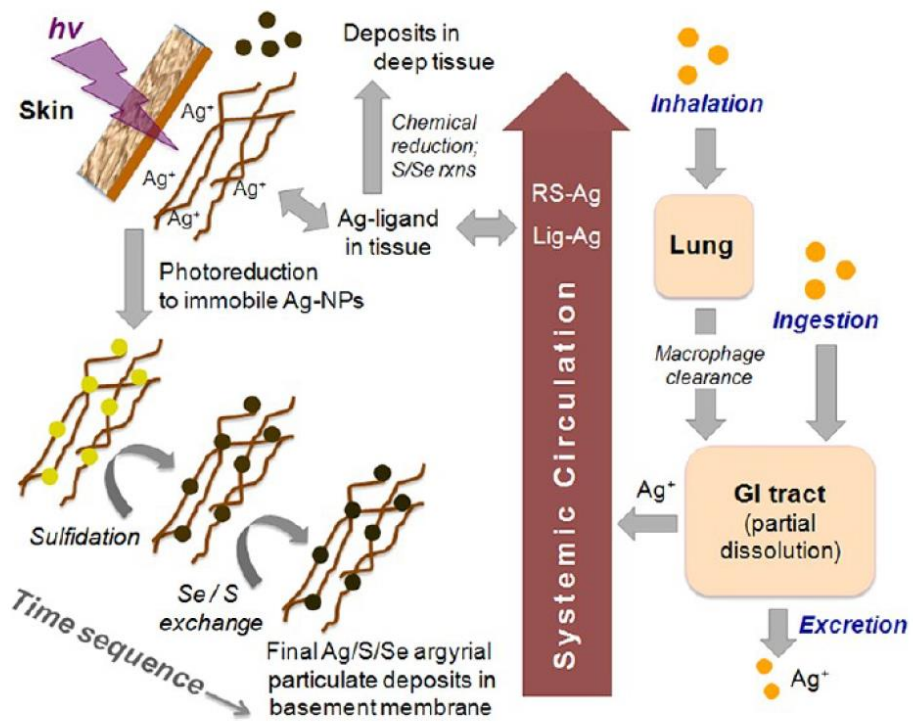


Fig. 9. Chemical transformation of Ag NPs in biological environment. ³⁴

3 SILVER NANOPARTICLES ANTIBACTERIAL ACTIVITY

3.1 Orthopedic implants infections

In the orthopedic field, one of the major complications that can cause the failure of a prosthetic installation is the bacterial infection associated with the formation of a bacterial biofilm.

It is caused by microorganisms that, once they have reached the implant surface, are able to bind to different molecules, proteins of the extracellular matrix and begin, within this highly hydrated environment, a process that leads to the growth and formation of the biofilm, structure within which the bacteria are organized in highly complex and organized structures which are, finally, extremely resistant against the host's defenses as well as against antibiotics ^{42,43}.

Over time, the odds of bacterial contamination have been greatly reduced thanks to perioperative antibiotic prophylaxis, improved surgical techniques and patient isolation in laminar airflow ambient but, despite this, the rate of infections is still high given the increasing need for implants and the bacteria strains more and more resistant to antibiotics ⁴⁴.

3.1.1 Micro-organisms responsible for infections

The microorganisms most involved in the process of colonization and infection are bacteria, which can be divided into two categories (*gram positive* and *gram negative*). In particular, among these, the most responsible, identified in 65% of cases, are *Staphylococcus aureus* (*S. Aureus*) and *Staphylococcus epidermidis* (*S. Epidermidis*) (Fig. 10) ^{42,43}.

The difference between the two types of bacteria lies at the level of the external structure.



Gram negative bacteria present a three layers envelope composed by an outer membrane, a peptidoglycan cell wall and an inner membrane (Fig. 11).

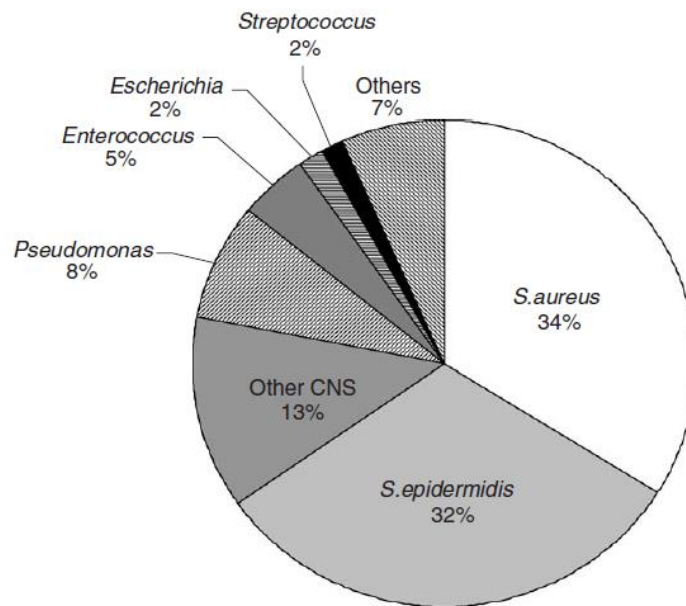


Fig. 10. Major bacteria involved in biofilm formation process. ⁴²

The outer membrane is a lipid bilayer made up internally by phospholipids and externally by glycolipids (lipopolysaccharide, LPS) and it plays an important role in the protection of the organism from the external ambient. The peptidoglycan cell wall (few nanometer thick) is a polymeric layer that determines the cell shape because of its rigidity. The inner membrane is a phospholipid bilayer in which are contained proteins with energy production, lipid biosynthesis, protein secretion and transport functions⁴⁵.



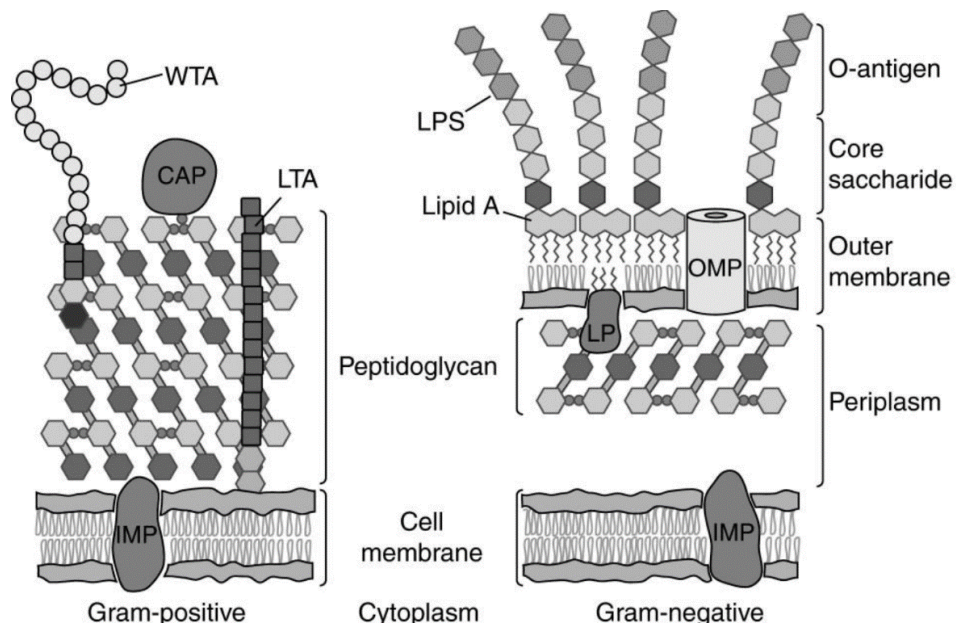


Fig. 11. Illustration of Gram negative cell envelope.⁴⁵

Gram positive bacteria present a different cell envelope (Fig. 11). They are deprived of the external protective membrane. The cell wall consists of several layers of peptidoglycan that form a rigid and much thicker (30-100 nm) structure.

Within this layer are also present other molecules such as teichoic acid that has the function of glue and regulates the presence of nutrients.

3.1.2 Biofilm formation mechanism

The biofilm growth is the result of an organized and coordinate mechanism of gene expression and high coordination and communication between cells.

The first step involved in the biofilm formation process is the attachment of microorganism to the surface.

The microbial cells adhere to a surface through their pilli and flagella and the contact is mediated by physical forces like Van der Waal's or electrostatic interactions. Other factors could be determinant like the surface properties. It has been evaluated a better attachment of bacteria to hydrophobic surfaces.



Subsequently, once the adhesion is stabilized, a process of multiplications and division occurs leading to the formation of cells clusters ^{42,46}.

These first two events are influenced by several ambient factors such as pH, oxygen, temperature, nutrients ⁴⁷.

The maturation and stabilization of the biofilm is regulated by the quorum sensing, a communication between microbial cells and micro-communities mediated by signaling molecules called auto-inducers (AI). The quorum sensing leads to biofilm growth, higher cell density, expression of genes inducing the production of extracellular polymeric substances (EPS), the main material into the biofilm, and the formation of voids into the structure acting as a circulatory system ^{42,46,48}.

The last phase consists in a detachment of fragments of biofilm. This process is due to the secretion of enzymes able to induce the EPS matrix lysis. The subsequent dispersion is responsible for the spread of infections in new sites ^{46,48}.

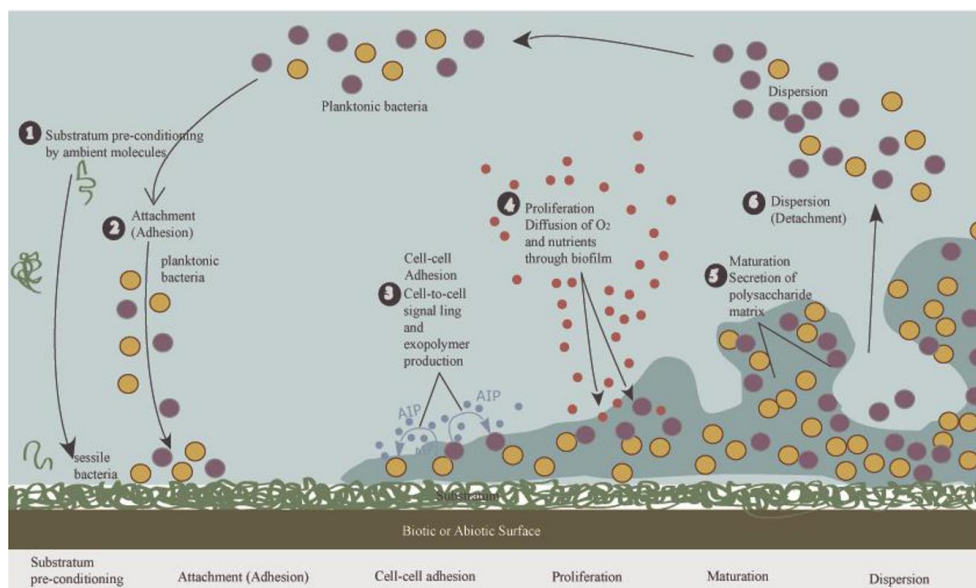


Fig.12. Schematization of biofilm formation process.⁴⁸



The biofilm formation mechanism is summarized step by step in Fig. 12. The complete biofilm is composed by microorganism aggregates (5-35%) immersed in an extracellular matrix of polymers (EPS, 50-90%). The matrix is mainly composed by proteins, exopolysaccharides and nucleic acids, it is usually thick 0.2-1 μm and it is responsible of the morphology and chemical-physical properties of the biofilm^{42,46}.

3.2 Silver nanoparticles antimicrobial activity

The widely diffused antimicrobial properties of silver nanoparticles resulted in its increasing use in biomedical applications and products. Although numerous studies and researches were conducted to better understand its mechanisms of action against bacteria and microorganisms, the complete and correct antimicrobial effect is not known. Silver nanoparticles are considered one of the most promising nanomaterials from the point of view of antibacterial behaviors but, possible toxic effects were highlighted not only against both gram negative and gram positive bacteria⁴⁹⁻⁵³ (*E. Coli*, *S. Aureus*) but also against other organisms such as fungi³², viruses^{54,55} and cells⁵⁶⁻⁵⁸. For this reason, it is of considerable importance the understanding at 360 degrees of the mechanisms by which nanoparticles act and essential to evaluate in what terms this action has deleterious effects in the different organisms so that we can exert the most from this behavior for disinfection and sterilization applications without acting negatively on healthy cells.

Three main mechanisms of action have been identified to be responsible for the bactericidal effect of silver nanoparticles⁵⁹. The main issues discussed are the release of Ag^+ ions, damage to the cell membrane and interactions with DNA, damage to metabolism and production of free radicals (ROS).



As discussed in the first chapter, silver nanoparticles in contact with aqueous biological fluids are characterized by a process of oxidative dissolution leading to the release, in the surrounding environment, of Ag^+ ions and depends on many factors.

Ag^+ ions generated have known antibacterial properties and, for this reason, their interactions with cells are commonly considered, at least in part, responsible for the antibacterial action of silver nanoparticles.

The toxicity mechanisms vary if silver nanoparticles or ions are taken into account.

In particular, in this context, the physico-chemical properties of nanoparticles such as size, superficial coatings and surface charge have a decisive impact on the interactions with the bacterial surfaces and the release and concentration of bioavailable ions⁶⁰.

Sotiriou et al.⁶¹ investigated the antibacterial activity of nanosilver on *E. Coli*. Silver was immobilized on silica particles obtaining Ag/SiO_2 particles. The antibacterial activity of Ag^+ ions and nanoparticles has been assessed by observing the growth of the bacterial population with the presence or not in solution of these particles.

The antibacterial activity was found to be dependent on particle size. Smaller nanoparticles are (around 10 nm), more consistent is the ions release and, consequently, the bactericidal effect is dominated by Ag^+ ions interactions.

3.2.1 Connection to the cell membrane

Multiple effects and interaction mechanisms of the Ag^+ ions and nanoparticles with cells were found. The behavior of ions has been assessed to be deleterious to the cell membrane.

Jung et al.⁵⁰ e Feng et al.⁴⁹ have conducted researches to evaluate the mechanisms by which Ag^+ ions interact with cellular microorganisms and inhibit bacterial growth.



Two bacterial strains have been commonly investigated, Gram negative (*E. Coli*) and Gram positive (*S. aureus*).

They were both treated with solutions containing Ag^+ ions, respectively AgNO_3 and electrically generated ions solution.

Ag^+ ions treatment on *E. Coli* and *S. aureus* has resulted in significant morphological changes.

Similarly, in both bacterial strains it is possible to notice a detachment of the cytoplasmic membrane, the appearance of an electron-light/low molecular weight zone in the center of the cell, within which is possible to notice a condensed form of DNA molecules (Fig. 13, Fig. 14, Fig. 15).

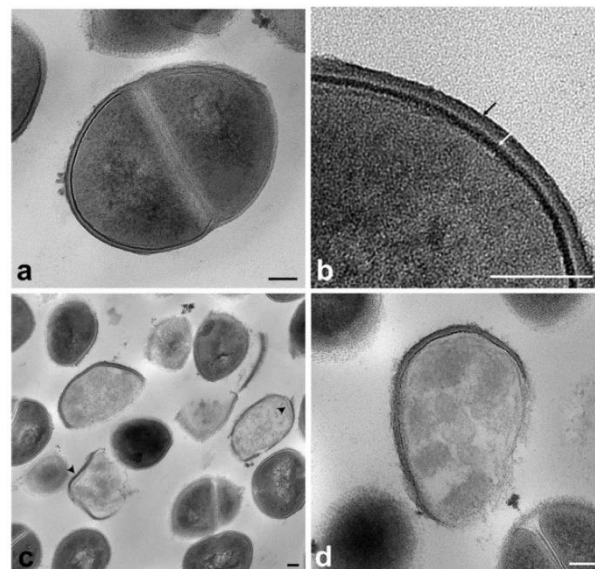


Fig. 13. Internal structure of *Staphylococcus aureus* observed by TEM. Bar=100nm. (a and b) Untreated bacteria. (c and d) Bacteria treated with silver ion solution (0.2 ppm). Black and white arrows indicate peptidoglycan layer and cytoplasmic membrane, respectively. Note the separation of cell membrane from the cell wall (arrowheads).⁵⁰

In this unrelaxed state, the DNA molecules lose their replication skills, the bacteria are carried in an "active but not curable state", in which the cells show signs of physiological activity but fail to grow ⁵⁰.

Further, within the cell, but outside the electron light zone, Ag^+ ions have been identified in correspondence with electro dense granules (Fig. 13).



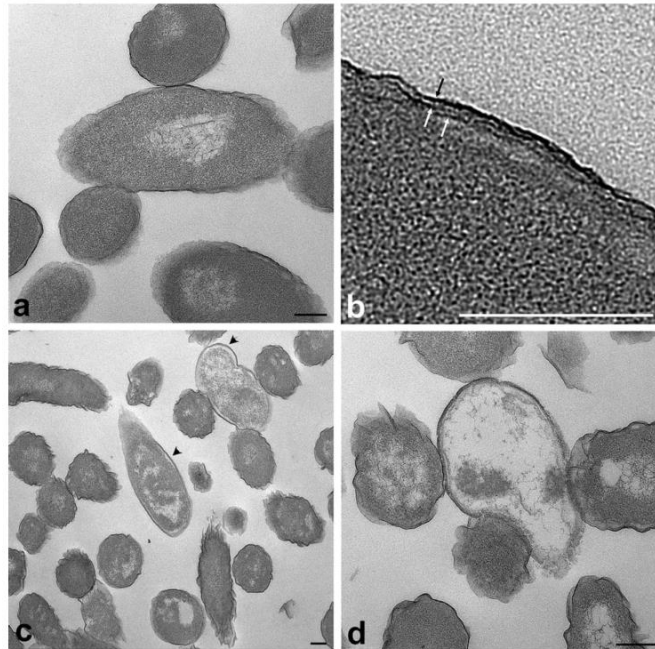


Fig. 14. Internal structure of Escherichia coli observed by TEM. Bar=200nm. (a and b) Untreated bacteria. (c and d) Bacteria treated with silver ion solution (0.2 ppm). Arrows indicate outer membrane, peptidoglycan layer, and cytoplasmic membrane from the outside of the cell. Arrowheads indicate separation of the cell membrane from the cell wall. ⁵⁰

These phenomena can explain one of the possible antibacterial mechanisms and at the same time the protective function that is established in the cell which seems to protect the DNA from the attack of ions by condensing it towards the center and leading to the generation of the electron light region.

Following treatment with Ag^+ ions, the cell undergoes a detachment of the cytoplasmic membrane followed by the rupture and release into the surrounding environment of the cellular content.

In general, the effects of ions treatment have been more effective against gram negative bacteria, probably due to the thickness of the peptidoglycan layer.

Differently, several interaction mechanisms have been found on bacteria treated with silver nanoparticles ^{52,53,62}.

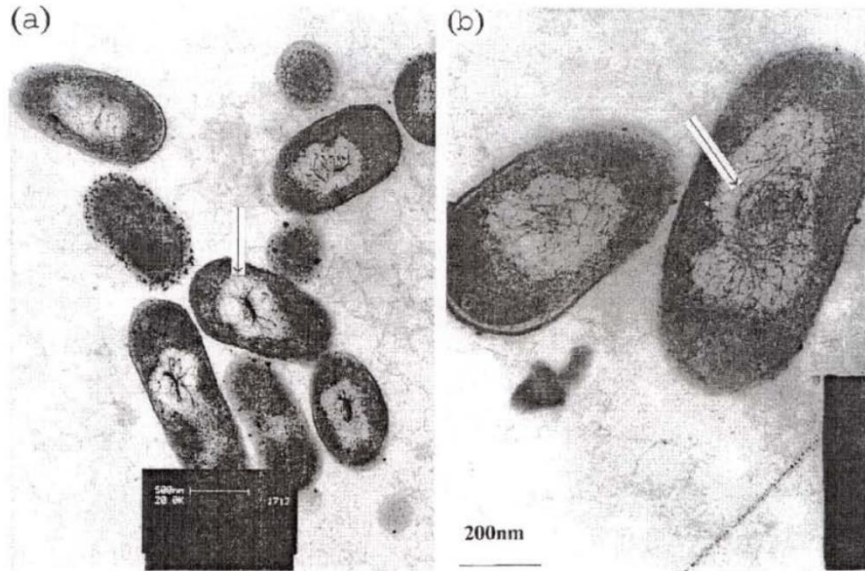


Fig. 15. Internal structure of silver ion treated E. Coli. (a) A remarkable electron-light region in the center of the cell and electro dense granules. (b) Condensed form of DNA in the center of the electron-light region. ⁴⁹

The interaction between the nanoparticles and the external membrane of the bacteria occurs through the binding affinity between silver and groups containing phosphorus and sulfur.

The interaction with these groups leads to structural and morphological changes of the membrane, degradation and its increased permeability. The nanoparticles induce on the membrane the formation of surface "pits" thanks to which the smallest nanoparticles are able to penetrate and, once inside the bacterium, to interact with the groups containing sulfur and phosphorus like DNA, which fidelity of replication of some genes is compromised, inhibiting replication activities and bacterial growth⁶³.

Unlike the action of Ag^+ ions, as far as nanoparticles are concerned, it is not possible to notice a low molecular weight zone in the center of the bacterium but, on the contrary, the bacterium presents a concentration of nanoparticles inside it ^{53,64} (Fig. 16).

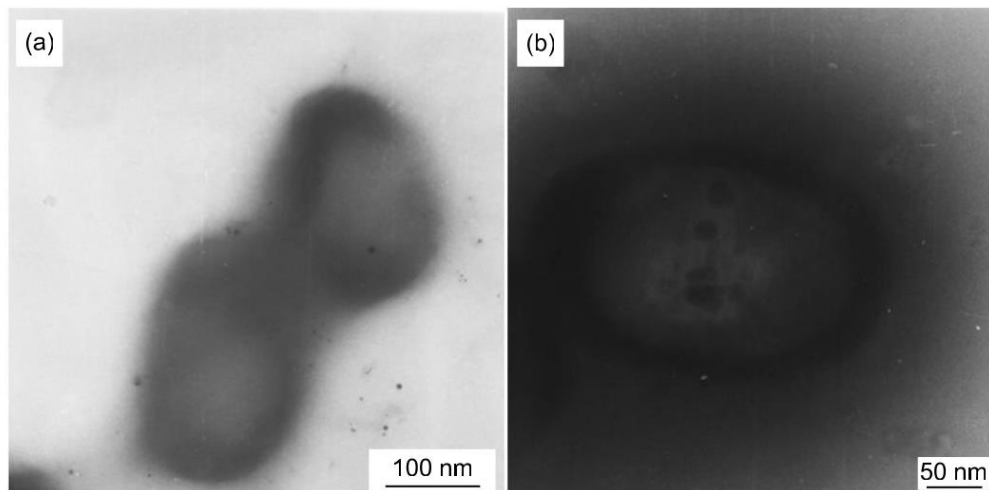


Fig. 16. (a and b) Interaction and penetration of silver nanoparticles in E. Coli. ⁶⁴

3.2.2 Interaction with the respiratory chain

A further mechanism of action by which silver nanoparticles and ions lead to their antibacterial effect has been found and concerns the negative incision of the Ag^+ ions with the respiratory chain and cellular metabolism.

Holt and Bard⁵¹ observed a mechanism of action that makes the cytoplasmic membrane permeable to protons and leads to the collapse of the proton gradient, essential for bacterial metabolism.

A mechanism of preferential interaction of Ag^+ ions with membrane-related proteins in the cytoplasmic membrane has been proposed.

The binding takes place with proteins involved in breathing and transport thanks to the remarkable affinity of the Ag^+ ions with thiol groups present in the cysteine residues^{65,66}.

During the respiration processes, in an electron transport system, the membrane-associated electron transporters (NADH , FADH_2) function in an integrated manner to transport the electrons to a final acceptor through a series of redox reactions.

When transferring electrons through a membrane-level transport system, protons (H^+) are transported through the membrane, resulting in the formation of a proton gradient and a proton-motive force required for the formation of ATP.

Coenzymes are oxidized to NAD and FAD by transferring electrons to some transport molecules.

The transfer of electrons through the respiratory chain requires the intervention of enzymes which contain a pair of electrons with a high transfer potential, also known as dehydrogenases (NADH, $FADH_2$).

In a first phase, the electrons deriving from the oxidation process of the NADH and $FADH_2$ coenzymes are transferred to the electron transport chain for the generation of a proton gradient in the intermembrane space of the mitochondria.

Subsequently, the proton gradient is used to activate transmembrane enzymes, for the synthesis of ATP molecules ^{67,68}.

Ag^+ ions interact with respiratory chain enzymes, such as NADH dehydrogenases, this binding leads to the inhibition of their functions with the consequent limitation of the efficient pumping effect of protons through the membrane.

The loss of the proton-motive force induces the decoupling of the respiration from the synthesis of ATP and the loss of the gradients that allow the production of energy for the vital transport mechanisms.

Similarly, Lok et al.⁶⁹ investigated the antibacterial activity of silver nanoparticles through a proteomic approach.

The analyzes carried out revealed an accumulation of envelope protein precursors, a phenomenon probably due to the loss of the proton-motive force, induced by treatment with Ag nanoparticles, which results, subsequently, in the destabilization of the membrane and the loss of cell viability.

Consistently with the previously discussed studies, the mechanism of action of Ag nanoparticles and ions was found to be similar, with the



greatest difference in the antibacterial concentration respectively in the nanomolar and micromolar range.

To compensate for the lack of the proton gradient, the cell has been observed to enter in an uncontrolled and faster breathing process that leads to the generation of superoxide and hydroxyl radicals due to the limited transfer of electrons to oxygen at the terminal acceptor⁵¹.

3.2.3 Generation of reactive oxygen species (ROS)

One of the mechanisms that induce toxicity mediated by nanoparticles of silver is the production of free radicals and the consequent condition of oxidative stress.

In this context, the physicochemical characteristics of nanoparticles (size, surface charge, chemical composition) are of great importance⁷⁰. Carlson et al.⁷⁰ performed toxicity evaluation using mitochondrial, cell membrane viability and reactive oxygen species. After 24h treatment a significant inflammatory response was observed by the release of inflammatory mediators confirming the ROS production and a size-dependent toxicity was determined.

ROS are reactive species of molecular oxygen, they include superoxide anion (O_2^-), hydroxyl radical (OH), hydrogen peroxide (H_2O_2), singlet oxygen (O_2) and hypochlorous acid (HOCl).

ROS are formed as a natural product of the normal metabolism of oxygen and have important roles in cell signaling and homeostasis.

ROS levels can increase significantly in response to various stimuli and induce so-called oxidative stress⁷¹.

Superoxide anion ($O_2^- \bullet$), the product of a one-electron reduction of oxygen, is the precursor of most ROS and a mediator in oxidative chain reactions. Further reduction of $\bullet O_2^-$ produces hydrogen peroxide (H_2O_2), which in turn may be fully reduced to water or partially reduced to hydroxyl radical (OH \bullet)⁷².



Physiologically, ROS are produced by processes such as mitochondrial respiration and the activity of neutrophils or macrophages which, under inflammation conditions, may induce ROS production as a defense mechanism⁷¹.

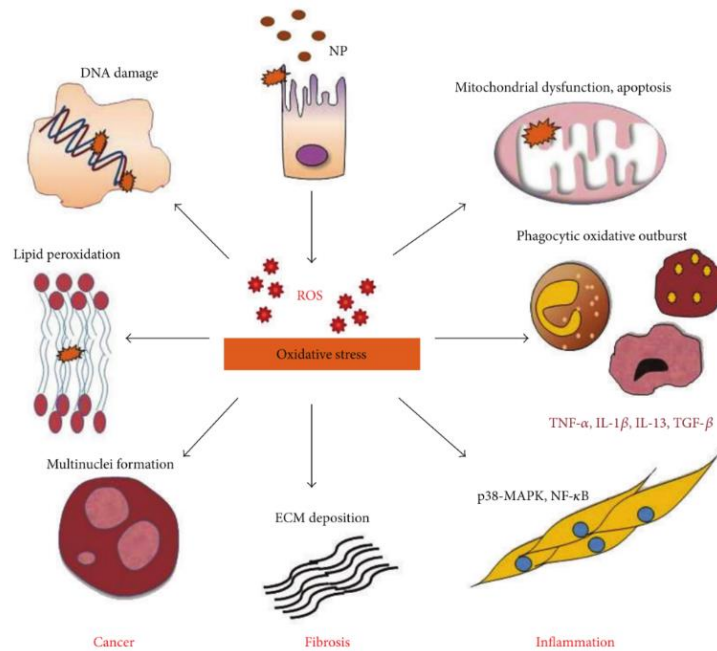


Fig.17. Oxidative stress dependent toxicity. ROS generation is capable of inducing DNA damage, strand breaks, protein denaturation, lipid peroxidation, mitochondrial membrane damage, transcription of genes responsible for fibrosis, carcinogenesis, EMT.⁷¹

Reactive oxygen species have a role in a number of cellular processes. High levels of ROS can lead to cellular damage, oxidative stress, DNA damage and apoptosis⁷³ (Fig. 17).

The human body naturally defends itself from the excess of free radicals producing enzymatic antioxidants such as dismutase, catalase, glutathione.

When ROS level is higher than the antioxidant capacity of the enzymes, they are no longer able to counteract the oxidizing action and the cell reaches the condition of oxidative stress.



Several sources have reported the generation of intracellular ROS as one of the mechanisms contributing to the bactericidal action of Ag⁺ ions and nanoparticles.

The inhibition of some enzymes due to affinity between the Ag⁺ ions and the thiol groups, as discussed above, causes the perturbation of the respiratory chain into bacteria and the possible formation of ROS has been proposed as a result of this phenomenon.

Park et al.⁷⁴, in their study, showed how Ag⁺ ions, released from nanoparticles, are involved in a toxicity mechanism mediated by ROS generation.

They investigated the activity of superoxide-sensor protein in *E. Coli* and *S. Aureus* bacterial strains.

The bactericidal activity of Ag⁺ ions was found to be greater against both bacterial strains under aerobic conditions, proving that the activity of ions is strongly linked to the presence of oxygen.

Moreover, the observation of the OxyR sensor for hydrogen peroxide showed that the superoxide-radical is the main ROS generated by the action of ions and involved in the antibacterial effect.

The generation of ROS and its oxidative stress induced in the cells was evaluated in the brain of mice following the treatment with Ag nanoparticles⁷⁵.

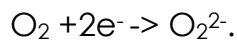
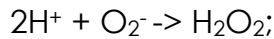
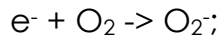
Gene expression variations have been assessed in three areas of the brain: caudal, frontal cortex and hippocampus.

The gene modification associated with the oxidative stress of selected genes indicated the possibility of disorders in the immune system leading to apoptosis and neurotoxicity.

Wang et al.⁷⁶ demonstrated the remarkable importance of the conductivity of the substrate treated with silver nanoparticles, in bacterial inactivation (Fig. 18).



Because of the different potential, galvanic pairs are formed between the titanium of the substrate and the nanoparticles of silver dipped in it. Titanium oxidizes, and the donated electrons are consumed for the production of ROS outside the cell with the following reactions:



At the same time, electron transfer of titanium can also occur within the cell by the action of silver nanoparticles by inducing the intracellular production of ROS, following, in that case, these reactions:

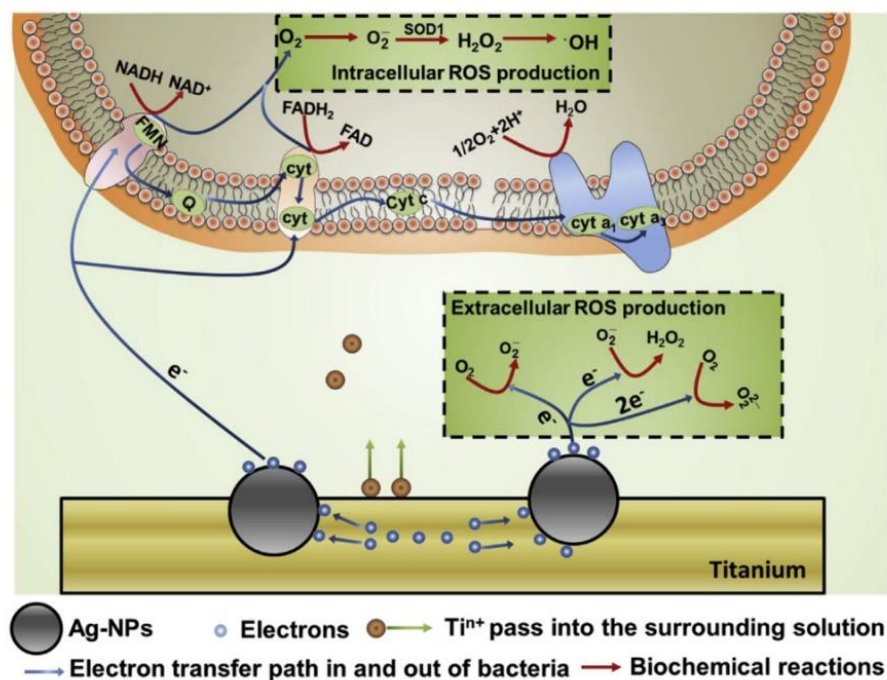
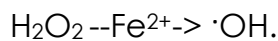


Fig.18. Generation of oxidative stress in the surrounding solution and within the bacteria. ⁷⁶

All mechanisms of Ag nanoparticles-bacterial cell interaction discussed in this section are summarized in Fig. 19.

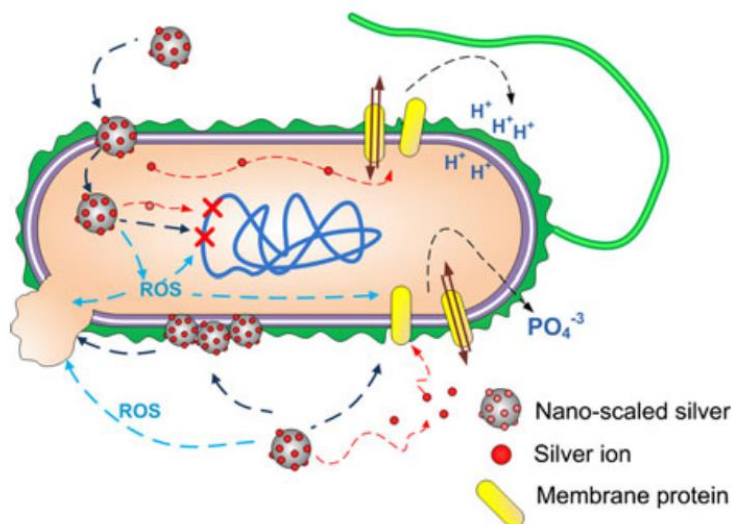


Fig.19. Diagram summarizing nano-scaled silver interactions with bacterial cell. ⁵⁹

3.2.4 Biofilm resistance

Biofilm is known to increase the resistance of a microorganism for antimicrobial agents and develop the human infection.

Since most applications of silver nanoparticles are related to counteracting bacterial infections, widespread bacterial resistance is a growing concern⁵⁹.

The increased antibiotic resistance of biofilm is due to different mechanisms of action (Fig. 20): limited diffusion of antimicrobial agents through the biofilm matrix; quorum sensing; resistance mediated by enzymes which bind bactericidal and bring them to sublethal concentrations; limited levels of metabolic activity inside the biofilm, cells are in a quiescence state and antibiotics need cellular activity to act; existence of persisters cells in the deepest area of the biofilm,

resistant to lethal doses of antimicrobial agents and can re-induce the growth of the biofilm; genetic expression of defense and regulatory genes encoding enzymes inducing repair and stress response; and modification of cell envelope^{42,77,78} (Fig. 20).

It was reported in one study that silver nanoparticles, stabilized by albumin, were not able to induce toxicity to different microorganism even at high concentration of silver⁷⁹.

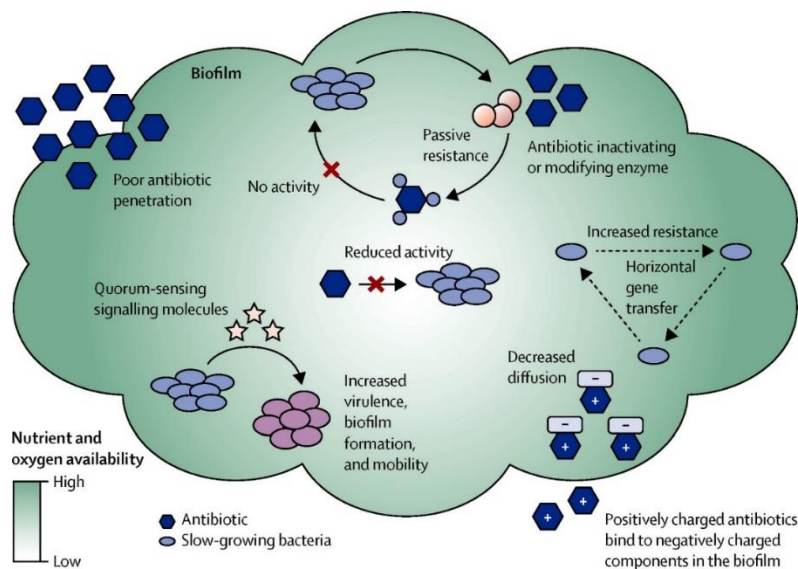


Fig. 20. Biofilm resistance mechanisms.⁷⁸

3.3 Enhanced cytocompatibility

Silver, as stated before, is commonly introduced into biomaterials surfaces with the aim to induce an antibacterial activity but, silver ions and nanoparticles could increase cytotoxicity limiting cell proliferation and adhesion in a time and dose dependent manner⁸⁰.

In order to inhibit the cytotoxic effect that accompanies the antibacterial action of silver, techniques and functionalities have been introduced on the surface for this purpose.



Zhang et al.⁸¹, in their work, modified polymer substrates (polyethylene) by adding Ag and N₂ through the plasma immersion ion implantation (PIII) technique to induce respectively an antibacterial activity and improve the cytocompatibility of the biomaterial.

First of all modified surfaces induced better protein adsorption resulting in an improved bone cell adhesion and proliferation rate due to the addition of N₂ functionalities.

Through the introduction of nitrogen functionalities, this technique has allowed to improve the cytocompatibility of the material compromised by the cytotoxic action of the released silver which accompanies its antibacterial action obtaining a surface modification that allows good biocompatibility and antibacterial effect of the biomaterial, in this case polyethylene.

In another study⁸² titanium surfaces have been modified with the co-implantation of zinc and silver by PIII.

The formation of micro-galvanic couples of Zn and Ag was observed to improve the corrosion resistance of the material.

The implanted Zn serves as the anode and releases Zn²⁺ ions, on the other hand silver nanoparticles serve as the cathode.

The Zn ions released in a appropriate quantity showed an improved osteogenic activity.

As a result, the co-implanted Zn and Ag are effective in obtaining better bone cell adhesion, proliferation and differentiation, corrosion resistance and antibacterial activity mitigating the cytotoxicity of implanted silver.



4 PROTEIN ADSORPTION ON BIOMATERIALS

The adsorption of proteins on solid surfaces is a fundamental phenomenon affecting nanotechnology, biomaterials and biotechnological processes.

When a solid material comes in contact with a biological environment containing proteins, a significant immediate and irreversible phenomenon of protein adsorption is observed on the surface leading to the generation of a protein layer.

This adsorbed protein layer, due to the large quantity of proteins present within biological fluids, will determine and modulate the behavior of the surface within the biological environment playing an important role in the incorporation of the implant.

Therefore, a comprehensive understanding of the mechanisms of formation, functioning and nature of proteins absorbed on the surface is necessary.

4.1 Kinetics of protein absorption

In addition to the determination of the protein components of the layer it is essential to study the stoichiometry and affinity of binding between proteins and surfaces.

Initially, the water molecules are the first to come in contact with the surface, they are followed by proteins which interact with the water molecules as well as the surface, and, are responsible for the formation of the protein layer.

The latter will be responsible for the interaction with the cellular organisms and its characteristics will depend on the initial properties of the surface of the material (topography, chemistry, surface charge, wettability).



Protein absorption can occur following different surface-proteins interaction mechanisms which can be identified as ionic or electrostatic interactions, hydrogen bonding, hydrophobic interaction and charge transfer interactions⁸³.

Initially, after the introduction of materials in contact with biological fluids, the absorption of proteins over the surface is believed to happen very fast within seconds to minutes, but a competition for surface absorption is observed between the biomolecules.

It is a dynamic mechanism including exchanges between surface-bound and bulk proteins over the time.

The proteins present in greater concentration in human plasma (e.g., albumin, fibrinogen)⁸⁴ will be the first to be absorbed on the surface and they will be replaced on different time scales by proteins with greater affinity, this phenomenon is called Vroman's effect ⁸⁵ (Fig. 23).

Therefore, the protein layer is not a fix layer, but its composition is controlled by the kinetic rate of adsorption and desorption on the surface of each protein and biomolecules.

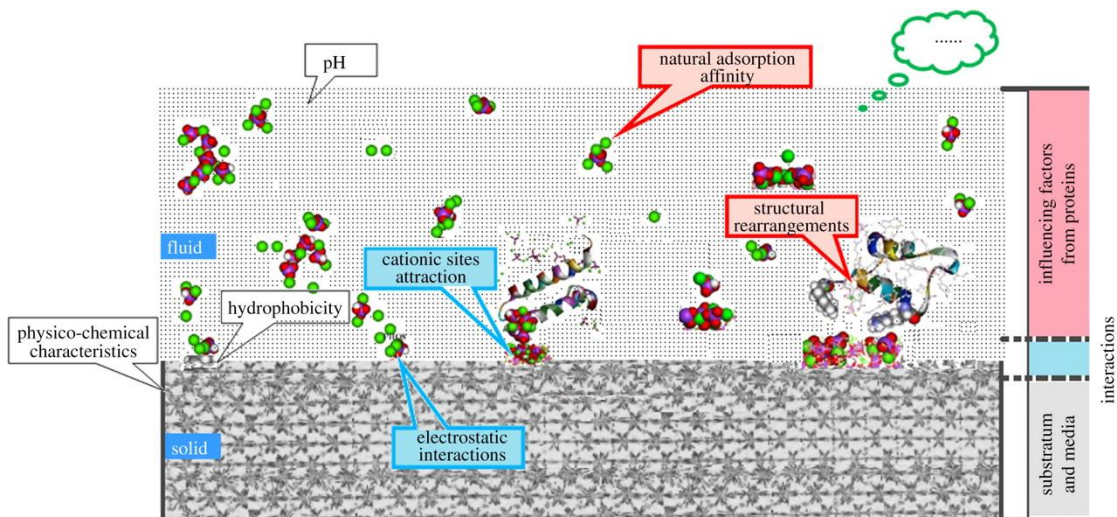


Fig.21. Influencing factors for protein adsorptions.⁸⁵



The interaction with the external proteins and cells will be controlled by the characteristics of the surface introduced by the adsorbed protein layer depending on amount of protein adsorbed, spatial organization, conformation, orientation, and biological activity.

Proteins, as soon as they come into contact with an implant surface, tend to change its structure by a conformation assumed in solution towards a new structure. The latter will depend on the characteristics of both the surface (hydrophobicity and surface chemistry ⁸⁶) and the proteins (structure, size, and structural stability ⁸⁷).

4.1.1 Surface properties

- Hydrophobic and hydrophilic surfaces

One of the main factors influencing the interaction of proteins and implant surfaces is the surface hydrophobicity or hydrophilicity⁸⁷.

The absorption of a protein on a hydrophobic surface takes place through the interaction between the internal portion of the protein (hydrophobic core) and the surface itself.

Initially, some hydrophobic protein domains are involved and subsequently a rearrangement of the protein structure is observed to allow the exposure of the hydrophobic domains and a closer bond.

This results in a loss of the native tertiary structure, an exposition away from the surface of hydrophilic domains and a reduction of the surface energy.

On the other hand, the interactions between proteins and hydrophilic surfaces include different behaviors.

First of all, the hydrophilic surface is covered with a layer of water adsorbed on it, which represents a barrier that the proteins must overcome to allow contact with the surface.

Protein absorption, in this case, does not occur through a conformational rearrangement of the protein structure but the protein



conformation is favorable to the bond which is generally weaker compared to the case of hydrophobic surfaces⁸⁷.

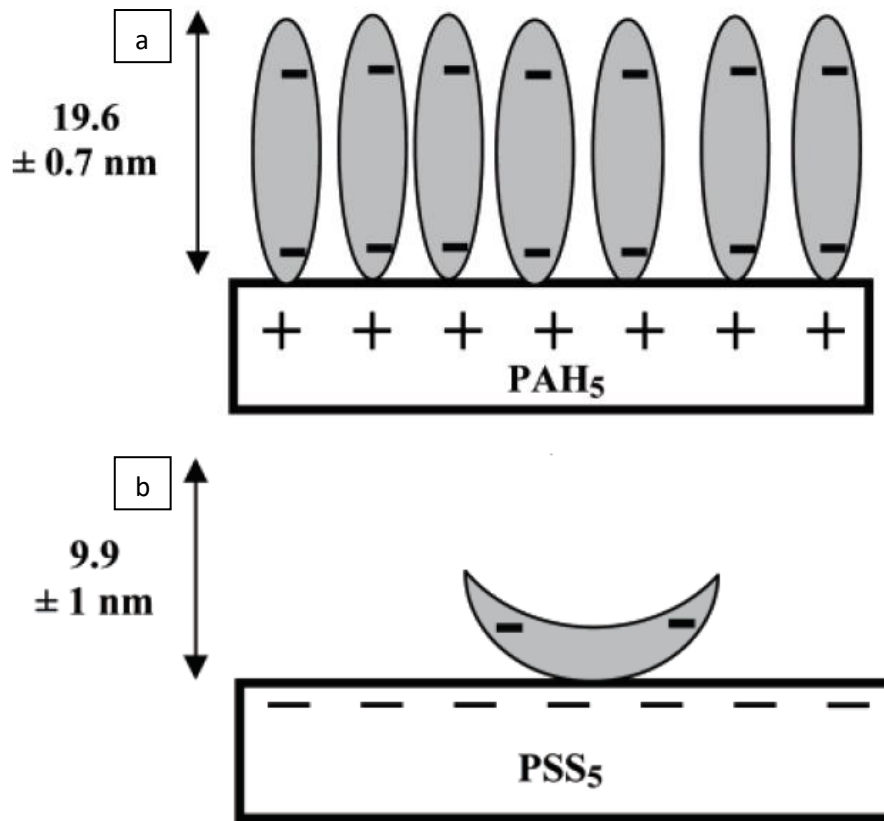


Fig. 22. Conformation adopted by fibronectin induced by surface charge.⁸⁹

- Surface charge

Surface charge is one of the factors that control body's initial responses to an implanted material ^{83,87}.

When a solid comes into contact with a liquid environment, it becomes electrically charged on the surface and the zeta potential of an implanted material is an index of its electric properties.

The presence of negative or positive charges on the surface is considered to promote strong links between proteins and surfaces when a significant portion of charged surface domains are capable of strong electrostatic interaction with those on the protein ^{83,87}.

Smith et al., in their study ⁸⁸, found a relationship between protein adsorption and zeta potential. Zeta potential on Ti6Al4V was evaluated to increase during the suspension with bovin serum albumin supplemented physiologic saline increasing the electronegativity gap and promoting electrostatic interactions.

The presence of a superficial charge was evaluated to be influential on the orientation of the adsorbed proteins. Ngankam et al.⁸⁹ showed, using AFM, that bronectin has different orientations depending on the substrate with which it comes into contact.

In particular, fibronectin was found to adsorb perpendicularly onto a polyallylamine hydrochloride surface (positively charged) and parallel to a polystyrene sulfonic acid surface (negatively charged) (Fig. 22)⁸⁹.

4.1.2 Protein properties

- Protein structure

Proteins structure makes possible to distinguish them in “hard” and “soft” proteins. Hard proteins are characterized by having greater structural stability.

Protein stability is conferred thanks to the presence of hydrophobic groups (in the inner core) and hydrophilic groups (surface groups), the greater the internal hydrophobicity and the external hydrophilicity more stable will be the protein.

The more stable a protein the less it will be the predisposition of it to change its structural conformation to maximize energetically favorable interactions with the surface.

As a result, the hard proteins will bind to the surface slowly and with a weaker bond because they will not be able to structurally rearrange themselves and this is manifested by the maintenance of the tertiary structure.



In addition, larger proteins that possess larger contact area bind preferentially to surfaces compared to smaller proteins.

Generally, larger proteins are soft proteins such as fibrinogen and they are reported to adsorb strongly on hydrophilic surfaces⁸⁷.

Moreover, the stability of proteins depends on many other factors. Between these temperature (sufficiently high temperatures could bring to protein denaturation), pH (pH changes could modulate kinetics and thermodynamic behavior of adsorbed proteins as well as the structure in the adsorbed phase), ionic strength (dissolved ions may mask charges on protein surface interacting with electrostatic interactions) and concentrations⁸⁷.

- Conformational changes

The entropy gain derived from rearranging the protein structure and the hydrophobic behavior determine the conformational changes of protein structure on the surface resulting in the minimization of the interfacial free energy between the protein, surface, and solution.

A minimization of the energy of the system is observed through a modification of the conformation of the protein secondary structure (relaxation of alpha helices and increase in random coils).

Roach et al.⁹⁰ studied the albumin and fibrinogen adsorption on hydrophobic (CH₃ modified) and hydrophilic (OH modified) surfaces.

They used grazing angle infrared spectroscopy (GA-FTIR) to study the conformational state of proteins adsorbed on surfaces.

For both proteins it has been observed a less organized secondary structure following the interaction with the hydrophobic surface compared to the hydrophilic one, with a greatest effect observed for BSA.

The energy of the system, upon proteins interaction with the surface, is minimized. Proteins can rearrange themselves to a more stable position,



causing an increase in conformational entropy and a decrease in Gibbs free energy, which involves the formation of solid interactions.

When the surface is hydrophobic, adsorption is thought to be more energetically favorable as stated before.

It results that interaction of a protein with a hydrophobic surface is expected to be greater than toward a hydrophilic surface.

4.2 Instrumental analysis for evaluating adsorbed proteins

Since, as previously stated, the formation of a protein layer will determine the interaction of the surface with the external environment, it is necessary to study the characteristics of the adsorbed proteins such as quantity, conformation and orientation. For this purpose, different techniques have been used and adapted for the study of protein absorption.

4.2.1 Optical techniques

One of the most widely used optical techniques for the determination of adsorbed proteins is Surface Plasmon Resonance (SPR).

Surface plasmon resonance is a technique used to measure molecular interactions, often used in many standard tools for measuring adsorption of proteins on surfaces or nanoparticles.

It is based on the change of the refractive index on the surface of a sensor (stimulated by incident light) caused by an alteration related to the link between ligand and analyte and directly proportional to the mass linked to the biosensor.

SPR has emerged as a useful tool for evaluate protein adsorption mechanisms on a surface in real time and without the necessity for radiolabelling techniques.



This technique has been used for the evaluation the adsorption of different plasma proteins on both metal and polymeric surfaces by Green et al.⁹¹.

They used SPR on polystyrene surfaces to detect adsorption profiles for albumin, revealing the impact of protein concentration on both protein adsorption kinetics and the time for a monolayer coating generation. SPR data highlighted the influence of both surface chemistry and protein solution on the adsorption kinetics and thickness of the adsorbed layer.

Ellipsometry is another optical method for the evaluation of different surface properties mainly on reflecting metal surfaces. It is based on the measure of the change of polarization of light as a result of the interaction between the radiation and the surface of the material (reflection or transmission) and its comparison with a model (Fig. 23).

It can be used to investigate surface properties like presence of coatings or films, and various aspects of protein adsorption⁹².

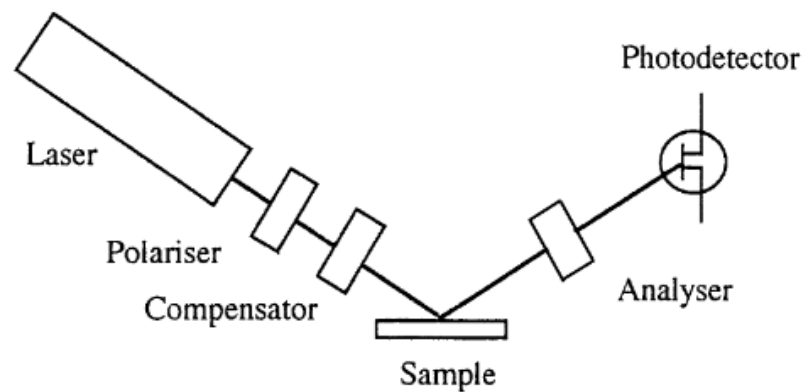


Fig. 23. Principle of ellipsometer.⁹²

4.2.2 Spectroscopic techniques

Differently from optical techniques, spectroscopic methods are based on the interaction of photons with some parts of the adsorbed protein molecules.



The output spectroscopic signals as the interaction spectra can be related to the amount of proteins adsorbed on the surface and to information on their conformation and orientation.

Examples from this category of techniques are infrared spectroscopy (IR) and x-ray photoelectron spectroscopy (XPS).

XPS is a technique used to obtain quantitative information about the chemical surface composition of a sample.

The sample, put under vacuum, is irradiated through x-rays.

The interaction between the radiation and the sample causes some phenomenon like the emission of the electron from the atom if the photon energy is greater than the electron binding energy.

The emitted photoelectrons are analyzed by a detector based on their kinetic energy (KE).

The flow of photoelectrons emitted from the surface following irradiation can be attenuated by the presence of a layer on the surface as can be that of the adsorbed proteins. The degree of attenuation is related to the thickness and the layer coverage rate⁹³.

4.2.3 Microscopic techniques

Microscopy techniques are commonly used for the observation of surfaces. Among these the most used is atomic force microscopy (AFM). Through this technique it is possible to obtain images of surfaces through contact and interaction between a physical probe and the sample⁹⁴.

Truong et al.⁹⁵ studied adsorbed protein conformation or orientation through scanning force microscopy (SFM).

They functionalized gold substrates with methyl- and carboxylate terminated alkane thiolate monolayers to detect the action of each functional group on bovine fibrinogen (BFG) adsorption.

SFM images detected variations of BFG adsorption on the different functional groups and, in addition, a contrast in the friction images was



observed and related to BFG orientation and conformation induced by methyl and carboxylate functional groups.

4.2.4 Spectrometric techniques

Time-of-flight secondary ion mass spectrometry (ToF-SIMS) is a technique employed to analyze complex biological systems, including proteins adsorbed and their conformation on surfaces.

In this technique, a sample is bombarded with high energy primary ions, which energy is transferred to the surface resulting in the ejection of different molecular fragments^{93,96}.

The secondary ions created by the collision are evaluated by a mass analyzer, in this case time of flight analyzer (ToF).

Flight time is dependent on the fragment mass (smaller species move faster) and it is possible to obtain a mass spectrum characterized by peaks.

Determining fragmentation patterns for each protein, the protein concentration on a substrate could be identified.

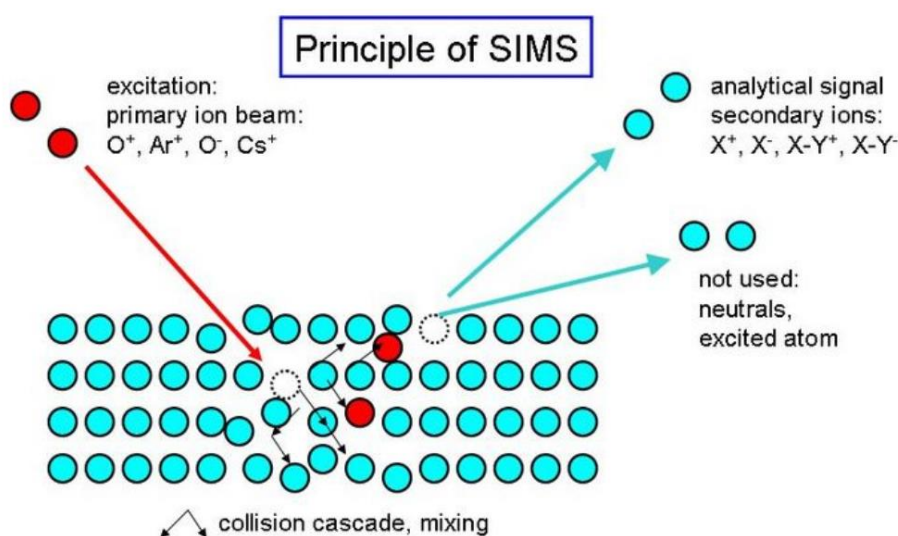


Fig.24. Principle of SIMS.⁹⁶



The relative amount of proteins, since the technique investigates only a surface depth of 2-3 nm (thickness lower than that of the surface protein layer), can be related to the protein orientations and conformations⁹³.

4.3 Influence of adsorbed proteins

The formation of a protein layer on biomaterials surfaces due to adsorption phenomenon avoids the direct contact of the material with the biological ambient and minimizes adverse effects.

Despite this, the protein adsorption could be also a problem because it may interfere with some behaviors such as the release of antimicrobial agents (antibiotics, antimicrobial metal elements) from implants as a solution to the problem of post-surgical infections.

The molecular mechanism of antibacterial toxicity of silver ions is related with their bond with structural and functional proteins.

The connection between silver ions and protein groups, especially thiol groups (-SH), is essential for silver ions antimicrobial activity resulting in inhibition of respiratory chain proteins that alter the ROS production inside the cell leading to oxidative stress and cell damage and death⁹⁷. On the other hand, the formation of insoluble precipitates such as silver chloride (AgCl) or interaction with other proteins (e.g., BSA) has been reported to limit and decrease the antibacterial activity of silver ions⁹⁸.

Sakthivel et al. studied gelatin-AgHAp composite and the influence of silver ions concentration on protein adsorption and biocompatibility (hemolysis).

They investigated protein adsorption founding that it decreases with the increase of silver ions concentration. A minimum amount of silver (150 µg/L) was found to cause an improved BSA adsorption.

The growth in the amount of silver causes the increase in the ionic strength diminishing the surface charge and consequently the protein-surface interaction.



In another study was also investigated BSA adsorption on plasma-deposited silver nanocomposite thin films⁹⁹. Silver release was observed before and after the incubation with protein solution. They found that BSA adsorb preferentially on silver treated surfaces and in addition was shown as BSA coating limits the silver release.

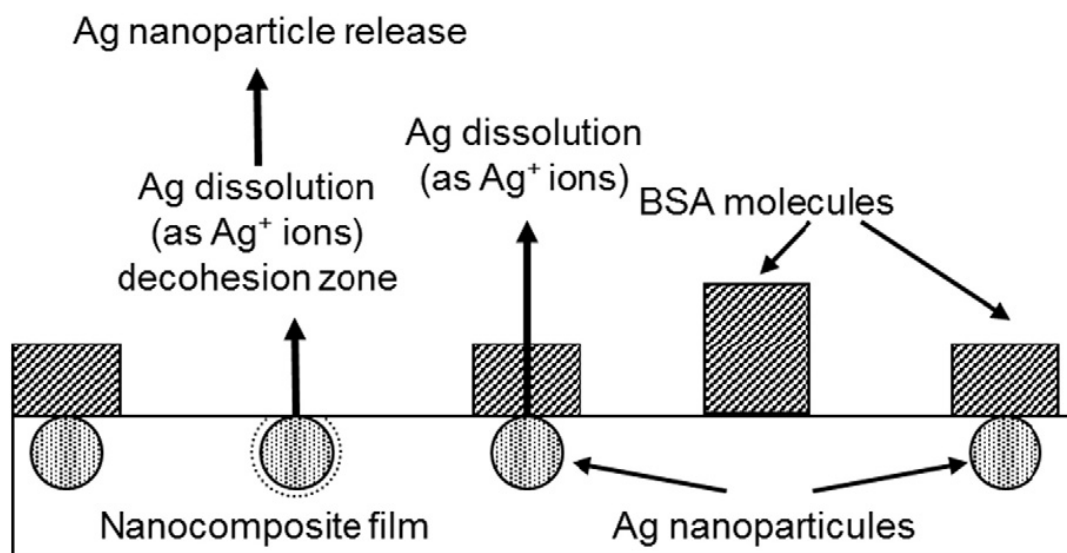


Fig. 25. Mechanisms proposed for silver release/dissolution in the case of surface covered with a discontinuous layer of BSA.⁹⁹

The scheme in fig.25 represents the mechanisms of silver release from the film covered by BSA in a discontinuous layer.

Since BSA preferentially adsorbs on silver instead of on the polymer, it was reported a blocking effect of the protein on silver nanoparticles release into the surrounding environment.

Despite this, the release of silver ions continues to take place. Some nanoparticles, being the protein layer discontinuous, are not covered, in these it can be observed a phenomenon of dissolution and ionic release starting from the outside of the nanoparticle through the formation of a decohesion zone at the interface.



In contrast, BSA adsorption on silver surfaces was evaluated to increase silver release in pH neutral aqueous solutions¹⁰⁰.

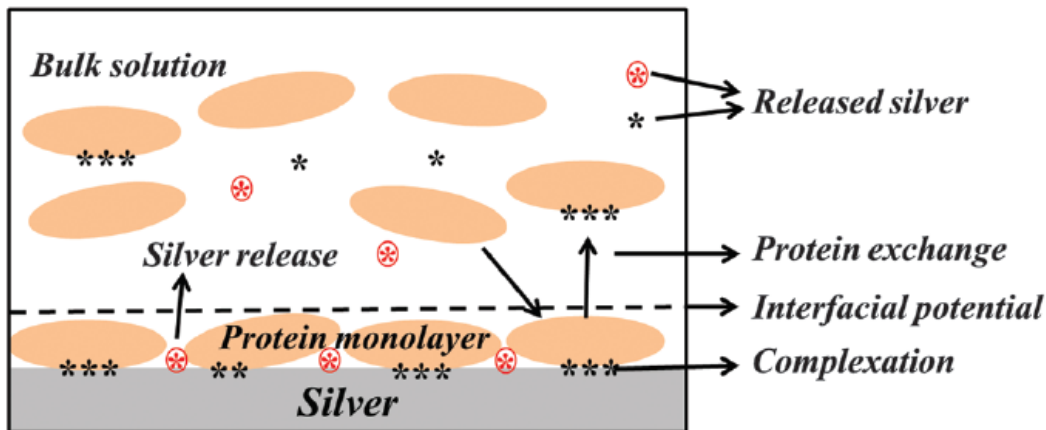


Fig.26. Mechanisms of silver release from silver surfaces in the presence of BSA in pH neutral aqueous solutions.¹⁰⁰

Different mechanisms of enhanced silver release are shown by Wang et al.¹⁰⁰ (Fig. 26).

The structure of adsorbed BSA (affected by low conformational changes) on the surface and the presence of BSA molecules in solution have been indicated as properties influencing the effect of BSA on silver release.

Especially, the increased release is attributed to the generation of BSA-silver complexes formed on the surface following the absorption of BSA (electrostatic interactions) and the subsequent exchanges process between the complexes and the proteins in solution leading to an enhanced amount of silver in solution.

The properties of the protein absorbed on the surface are fundamental. For example, lysozyme (LSZ) adsorption on silver has been studied resulting in an inhibition of silver release¹⁰¹. This can be explained by the interfacial potential of the adsorbed protein layer, positively charged LSZ adsorbs on the surface strongly reducing silver release due to the



electrostatic repulsion between the positively charged silver ions and LSZ.

In conclusion, depending on the material properties (charge, surface properties) and the type of protein (physico-chemical conditions, charge, conformation) the release of metals from biomaterials can be either enhanced or inhibited.



5 MATERIALS AND METHODS

5.1 Samples preparation

Ti6Al4V alloy (ASTM B348, Gr 5, Titanium Consulting and Trading) was used for this thesis work. Ti6Al4V is a high strength α/β alloy commonly used in orthopedic, craniofacial and dental applications. The specimens in the form of disks of about 2 mm thickness and 10 mm in diameter were obtained from the cutting of cylindrical bars. The cut was performed using an automatic cutter (ATM Brillant 220 (Fig. 27)) provided with an alumina blade (356 CA) suitable for metal cutting, speed was set at 0.020 mm/s in horizontal cutting mode. In this way 62 Ti6Al4V specimens were obtained.



Fig. 27. ATM Brillant 220 automatic cutter.

The samples obtained from the cut were subsequently polished (Table 5). The polishing process was accomplished by means of a polishing machine model Struers "LaboPol-2" using SiC abrasive papers.

In a first polishing step was used an abrasive paper with grain 120 on both sides of the samples allowing to remove the evident signs of cutting and imperfections on the disks.

Number of polished samples	Polishing steps
57 samples	<ul style="list-style-type: none"> • Up to 120 grit on one side. • Up to 500 grit on the other side.
5 samples (mirror polished)	<ul style="list-style-type: none"> • Up to 120 grit on one side. • Up to 4000 grit on the other side and final finishing with a colloidal silica suspension.

Table 5. Polishing protocol.

Subsequently by means of an electric pen one side of the samples was marked with a number.

The following polishing steps have been carried out on the unmarked side with abrasive sandpapers of grit 320 and 500 for 57 samples (Fig. 28). The remaining 5 were mirror polished (Fig. 29) using in sequence abrasive papers with grit 320, 500, 600, 800, 1000, 2500 and 4000 and a colloidal silica suspension (colloidal silica 0.04 μm and distilled water) for surface finishing.

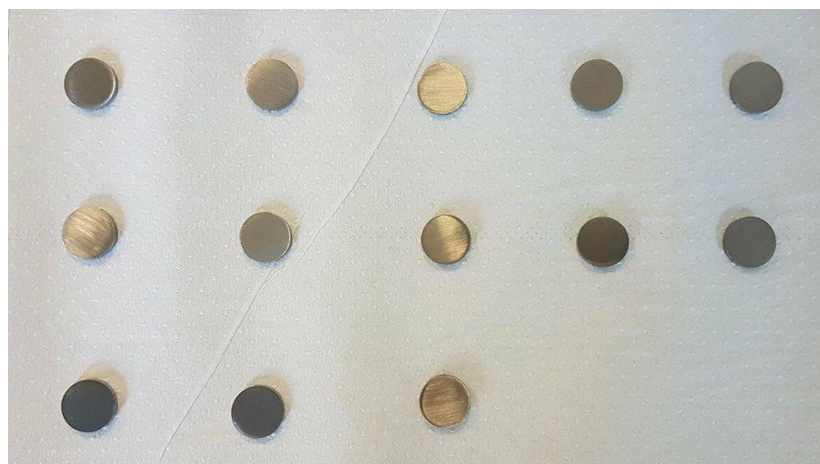


Fig. 28. Some of the samples polished up to 500 grit on one side.



Fig. 29. Mirror poished samples.

All samples in the end have been washed in ultrasonic bath with the purpose of removing any contaminations introduced on the surfaces.

By means of ultrasounds, by the transmission of vibratory effects, it is possible to quickly remove the most tenacious and resistant deposits and impurities accumulated during the processing previously carried out.

The instrument used is the ultrasonic bath Sonica 2400 ETH S3 (Fig. 30).

Each sample has been subjected to 3 washes, first in acetone for 5 min. and then two washes in distilled water for 10 min.



Fig. 30. Sonica 2400 ETH S3.

Once the ultrasonic bath is completed the samples were placed to dry in the hood under laminar flux and finally packed for subsequent superficial treatments.

5.2 Surface treatments

Surface modifications have been carried out on the samples with the aim of giving the titanium alloy a nanostructured surface enriched with hydroxide groups, and bioactive and antibacterial behavior.

The surface modifications were carried out following a patented thermo-chemical process¹⁰².

The process consists of a first acid etching through which the removal of the native oxide layer is achieved, and a subsequent controlled oxidation. The antibacterial properties are conferred by the addition of the antibacterial agent, in this case silver, within the reformed oxide layer¹⁰³.

The first 25 samples were treated without the addition of the antibacterial agent.

Each sample was initially acid etched in diluted hydrofluoric acid, the acid-on-surface attack ensures the dissolution and removal of the natural surface oxide.

Subsequently, the samples were immersed in hydrogen peroxide at 60°C thermostatic bath (Julabo, SW23) with 120 rpm shaking.

Finally the samples were removed and allowed to dry in the hood under laminar flow.

For the other samples the controlled oxidation process was done with the addition of a silver nitrate solution (AgNO_3 , Silver Nitrate PA-ACS-ISO 131459,1611, Panreac) in hydrogen peroxide at a half of the treatment. Simultaneously, gallic acid (GA, 0.1 g/l), a stabilizing agent, and polyvinylalcohol (PVA, 0.1 g/l), a reducing agents, were added to



control silver nanoparticles size, distribution and ion release. The final concentrations were, respectively, 0.1 g/l and 0.01 g/l.

Silver nitrate was added in order to reach a concentration of 0.001M, which in a previous research was found to be a concentration not capable of causing cytotoxic effects ¹⁰³.

Also were provided by the Politecnico di Torino for this research further 12 samples treated with a greater concentration of silver (0.005M), for comparison purposes.

The solvent for all treatments above was ultrapure water.

After the treatment all samples were placed in the laminar flux hood for drying and were finally packed in closed plastic bags.

Table shows all the samples prepared and available for this thesis work.

The preparation and treatments of all the samples (Fig. 31) were carried out in the laboratories at the Politecnico di Torino.

Nome campioni	Numero
Ti6Al4V-CT	25
Ti6Al4V-CT + Ag (0.001M)	32
Ti6Al4V-MP	5
Ti6Al4V-CT + Ag (0.005M)	12

Table 6. All samples available for this research.



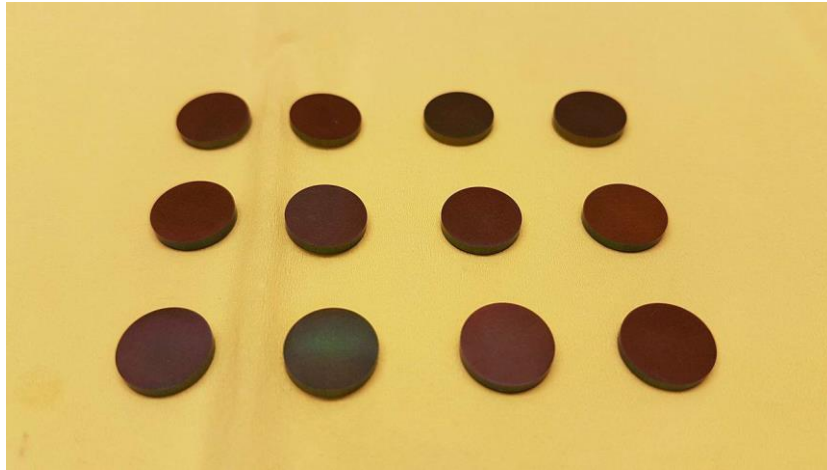


Fig. 31. Some samples after the surface treatments.

5.3 Samples characterization

The morphological characteristics of selected samples were examined by means of a scanning electron microscope (SEM, PHILIPS XL30ESEM) equipped with Energy Dispersive X-ray Spectroscopy (EDS, X-MAX Oxford instruments, 20 mm² detect.) in order to evaluate surface compositional information.

Four samples were observed: Ti6Al4V-MP, Ti6Al4V-CT, Ti6Al4V-CT + Ag (0.001M) and Ti6Al4V-CT + Ag (0.005M).

The SEM instrument uses a high-energy primary electron beam focused on the sample through a lens system, the beam is driven sequentially on a small area.

The interaction between the beam and the atoms constituting the surface allows the emission of different signals, among these the secondary electrons, the back scattered electrons and the characteristic x-rays, which are collected and analyzed by a series of detectors each sensitive to a particular signal so that they can be processed images and data¹⁰⁴ (Fig. 32).

These signals give us morphological and chemical informations.

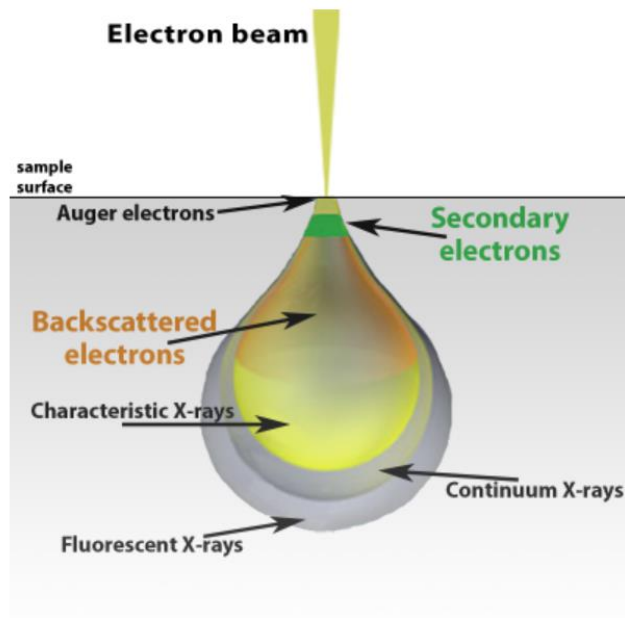


Fig. 32. Schematic representation of the signals emitted from the surface affected by the electron beam.¹⁰⁴

The secondary electrons (SE) have low energy (few eV) and represent the most frequently used signal. They are generated when an electron of the beam raises an electron from an atom on the surface of the sample and, commonly, give high-resolution topographical information. The back scattered electrons (BE) are generated by the elastic scattering of electrons bouncing back from the sample without crossing it. They have a high energy (1-50 KeV) and therefore come from deeper areas.

They are detected to obtain information about the relative atomic density along with information about the topography of the samples ¹⁰⁵. The SEM allows to obtain also an EDS microanalysis, analytical technique for the chemical characterization of a sample.

The technique is based on the detection of the characteristic x-rays that the electrons emit when collide with different atoms.



5.4 Exposure plan

All the available samples, in order to evaluate the release of metal ions, were subjected to a plan of exposure in different physiological simulated solutions mainly consisting of phosphate buffered saline (PBS) with the addition of variable concentrations of hydrogen peroxide (H_2O_2), to simulate inflammation condition, and albumin (BSA) which is one of the most present protein in the blood, to evaluate the effect of proteins on ions release.

Prior to exposure, all vessels and equipment in contact with the solutions were acid-cleaned in 10% HNO_3 , for at least 24 h, rinsed 4 times with ultrapure water (18.2 $M\Omega cm$, Millipore, Sweden) and then dried in ambient laboratory air.

All disks were positioned, with the entire surface area exposed, in 15 ml polyethylene vessels keeping the surface area to solution volume ratio constant at 1 cm^2/ml (Fig. 33).

Depending on the available specimens, a different number of samples and one blank sample (no metal disk) were exposed in parallel for each specimen type, time period and solution.



Fig. 33. Polyethylene vessels used for disks exposition.

All exposures were conducted at 37 °C +/- 0.5 °C, at dark condition and bilinear shaking (12° inclination, 22 cycles/minute) for two different time periods (4h and 336h) (Table 7).

After exposure, all samples were removed from the solutions, rinsed with 0.5 mL of ultrapure water, dried with nitrogen gas (N₂), and stored in a desiccator prior to surface analysis.

The test solutions and the 0.5 mL of ultrapure rinsing water (as this probably contains precipitated metals and proteins), were combined. Subsequently, the solution was centrifuged (Eppendorf MiniSpin microcentrifuge in Fig. 34, 30 min, 13400 r.p.m.), separated into supernatant and remaining solution (0.75 mL and 1 mL), and stored at -20 °C.

The remaining (non-supernatant) solution was also investigated in addition to the particle-free supernatant, since possible released silver nanoparticles and precipitated metals/proteins were expected in that solution.



Fig. 34. Eppendorf minispin microcentrifuge



5.5 Simulated physiological fluids

Physiological solutions were based on phosphate buffered saline (PBS) with varying hydrogen peroxide (H_2O_2 , Sigma Aldrich, Sweden) and bovine serum albumin (BSA, A7906, Sigma Aldrich) concentrations.

Three simulated biological fluids were used:

- PBS with 10 μM H_2O_2 and 40 g/L BSA (PBS+10 μM H₂O₂+BSA),
- PBS with 30 mM H_2O_2 and 40 g/L BSA (PBS+30mMH₂O₂+BSA),
- PBS with 30 mM H_2O_2 (PBS+30mMH₂O₂).

Phosphate buffered saline (PBS) was composed of 8.77 g/L NaCl, 1.28 g/L Na_2HPO_4 , 1.36 g/L KH_2PO_4 in ultrapure water, and its pH was adjusted to 7.2-7.4 with 50% NaOH.

After exposure, pH changes of less than 0.25 pH were measured as compared to the initial pH.

An amount of about 40 g/L BSA was selected because relevant for human blood¹⁰⁶, 10 μM hydrogen peroxide has been suggested to be physiologically relevant at inflammatory conditions¹⁰⁷.

A 30 mM hydrogen peroxide concentration was also selected because macrophages and neutrophils can induce very oxidative conditions¹⁰⁸, which could imply that a high redox potential, like that induced by intermediate or high hydrogen peroxide concentrations, could be physiologically relevant.

All chemical used were of analytical grade (p.a.) or puriss p.a. (hydrogen peroxide).

Solution	Exposure times
1. PBS + 10 μM H_2O_2 + 40 g/l BSA	4h, 336h
2. PBS + 30mM H_2O_2 + 40 g/l BSA	4h, 336h
3. PBS + 30mM H_2O_2	4h, 336h

Table 7. Solutions used for the exposure and related exposure times



5.6 UV Digestion

Prior to the solutions analysis by means of graphite furnace atomic absorption spectroscopy (GF-AAS) all solutions were digested in order to avoid silver precipitation and protein aggregation, ensuring accurate trace metal analysis.

Unfrozen solutions were digested by adding 0.5 mL of 30% H₂O₂, 0.15 mL of 30% HCl and about 8 mL ultrapure water to 0.75 mL of solution sample and by means of a Metrohm 705 UV digester (Fig. 35) for about 1 h at 90 °C until the solution was transparent and odorless.

After the digestion process, the final volume of all solutions was measured and the dilution factor calculated (final volume after digestion divided by the initial solution volume).

The digestion process is performed to obtain the UV photolysis of liquid samples inside which there is a certain amount of organic component.



Fig. 35. Metrohm 705 UV Digester

This method allows the elimination of dissolved organic matter (DOM) that interferes in the trace analysis of heavy metals, as in the case of AAS.

5.7 Photon cross-correlation spectroscopy (PCCS)

Photon cross-correlation spectroscopy (PCCS, NanoPhox, Sympatec in Fig. 36) dynamic light scattering was used to investigate the particle size distribution in the supernatant and non-supernatant solutions.

For these measurements, non-digested unfrozen solutions were tested. Each sample was measured with two replicate measurements of 120 s. First tests showed that 0.2 μm membrane (PTFE) filtering lowered the particle concentration to undetectable levels, why all solutions were first measured without filtering, and only in some cases (where some large particles were present) reanalyzed after filtering. If the correlation function was acceptable (good fitting and no positive values at long lag times), a non-negative least square (NNLS) algorithm was used by the instrument to determine the intensity size distribution.

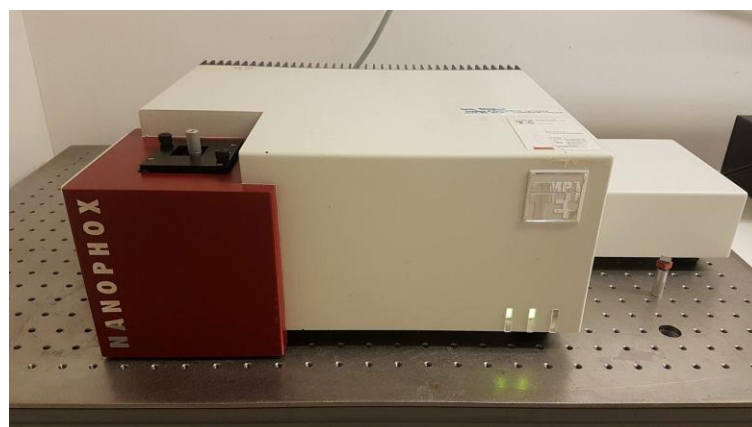


Fig.36. PCCS, NanoPhox, Sympatec

5.8 Grafite furnace Atomic Absorption spectroscopy

Atomic Absorption Spectrometry (AAS) is a technique for measuring amounts of metal elements present in solution samples by measuring the absorbed radiation by the element of interest.

The released amounts of metals from disks in contact with the simulated physiological solutions were analyzed by means of graphite furnace atomic absorption spectroscopy (GF-AAS) using a Perkin Elmer AAnalyst 800 instrument (Fig. 37).

Titanium (Ti), aluminium (Al), vanadium (V) and silver (Ag) concentrations ($\mu\text{g/L}$) were determined using calibration curves based on 0 (1% HNO_3), 10, 30, 60 and 80 $\mu\text{g/L}$ for Ti; 0, 30, 60 and 100 $\mu\text{g/L}$ for Al; 0, 10, 30, 80, 120 $\mu\text{g/L}$ for V and 0, 7.5, 15, 30, 45 $\mu\text{g/L}$ for Ag.

Every 4-5 samples, quality control samples of known concentration were analyzed. For each solution sample, three measurements were conducted.

The released metal content in solution ($\mu\text{g/cm}^2$) was determined as follows:

$$Me_{aq} = \frac{\left((c_{sample,s} \left(\frac{\mu\text{g}}{\text{L}} \right) - c_{blank,s} \left(\frac{\mu\text{g}}{\text{L}} \right)) * DF + (c_{sample,n} \left(\frac{\mu\text{g}}{\text{L}} \right) - c_{blank,n} \left(\frac{\mu\text{g}}{\text{L}} \right)) * DF \right) * V \text{ (L)}}{A \text{ (cm}^2\text{)}}$$

Where $c_{sample,s}$ is the concentration of the supernatant measured by AAS, $c_{sample,n}$ is the concentration of the non-supernatant, $c_{blank,s}$ and $c_{blank,n}$ are the corresponding blank concentrations (amount of metal ions revealed into the solution exposed without samples), V is the exposure volume (0.0015 L), A is the sample surface area (1.57 cm^2) and DF is the dilution factor calculated after the UV digestion process.



Furthermore, the supernatant and non-supernatant concentrations are compared by normalizing to the dilution factor and subtracting the corresponding blank value according to:

$$\left(c_{sample,s/n} \left(\frac{\mu g}{L} \right) - c_{blank,s/n} \left(\frac{\mu g}{L} \right) \right) * DF$$



Fig.37. GF-AAS Perkin Elmer AAnalyst 800

5.9 X-ray photoelectron spectroscopy (XPS)

XPS spectra were recorded using a Kratos AXIS UltraDLD X-ray photoelectron spectrometer (Kratos Analytical, Manchester, UK in Fig. 38) using a monochromatic Al x-ray source (1486.6 eV) operated at 300W on not exposed disks and on exposed disks for each solution and exposure time.

The analyzed areas were smaller than 1 mm² (most of the signal originates from an area of 700 × 300 μm²) collecting overview spectra and detailed high resolution spectra (20 eV) of C 1s, O 1s, etc.



The elemental peak positions on the binding energy scale provide information about the chemical state. The hydrocarbon peak at 285.0 eV was used as internal standard.

XPS is a spectroscopic technique based on the photoelectric effect: a sample, invested by an electromagnetic radiation having energy ($E = h\nu$) in the X-ray range, emits electrons from the most internal energy levels.

The electrons contained in the atoms of the material are found on energy levels (orbitals) characterized by a precise binding energy (BE), which can be determined by measuring the kinetic energy (KE) of the photoemitted electrons.

The binding energy of the electrons of a given atom is related to the chemical element to which they belong and from their energy level so by analyzing the spectrum of the photoemitted electrons it is possible to determine the elements forming the material.

5.10 In vitro bioactivity

Two of the available samples were used to analyze in vitro bioactivity. They were immersed in simulated body fluid (SBF) for two and four weeks respectively and incubated in an incubator at 37 °C.

SBF is a solution composed of an ionic concentration similar to that of human plasma and was prepared following the protocol described by Kokubo¹⁰⁹ (Table 8).

After each week of exposition the solution was refreshed to mimic the physiological exchange of body fluids and the solution pH measured.

At the end of the exposure the samples were rinsed with ultrapure water and have been observed at FE-SEM to evaluate the possible growth of hydroxyapatite on the surface.

Since the main mineral component of the bone is hydroxyapatite, the formation of a superficial layer of apatite is of fundamental importance



for an artificial material that must bind to the bone tissue after implantation. Soaking a sample in SBF it is possible to study in vitro the possible growth of a superficial layer of apatite and, therefore, to predict what the bioactivity will be in vivo. In fact, when a biomaterial is immersed in SBF, the calcium and phosphorus originally within the solution give rise to the precipitation of apatite nuclei which then grow on the surface of the material¹⁰⁹.

Reagents for 1L SBF	
NaCl	8.035g
NaHCO ₃	0.355g
KCl	0.255g
K ₂ HPO ₄ ·3H ₂ O	0.231g
MgCl ₂ ·6H ₂ O	0.311g
1M-HCl	39ml
CaCl ₂	0.292g
Na ₂ SO ₄	0.072g
TRIS	6.118g
1M-HCl	0-5ml

Table 8. Reagents used to prepare 1L SBF. ¹⁰⁹

5.11 Zeta potential measurements

The zeta potential, also defined as an electrochemical potential, is used for the characterization at the solid-liquid interface, in fact the electric charge on the surface is one of the factors influencing the interaction between biomaterials and the biological environment and consequently can take part to the evolution of the tissue around the implant.



The surface of a solid material, in contact with water based media (such as biological fluids), leads to the formation of an electronic double layer at the solid-liquid interface.

It is initially observed the formation of an absorbed layer of charges opposite to the surface charge called “stationary layer” which attracts other mobile charges which form the so-called “stern layer” (Fig. 38).

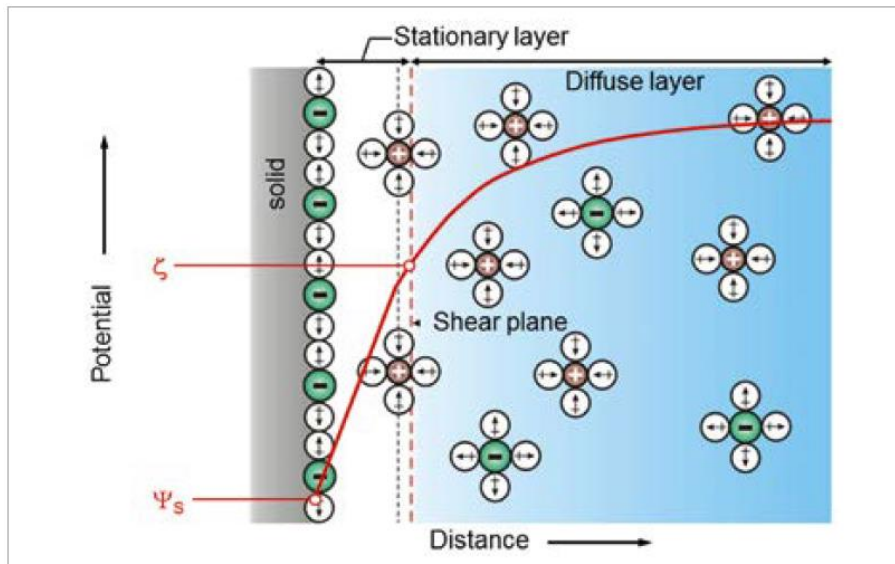


Fig. 38. Schematization of the formation of the double layer on material surface. ¹⁰⁶

The zeta potential is defined as the potential at the boundary between the stationary layer and the stern layer (shear plane).

The streaming potential technique has been used for the determination of the isoelectric point (PI) and of the zeta potential as a function of the pH in the present research.

An electrokinetic analyzer for solid surfaces (SurPASS, Anton Paar) was employed at this purpose (Fig. 39).

The technique is based on the passage of a flow of aqueous solution into a capillary system obtaining an electronic response evaluated as a dc voltage¹¹⁰ (Fig. 40).





Fig.39. SurPASS Anton Paar analyzer.

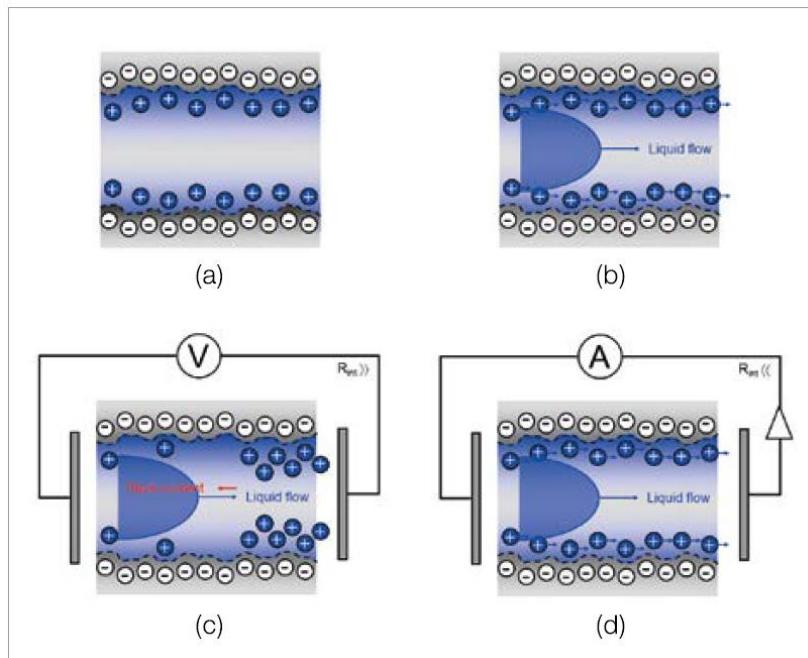


Fig. 40. Generation of the streaming potential and streaming current. ¹⁰⁶



6 RESULTS AND DISCUSSION

6.1 Scanning electron microscopy (SEM)

SEM measurements have been carried out in order to characterize the surface of the samples. Each type of sample (Ti6Al4V-MP, Ti6Al4V-CT, Ti6Al4V-CT + Ag 0.001M, Ti6Al4V-CT + Ag 0.005M) have been observed and, in parallel, the EDS analysis was performed to show the superficial elemental composition (wt%).

6.1.1 Ti6Al4V-MP

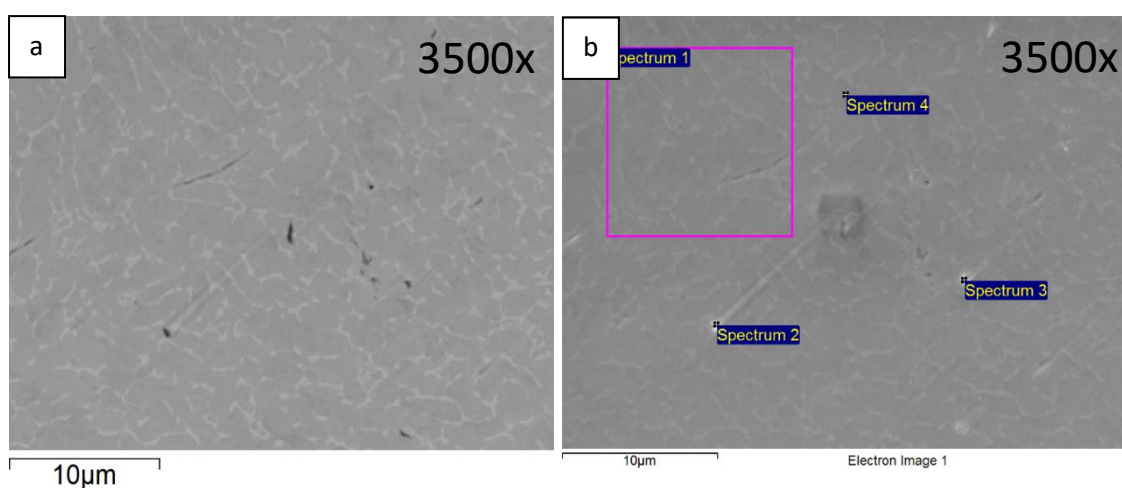


Fig. 41. SEM images of Ti6Al4V-MP.

Spectrum	C	N	Al	Si	Ti	V
Spectrum 1	1.61	0.00	6.57	0.00	88.36	3.46
Spectrum 2	2.91	0.00	4.32	3.05	83.48	6.24
Spectrum 3	2.62	0.00	4.98	1.01	83.80	7.59
Spectrum 4	1.79	0.00	6.86	0.00	91.35	0.00
Mean	2.23	0.00	5.69	1.01	86.75	4.32
Std. deviation	0.63	0.00	1.23	1.44	3.79	3.36

Table 9. EDS analysis of Ti6Al4V-MP.

The Ti6Al4V-MP (Fig. 41) and Ti6Al4V-CT (Fig. 42) samples are as expected.

On Ti6Al4V-MP samples points having silicon impurities have been identified.

The presence of these impurities is probably due to the polishing process obtained through the use of SiC abrasive papers and the colloidal silica suspension in the finishing process for mirror polishing.

6.1.2 Ti6Al4V-CT

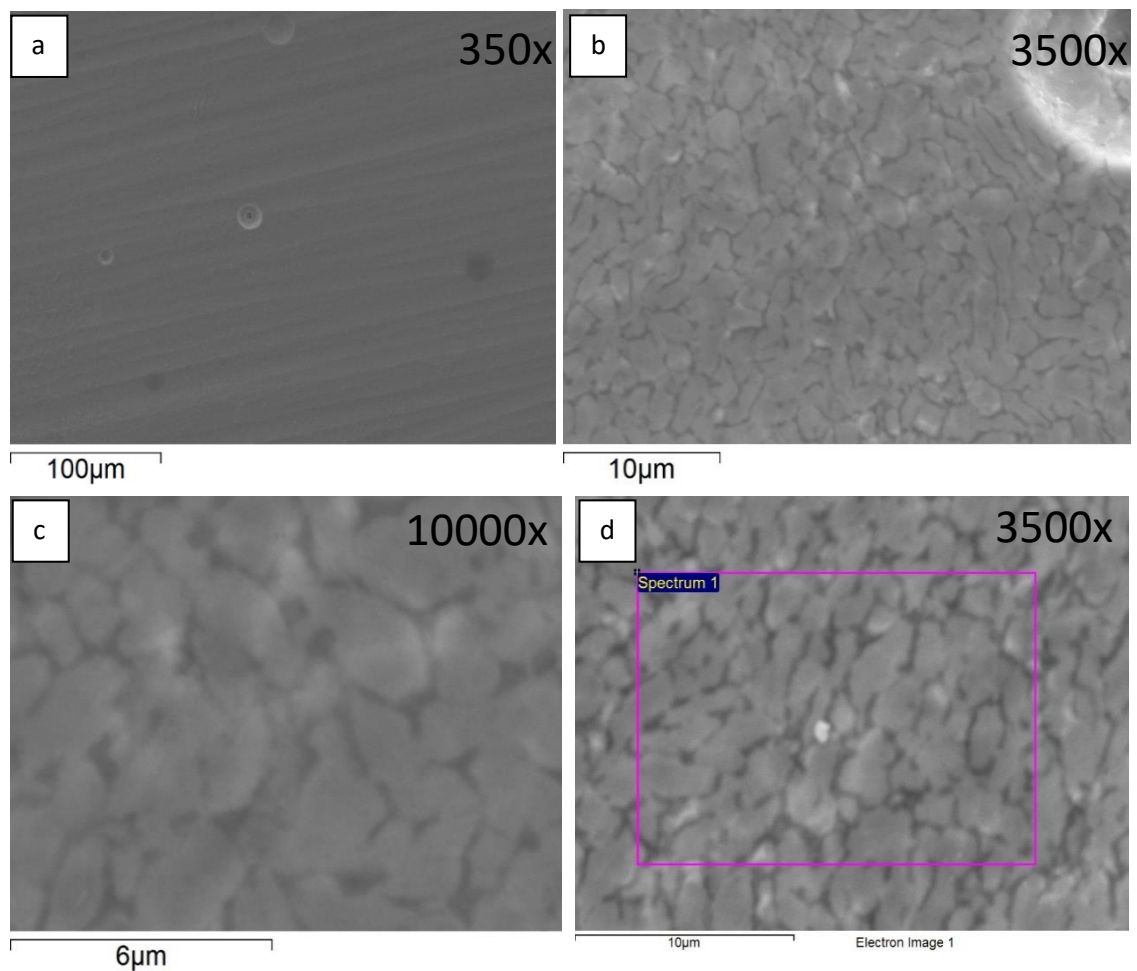


Fig. 42. SEM images of Ti6Al4V-CT.



Spectrum	C	O	Al	Ti	V
Spectrum 1	1.81	30.81	3.81	61.89	1.68

Table 10. EDS analysis of Ti6Al4V-CT relative to the area in fig. 42d

6.1.3 Ti6Al4V-CT + Ag (0.001m)

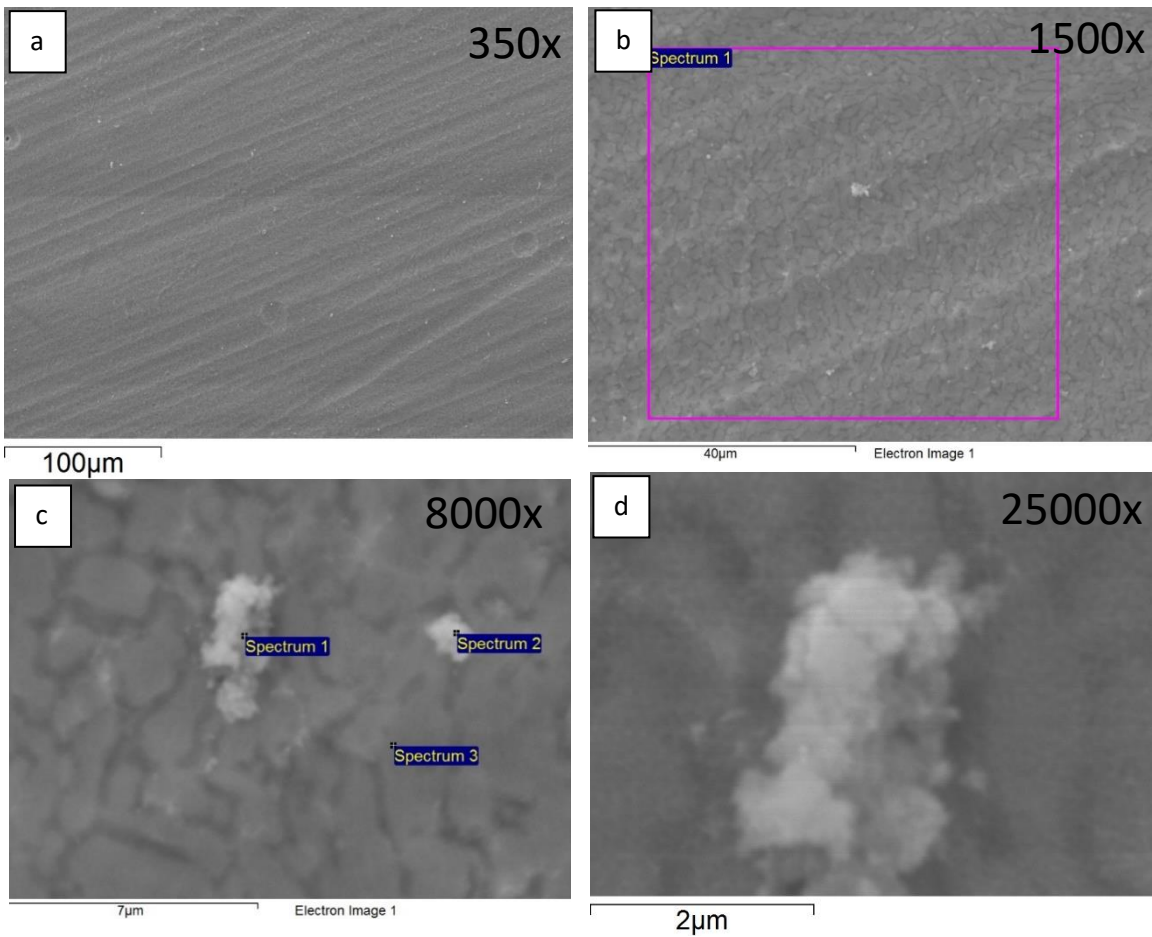


Fig. 43. SEM images of Ti6Al4V-CT + Ag (0.001M).

Spectrum	C	O	Al	Ti	V	Ag
Spectrum 1	3.32	31.53	3.56	58.88	2.00	0.71

Table 11. EDS analysis of Ti6Al4V-CT + Ag (0.001M) relative to area in fig. 43b.



Spectrum	C	O	Al	Ti	V	Fe	Ag
Spectrum 1	3.19	38.55	3.11	51.57	1.21	0.36	2.01
Spectrum 2	3.59	46.57	3.05	43.73	1.12	0.23	1.70
Spectrum 3	2.21	27.50	4.06	63.98	1.48	0.16	0.62
Mean	3.00	37.54	3.41	53.10	1.27	0.25	1.44
Std. deviation	0.71	9.58	0.56	10.21	0.19	0.10	0.73

Table 12. EDS analysis of Ti6Al4V-CT + Ag (0.001M) relative to fig. 43c.

6.1.4 Ti6Al4V-CT + Ag (0.005m)

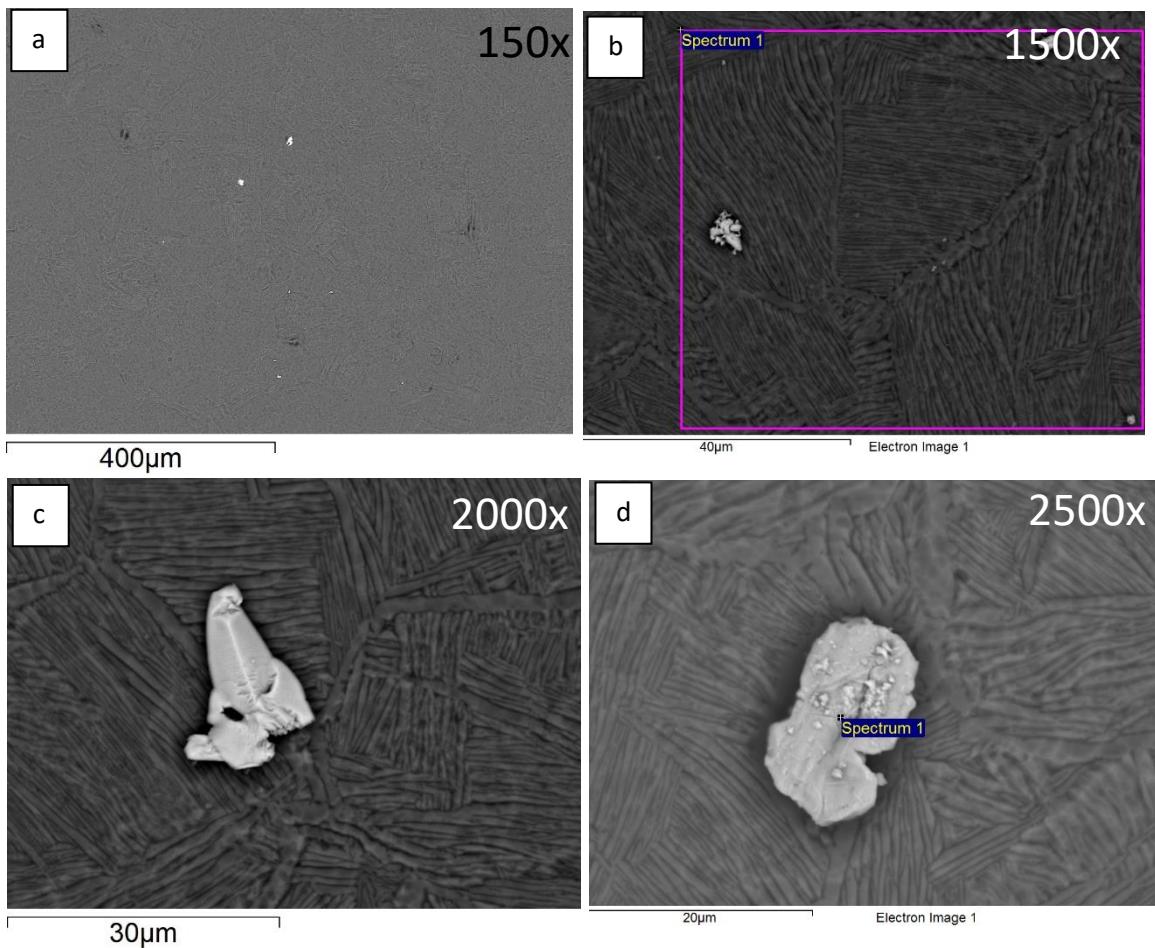


Fig. 44. SEM images of Ti6Al4V-CT + Ag (0.005M).

Spectrum	C	O	S	Ti	Ag
Spectrum 1	28.31	10.93	3.30	2.96	54.49
Mean	28.31	10.93	3.30	2.96	54.49
Std. deviation	0.00	0.00	0.00	0.00	0.00

Table 13. EDS analysis of Ti6Al4V-CT + Ag (0.001M) relative to area in fig. 44b.

Spectrum	C	O	Al	Ti	V	Ag
Spectrum 1	3.21	29.00	3.66	60.44	1.83	1.86

Table 14. EDS analysis of Ti6Al4V-CT + Ag (0.005M) relative to fig. 44d.

On silver-treated samples (Fig. 43, Fig. 44, Fig. 45) it is possible to notice the formation of silver particles (10-50 nm) (Fig. 45) which are lighter and brighter than the sample surface. They seem to be strictly bonded to the superficial oxide because they are present after the washing of the samples at the end of treatment.

The formation of the particles takes place by the reduction of the silver nitrate (AgNO_3) induced by the hydrogen peroxide (H_2O_2) which causes the precipitation of silver crystals of different dimensions.

Moreover, large precipitates (10-50 μm) containing a high quantity of silver can be seen (Fig. 44c). These crystals are possibly derived from pre-existent carbon impurities in which the precipitation of silver is concentrated.

The EDS analyzes performed on areas of about $60 \times 60 \mu\text{m}^2$ measured percentages in weight (wt%) of silver on the two treated samples



(Ti6Al4V-CT + Ag 0.001M and Ti6Al4V-CT + Ag 0.005M) respectively of 0.70% and 1.86%.

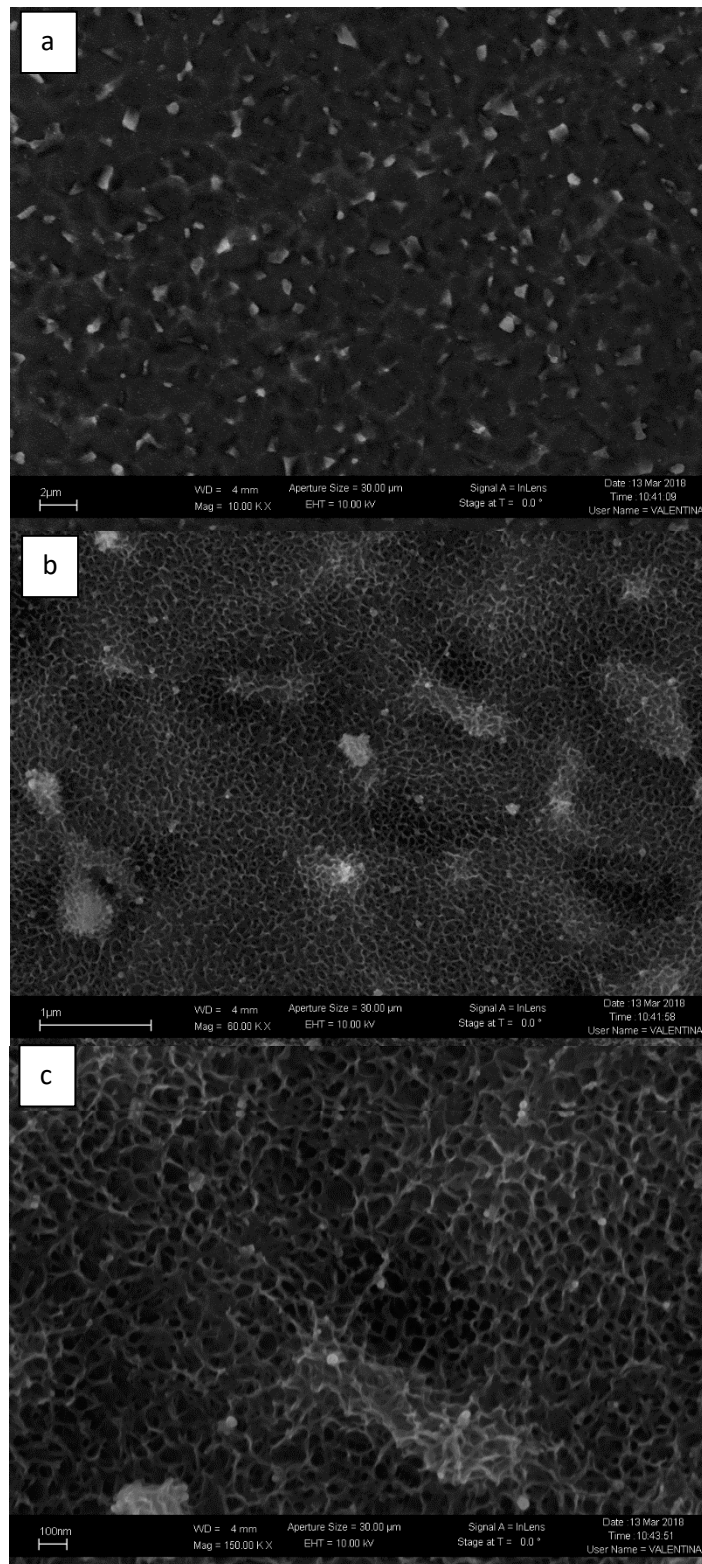


Fig. 45. FE-SEM images of Ti6Al4V-CT + Ag (0.001M) prior to SBF exposure, a) 10000x, b) 60000x, c) 150000x.



From the observation of the samples it is possible to identify the presence of a nanostructure on the surface (Fig. 45c).

This is due to the method used for the treatment (acid etching and immersion in H_2O_2) and is of considerable importance for the behavior of the material since it is essential for its bioactivity.

6.2 Photon cross-correlation spectroscopy (PCCS)

In order to identify the presence of silver nanoparticles or precipitates in PBS solutions, photon cross-correlation spectroscopy (PCCS, NanoPhox, Sympatec) was used.

First tests showed that 0.2 μm membrane (PTFE) filtering lowered the particle concentration to undetectable levels, why all solutions were first measured without filtering, and only in some cases (where some large particles were present) reanalyzed after filtering.

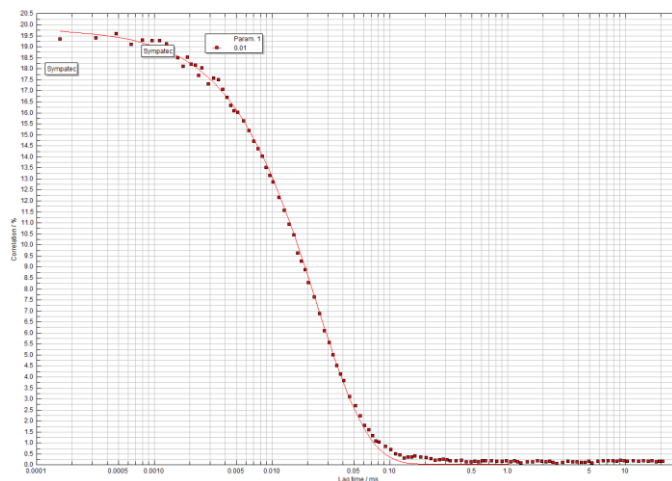


Fig. 46. Correlation function from PCCS analysis.

If the correlation function was acceptable (Fig. 46) (good fitting and no positive values at long lag times), a non-negative least square (NNLS) algorithm was used by the instrument to determine the intensity size distribution.



Comparisons between the different solutions, exposure times and supernatant/non-supernatant have yielded almost identical results identifying particles of average size of approximately 7-10 nm (Fig. 47, Fig. 48).

No results are available for the solution PBS + 30mMH₂O₂ (without BSA) because in no case did they have reliable results based on the correlation function.

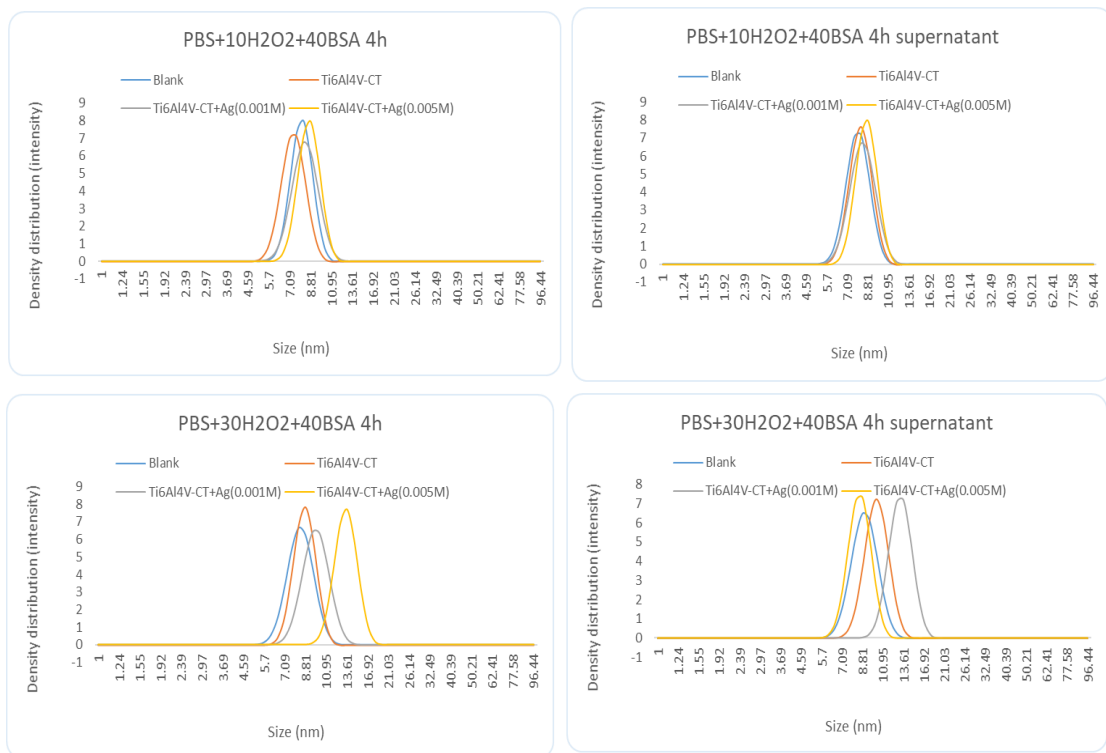


Fig. 47. PCCS results relative to 4h exposure samples.

The trend of the 50 percentile has been also evaluated on the different samples solutions to detect possible increases in particle size in the solutions exposed to containing Ag samples. No trends have been identified.

These results suggest that the detected particles are aggregates due to the presence of BSA, since, according to available data, its dimension in solution should be around 9-10 nm.



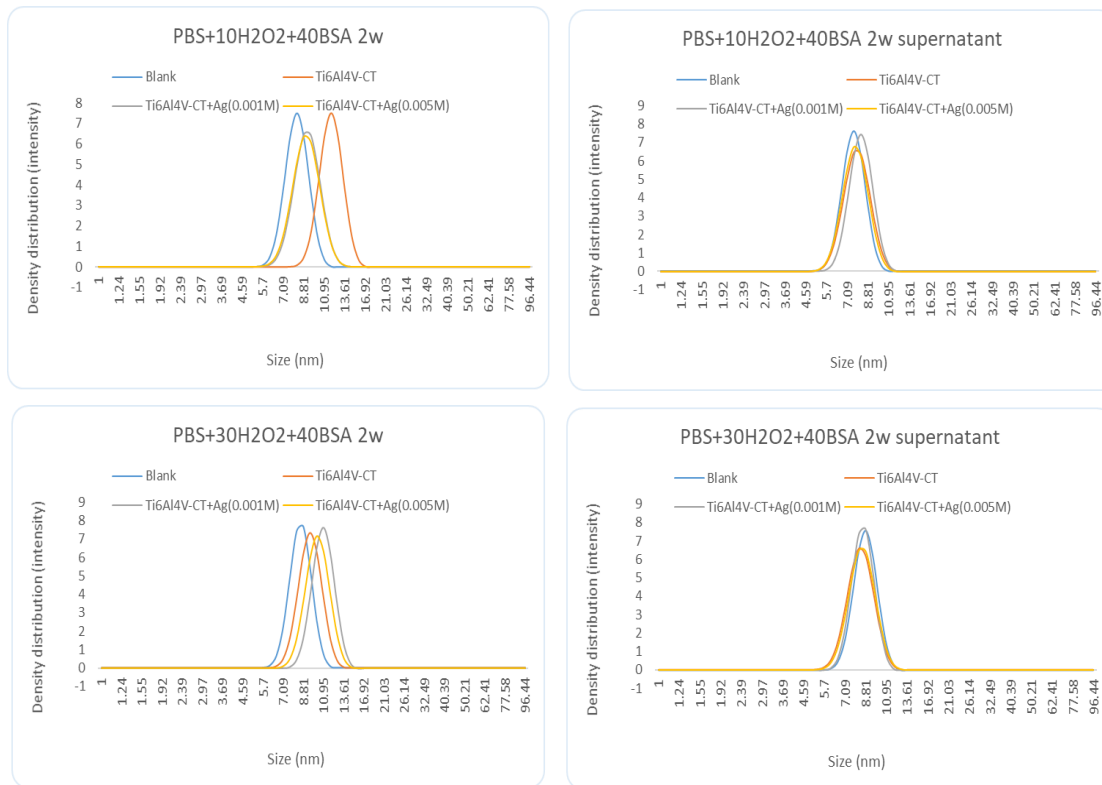


Fig. 48. PCCS results relative to 2w exposure samples.

6.3 Total metal release

The concentrations of titanium, aluminum, vanadium and silver released from the samples into the PBS solutions have been investigated by means graphite furnace atomic absorption spectroscopy (GF-AAS, Perkin Elmer AA800 analyst).

Measured release amounts of Ti, Al, V and Ag ($\mu\text{m}/\text{cm}^2$ of surface area) ions from Ti6Al4V disks following 4h and 336h of incubation in the different biological solutions are presented in Fig. 49, Fig. 50, Fig. 51, Fig. 52, Fig. 53, Fig. 54 and Fig. 55.

The release values from the Ti6Al4V-MP samples exposed for 336h into the three solutions are reported, for each solution, in Fig. 49, and, as a threshold line, in Fig. 51, Fig. 53 and Fig. 55 for comparison.



The analysis of variance (ANOVA) was performed between data sets on different samples and at different time points. A statistically significant difference is considered between the groups when the p-value is below 0.05.

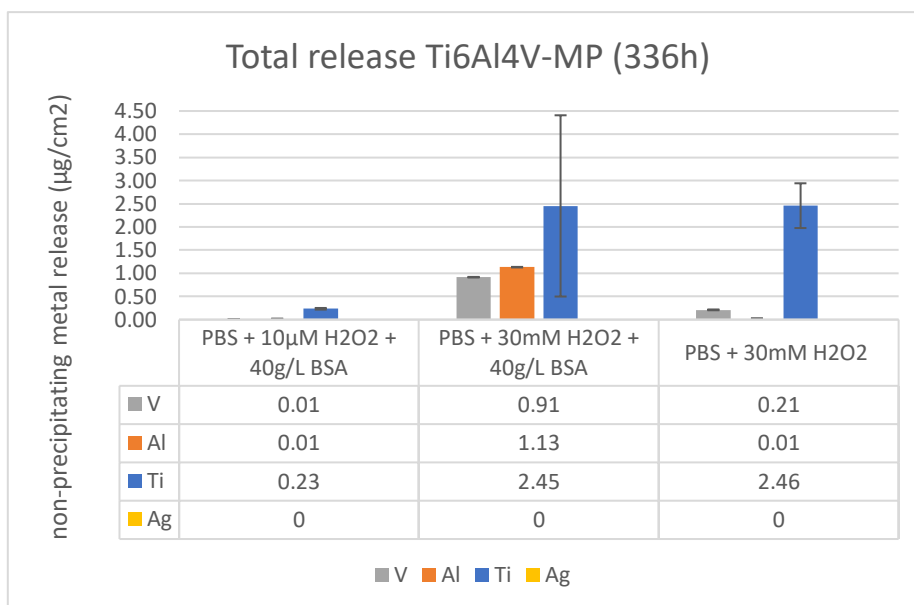


Fig. 49. AAS analysis of Ti6Al4V-MP.

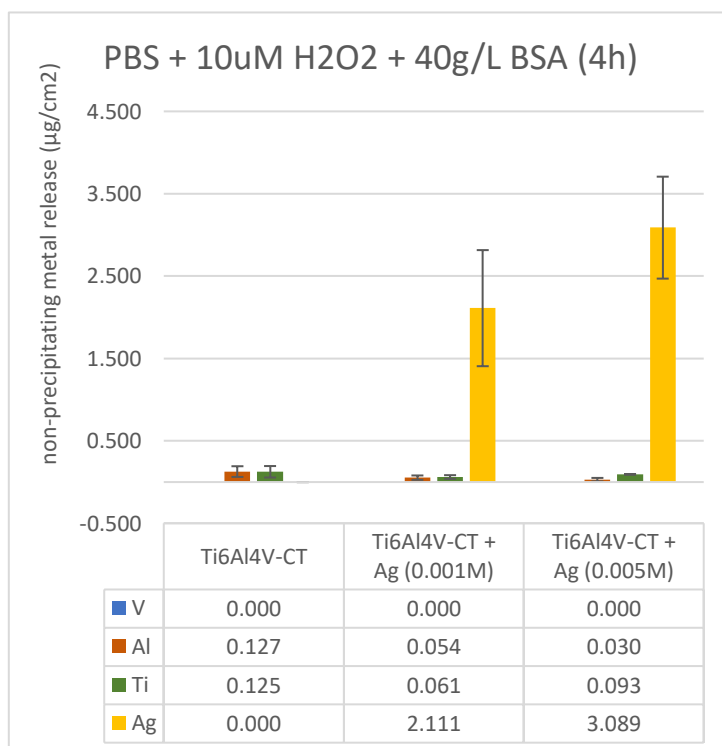


Fig. 50. AAS analysis of Ti6Al4V-CT, Ti6Al4V-CT + Ag (0.001M) and Ti6Al4V-CT + Ag (0.005M) exposed 4h in PBS+10uM H2O2+40g/L BSA



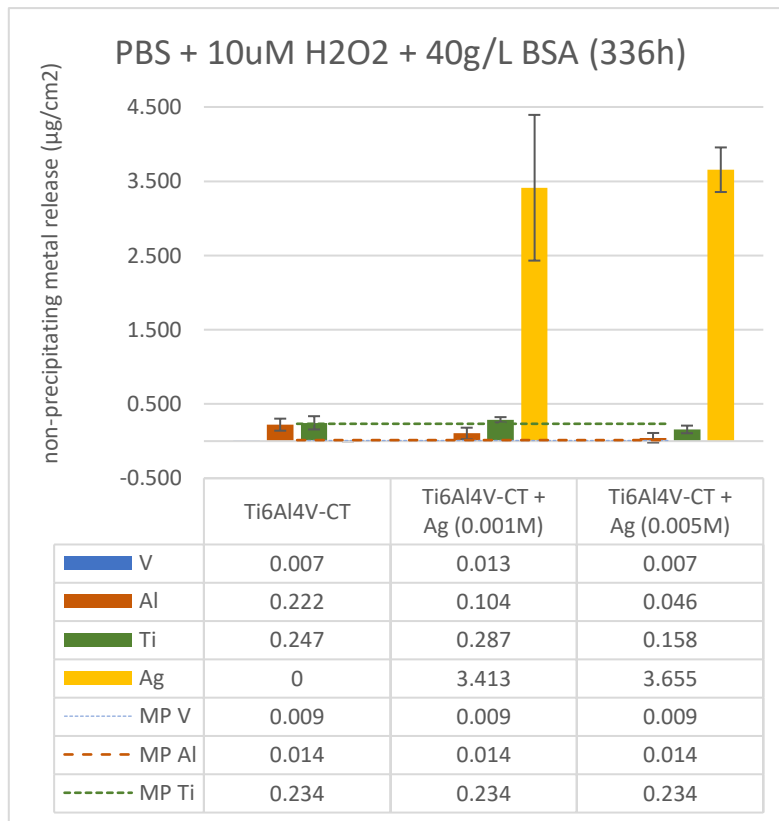


Fig. 51. AAS analysis of Ti6Al4V-CT, Ti6Al4V-CT + Ag (0.001M) and Ti6Al4V-CT + Ag (0.005M) exposed 2w in PBS+10uM H₂O₂+40g/L BSA

Based on the available data analyzed, it is possible to see from the comparison between the analysis of the mirror polished and superficially treated samples as the presence of the superficial modifications does not substantially influence on the released and non-precipitated amount of titanium, aluminum and vanadium.

This is confirmed by the statistical tests in which $p > 0.05$ in all cases except for the aluminum in the sample exposed for 336h in PBS+10µM H₂O₂ + 40g/L BSA ($p=0.018$).

Significant differences in release values, on the other hand, can be noticed by observing the samples exposed into the different solutions (PBS+10H₂O₂+BSA, PBS+30H₂O₂+BSA, PBS+30H₂O₂).

In particular, the presence of hydrogen peroxide and bovine serum albumin is strongly influential on release.



With the presence of both H₂O₂ and BSA, the metal release rate assessed by the exposure tests is very high compared to releases in solutions with only one of the two species.

In particular, as the concentration of hydrogen peroxide increases, there is an increase in the metal release of Ti, Al, V with a lesser influence of the presence of BSA.

The release seems to be more dependent on the presence of H₂O₂ especially for titanium. An increase in the release can also be observed on aluminum and vanadium, but less evident and non-statistically significant.

This behavior has been previously reported on Ti6Al4V alloy by Yu et al.¹¹¹. They showed through electrochemical techniques a synergistic effect of H₂O₂ and BSA on the corrosion resistance of the alloy in question.

H₂O₂ has been reported increasing both the rates of anodic and cathodic reactions, while albumin limits them. The combined effect was attributed to the effect of adsorption of albumin in decreasing the rate of the cathodic reaction and thus lowering the open circuit potential (OCP) into the active region of titanium where complexation by H₂O₂ increased the corrosion rate.

In contrast, the concentration of BSA in the solutions to which the samples were exposed strongly modifies the release of silver.

In particular, in the samples Ti6Al4V-CT + Ag (0.001M) and Ti6Al4V-CT + Ag (0.005M) a remarkable release of silver ($p < 0.04$) in the solutions containing a greater quantity of BSA (PBS+10H₂O₂+BSA, PBS+30H₂O₂+BSA) is highlighted compared to the amount of silver detected in the solution without BSA (PBS+30H₂O₂).

This is probably due to the presence of the protein forming complexes with silver ions resulting in sedimentation and loss of metal from the solution.



Moreover, generally, the released amounts of Ti, Al, V and Ag at 366h are, in almost all cases, larger with statistically significant differences compared with 4h releases, as expected.

The only exception concerns Ti6Al4V-CT + Ag (0.005M) samples in which the release of silver turns out not significantly different ($p>0.36$) into PBS+10H₂O₂+BSA and PBS+30H₂O₂+BSA solutions after 336h compared with 4h suggesting that the silver release, in this case, occurs in the first hours of exposition.

Further, the silver amount released by Ti6Al4V-CT + Ag (0.005M) is higher but not statistically different ($p>0.3$) from silver released by Ti6Al4V-CT + Ag (0.001M) despite the greater amount of silver with which the samples were treated.

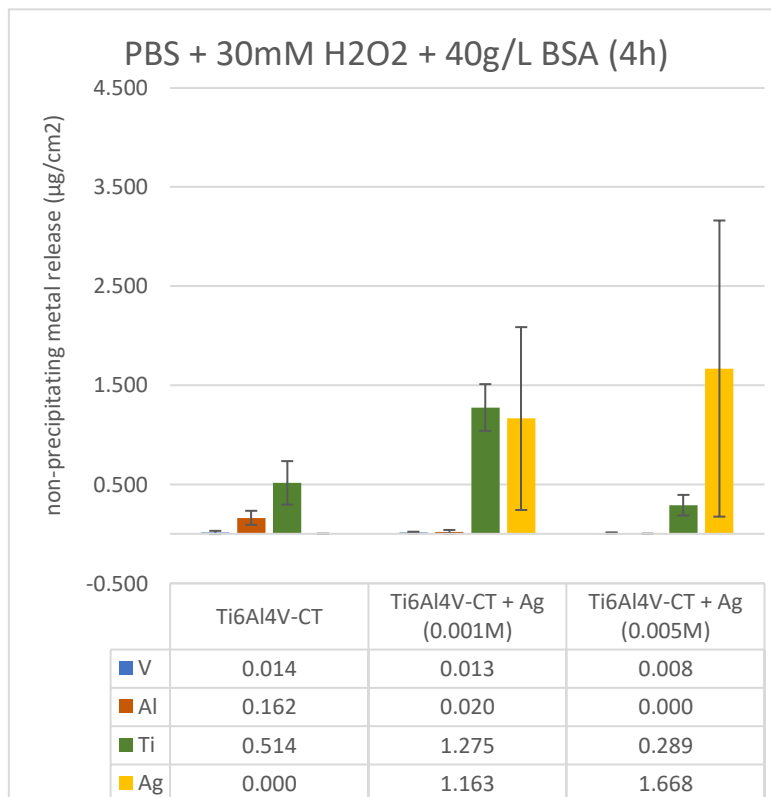


Fig. 52. AAS analysis of Ti6Al4V-CT, Ti6Al4V-CT + Ag (0.001M) and Ti6Al4V-CT + Ag (0.005M) exposed 4h in PBS+30uM H₂O₂+40g/L BSA



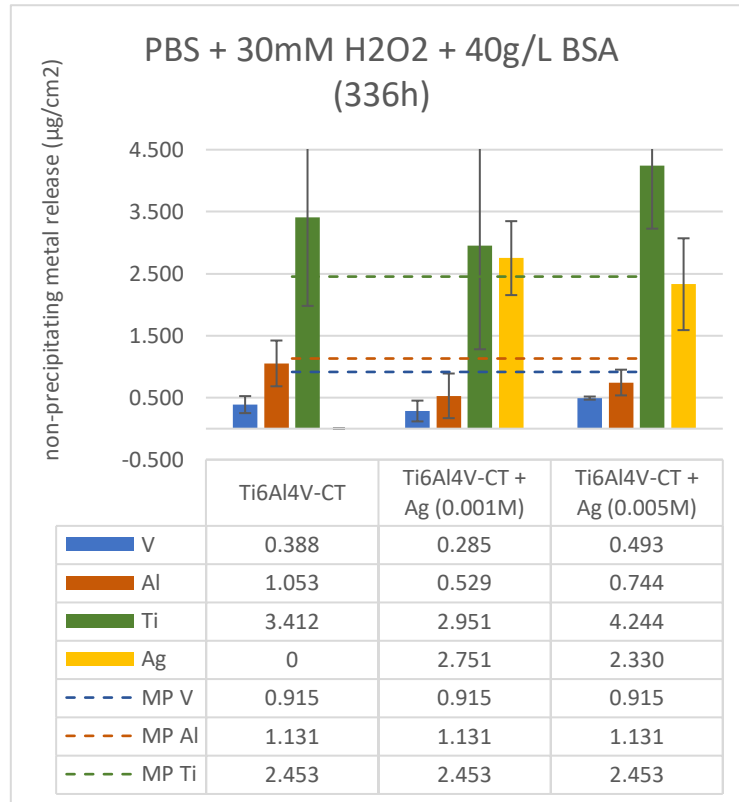


Fig. 53. AAS analysis of Ti6Al4V-CT, Ti6Al4V-CT + Ag (0.001M) and Ti6Al4V-CT + Ag (0.005M) exposed 2w in PBS+30uM H₂O₂+40g/L BSA

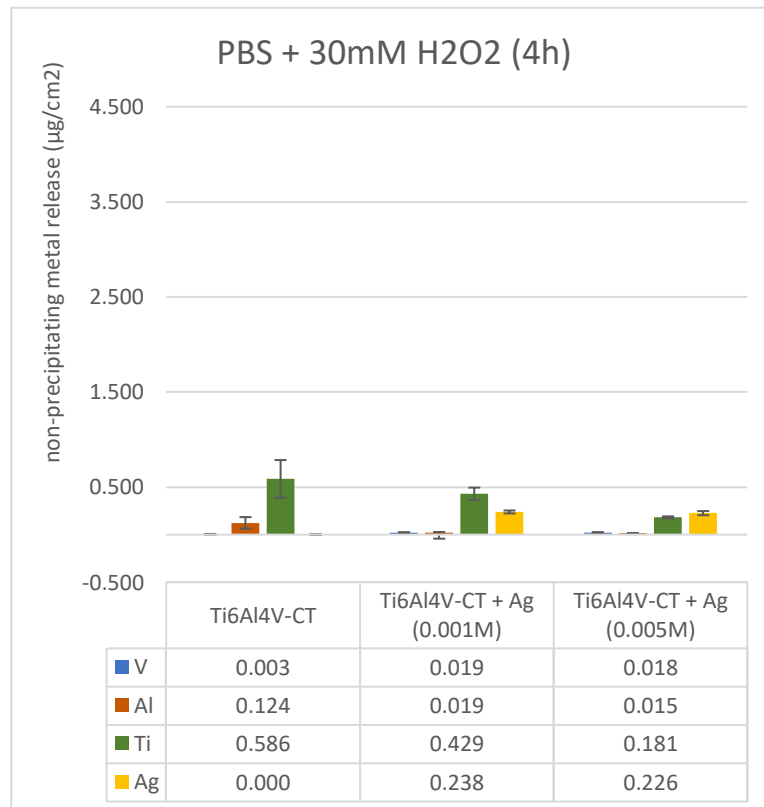


Fig. 54. AAS analysis of Ti6Al4V-CT, Ti6Al4V-CT + Ag (0.001M) and Ti6Al4V-CT + Ag (0.005M) exposed 4h in PBS+30uM H₂O₂



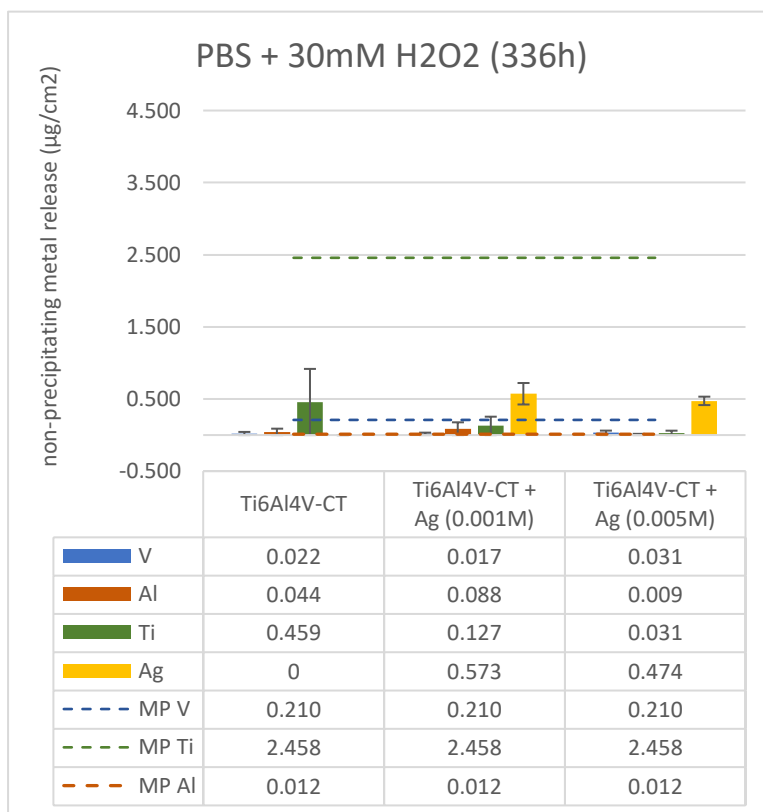


Fig. 55. AAS analysis of Ti6Al4V-CT, Ti6Al4V-CT + Ag (0.001M) and Ti6Al4V-CT + Ag (0.005M) exposed 2w in PBS+30uM H₂O₂

Silver concentration were compared in supernatant and non-supernatant solutions since possible released silver nanoparticles and precipitated metals/proteins were expected in non-supernatant solution.

It is not possible to observe substantial differences of silver released from the supernatant and non-supernatant solutions (Fig. 56), which suggests the presence mostly of ions instead of nanoparticles released into the solutions.

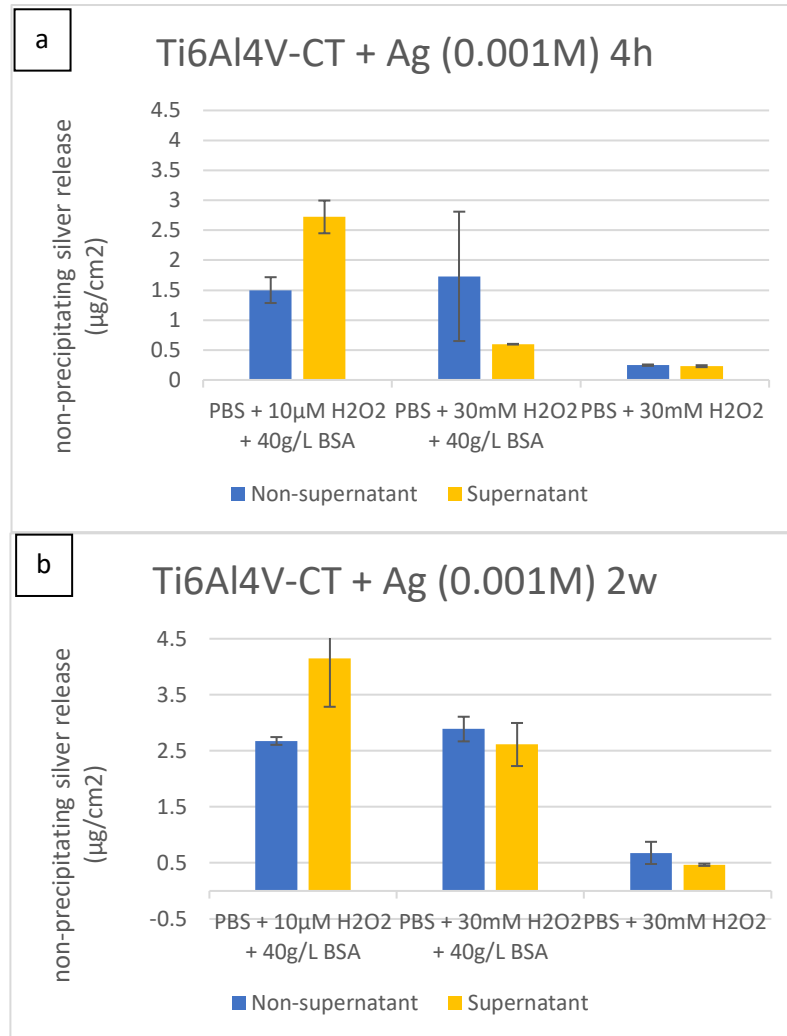


Fig. 56. AAS analysis on sample solutions of Ti6Al4V-CT + Ag (0.001M), comparisons between silver concentrations in supernatant and non-supernatant solution.

6.3.1 Other works

For comparisons, metal releases from a Ti6Al4V alloy from Hedberg et al. research¹¹² are reported.

This study investigated, as a function of different amounts of hydrogen peroxide and bovine serum albumin, the mechanism of the combined action on the metal release.

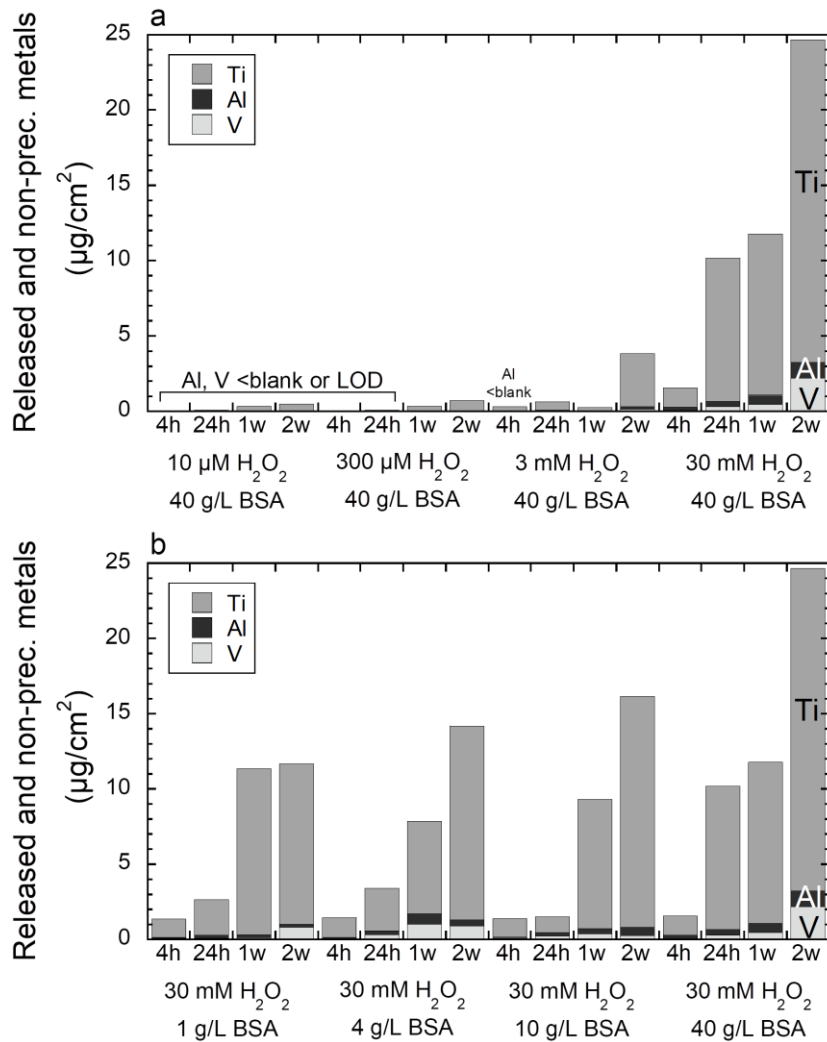


Fig. 57. Metal release from Ti6Al4V alloy dependent on H₂O₂ and BSA amount².

Confirming our results, the metal release was strongly affected by hydrogen peroxide and bovine serum albumin (Fig. 57) with a more pronounced effect of H₂O₂.

Are shown, further, for comparison, data of antibacterial activity and the analysis of their culture broths on samples prepared in a previous work.

The analysis of the broths (LB medium) were made by ICP on samples Ti6Al4V-CT, Ti6Al4V-CT + Ag (0.001M) and Ti6Al4V-CT + Ag (0.005M) (Fig.58).



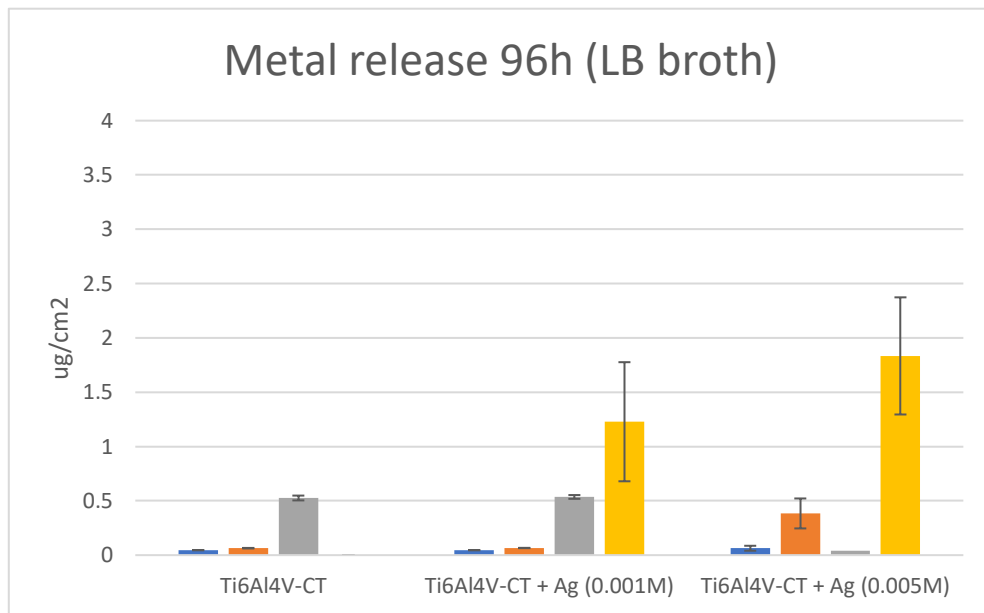


Fig. 58. Metal release in LB broth after 96h of incubation.

The samples were treated in the same way and immersed in 1 mL of the culture broth containing bacteria for the study of the antibacterial effect.

The results (Fig.58) of 96h of exposition are comparable with those obtained in this thesis work. The releases measured in broths are significantly lower taking into consideration the solutions containing H₂O₂ which was reported to be very influential on the release of metals in solution. In addition, in this case the solutions were not digested before the release tests and some elements could be precipitated and have formed undetected complexes.

As regards the silver, a smaller amount detected in broths may be due to the presence of bacteria.

Silver, in fact, to carry out its antibacterial action can be internalized by the bacteria and therefore detected in a lower amount in solution.

Moreover, cytocompatibility tests were conducted on human osteoblasts progenitor observing a marked reduction of cell viability due to the direct contact of Ag-doped samples with cells.



6.4 X-ray photoelectron spectroscopy (XPS)

XPS measurements have been conducted in order to analyze the surface oxide composition with an information depth less than 10 nm on non-exposed and exposed samples.

Fig. 59, Fig. 60 and Fig. 61 show the elemental composition (at%) of the surface oxide layer of Ti6Al4V alloy.

From the XPS measurements in this work, it is evident that significant changes in the surface oxide composition occur after a certain time period of incubation.

The percentages of the elements present on the surface are in agreement with the results obtained from the analysis of the ionic release.

As far as it regards the alloying elements (Ti, Al, V), their presence in the superficial oxide (at%) modified subsequently to the superficial treatment and to the contact with the physiological solutions.

The Ti6Al4V-MP samples, even if minimally, show percentages of all three elements differently from the superficially treated samples (Ti6Al4V-CT) on which, following the treatment, there are no traces, excluding sporadic cases, of aluminum and vanadium.

Ti decreases gradually with increasing exposure time to physiological solutions. In fact, it is partially released in solution from the samples.

Otherwise, silver, inserted in a minimal manner in the form of nanoparticles in the oxide layer, is no longer present (or in very small percentages) following exposure. It disappears from the surface almost completely following two weeks of incubation in the two solutions in which a greater release has been found by AAS analysis (PBS +10 μ M H₂O₂ + 40g/L BSA e PBS +30mM H₂O₂ + 40g/L BSA) confirming the results obtained from release tests.



The almost total release of surface silver introduced by the treatment is an appreciated result for orthopaedical field given that the risk of post-surgical infections is greater in the early days after intervention.

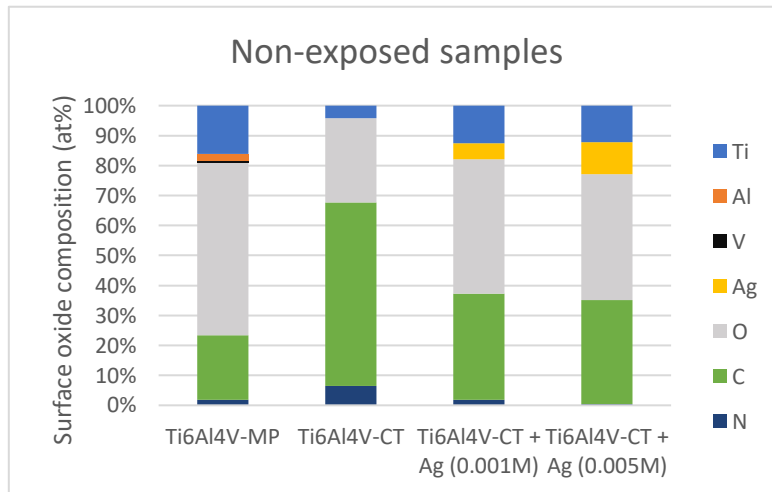


Fig. 59. XPS measurements on non-exposed samples.



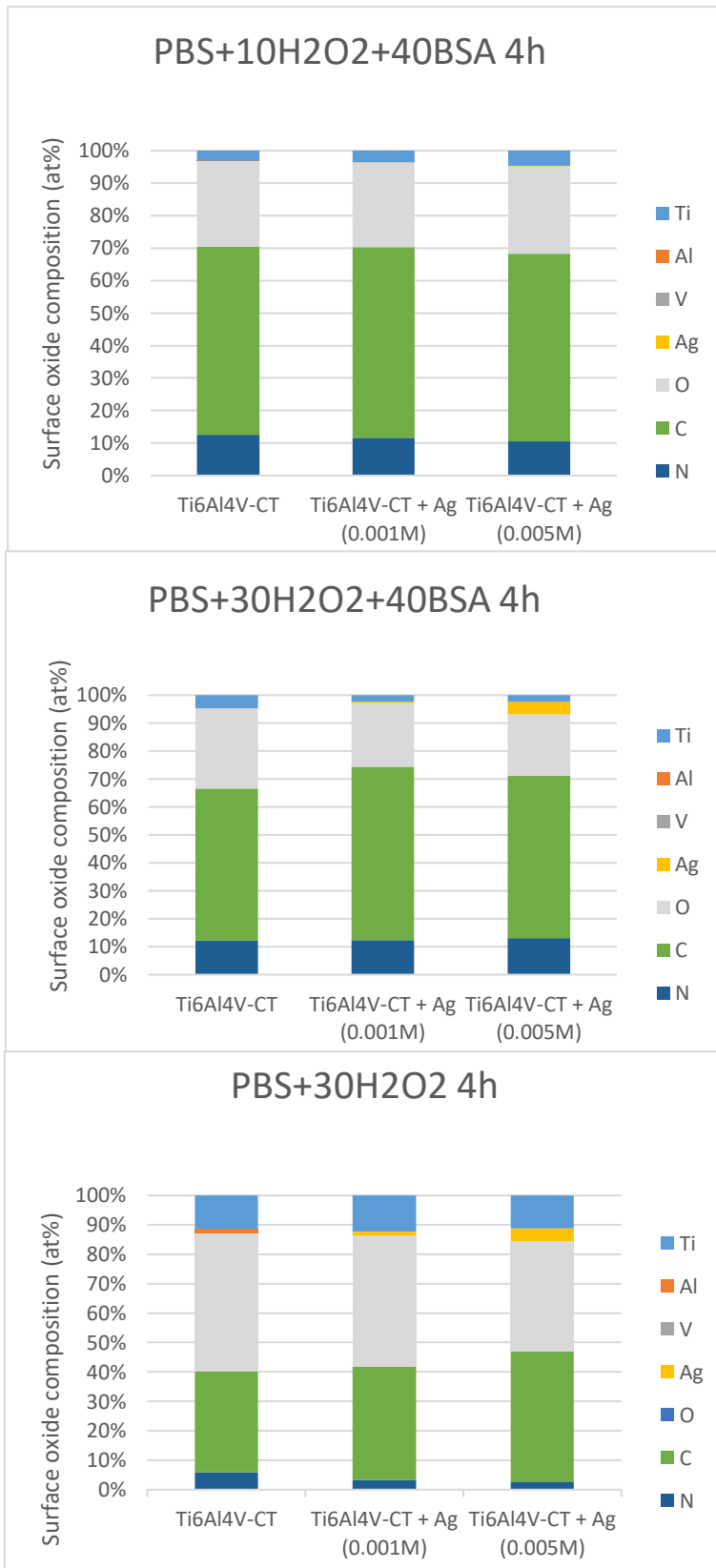


Fig. 60. XPS measurements on 4h exposed samples into the different solutions.



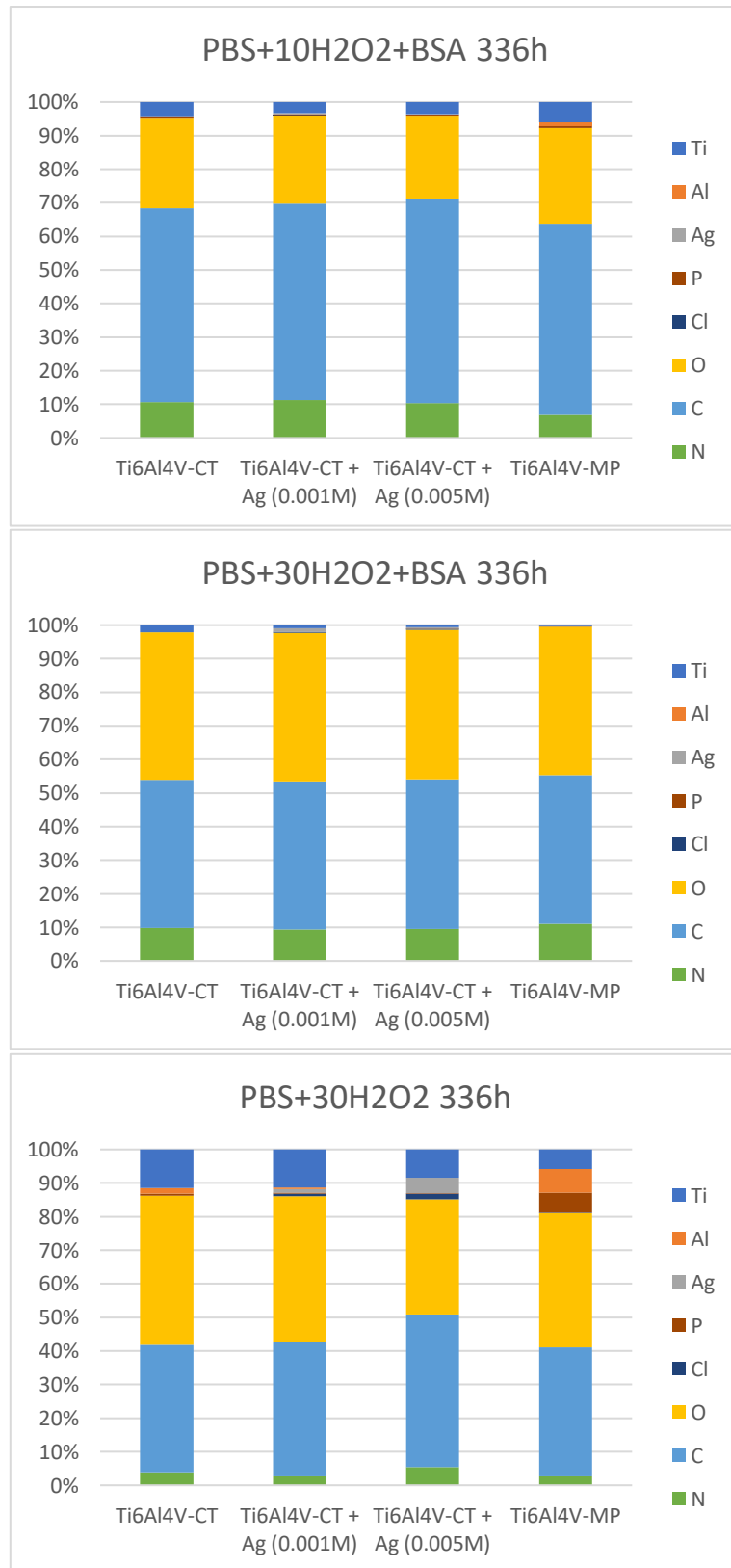


Fig. 61. XPS measurements on 336h exposed samples into the different solutions.



6.5 In vitro bioactivity tests

In order to evaluate the bioactivity of the treated surfaces and the related precipitation of hydroxyapatite, two samples (Ti6Al4V-CT + Ag 0.001M) were immersed in simulated body fluid respectively for 14 and 28 days (refreshing the solution every week) and finally analyzed by means of FESEM-EDS.

A refresh of the solution was performed every week and pH at every refresh was measured founding fluctuations between 7.17 and 7.46 (Table. 15) within the physiological limits of tolerability (7.00-7.80).

Samples	Initial pH	7° day	14° day	21° day	28° day
Ti6Al4V-CT+Ag (0.001M)	7.41	7.36	7.46	-	-
Ti6Al4V-CT+Ag (0.001M)	7.41	7.34	7.42	7.27	7.17

Table 15. pH measurements after every refresh of the SBF solution.

After SBF soaking, the FESEM-EDS observations showed an enrichment in Ca and P on the surface of both the samples.

On both samples exposed to SBF micrometric Ca and P precipitates with the typical form of hydroxyapatite (particle agglomerates) and a nanotexture, given by chemical treatment, are clearly visible (Fig. 62).



6.5.1 Ti6Al4V-CT Ag (0.001M) 14 days in SBF

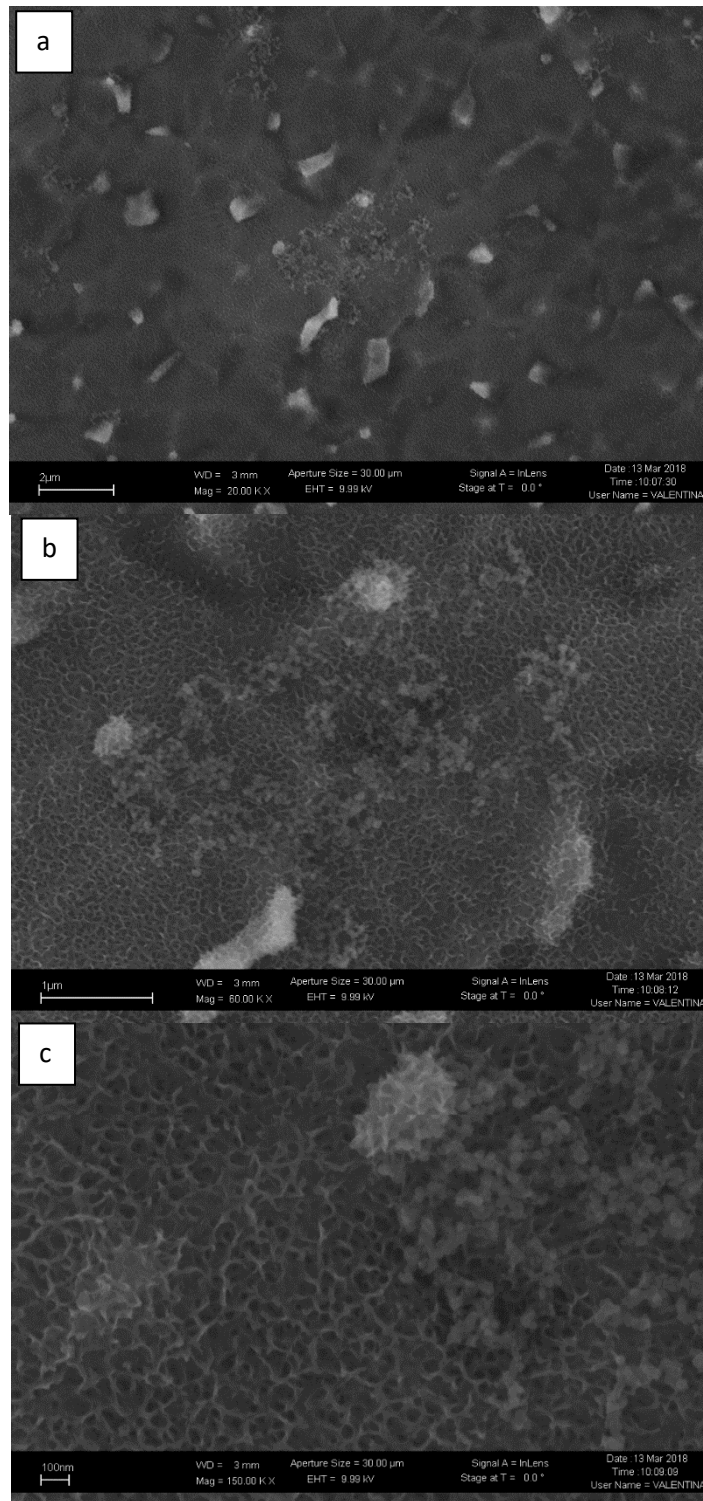


Fig. 62. FESEM images of Ti6Al4V-CT + Ag (0.001M) exposed to SBF for 14 days, a) 20000x, b) 60000x, c) 150000x.



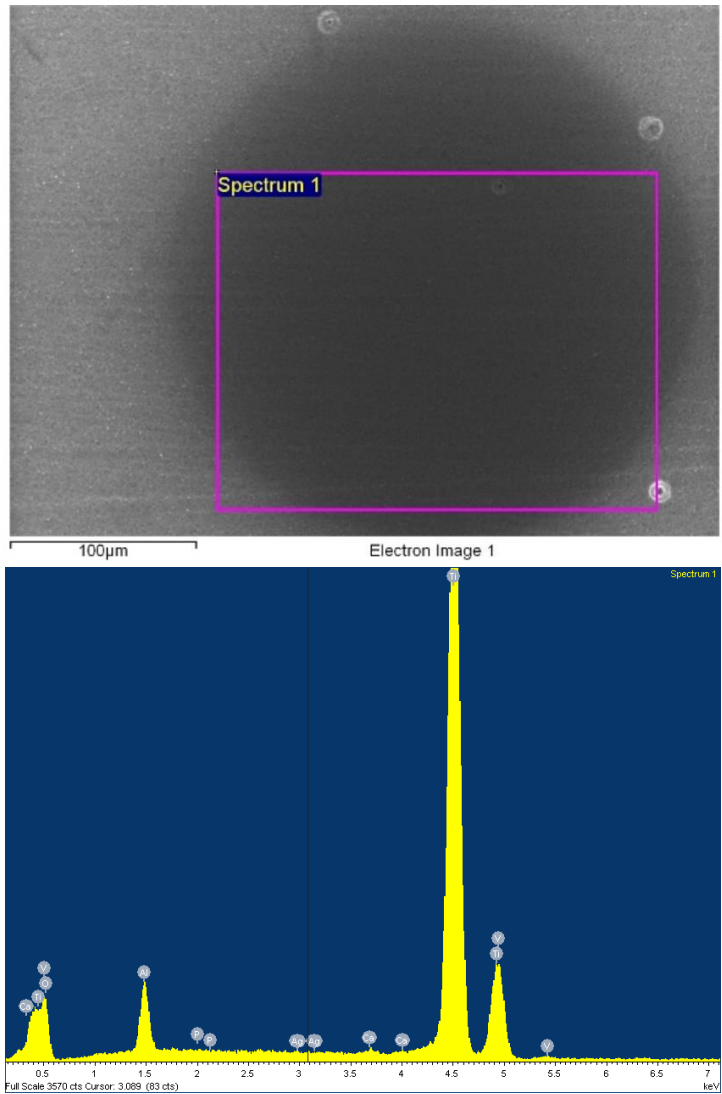


Fig. 63. EDS analysis of Ti6Al4V-CT + Ag (0.001M) exposed for 14 days in SBF.

The atomic percentages of Ca and P identified by the EDS analysis on areas and points for the two samples exposed in SBF are shown in Table.16.

It can be noticed that both samples surfaces (14 and 28 days in SBF) present an apparently similar bioactivity based on Ca and P amounts suggesting a limited bioactivity after 14 days.

Samples	Area analysis		Point analysis	
	Ca (at%)	P (at%)	Ca (at%)	P (at%)
Ti6Al4V-CT+Ag (0.001M) 14 days in SBF	0.19	0.03	0.29	0.13
Ti6Al4V-CT+Ag (0.001M) 28 days in SBF	0.17	0.00	0.21	0.21

Table 16. Ca and P amounts measured by EDS relative to Fig.19, Fig.20, Fig.22 and Fig.23.

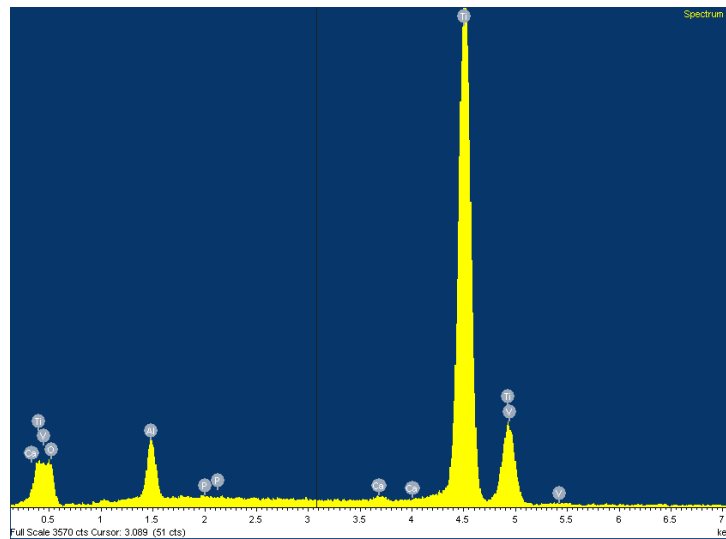
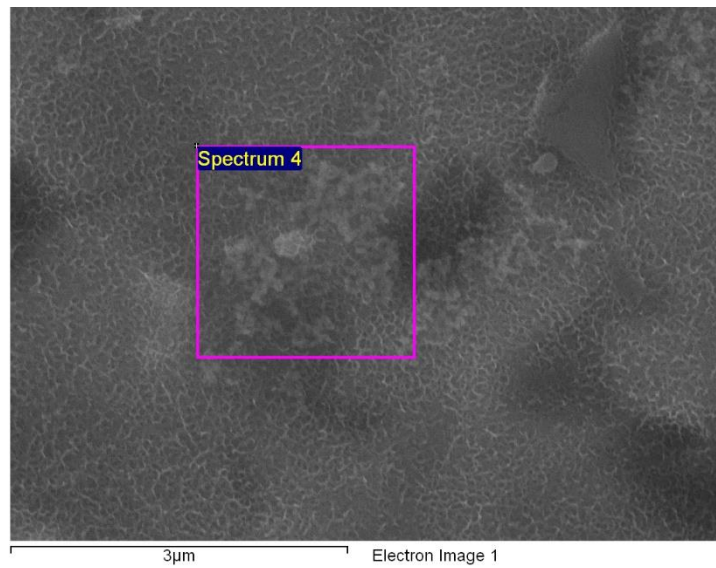


Fig. 64. EDS analysis of Ti6Al4V-CT + Ag (0.001M) exposed for 14 days in SBF.

6.5.2 Ti6Al4V-CT Ag (0.001M) 28 days in SBF

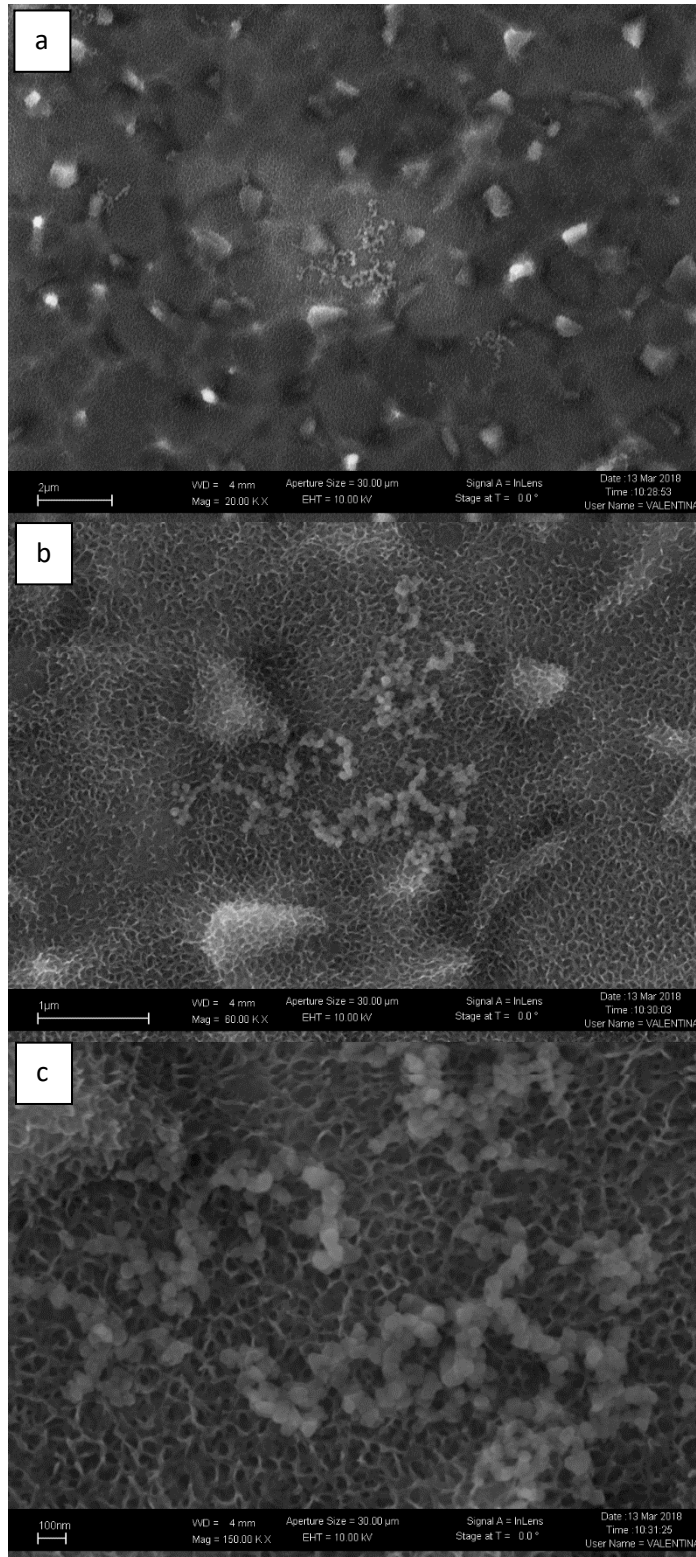


Fig. 65. FESEM images of Ti6Al4V-CT + Ag (0.001M) exposed to SBF for 28 days, a) 20000x, b) 60000x, c) 150000x.

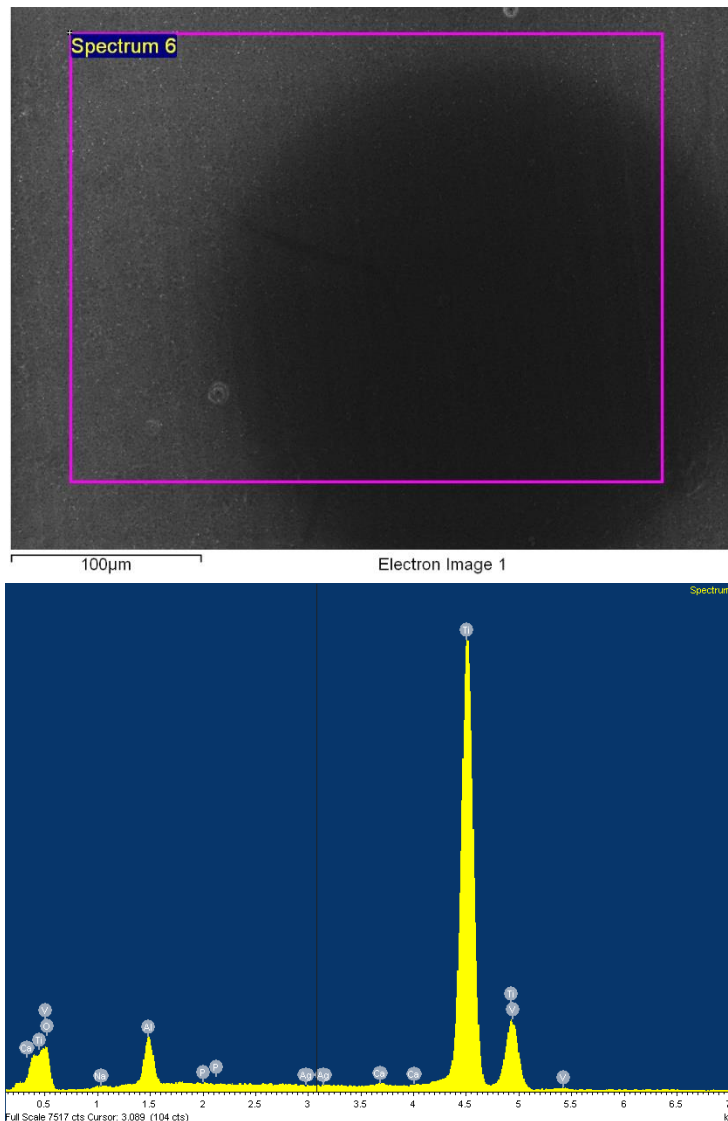


Fig. 663. EDS analysis of Ti6Al4V-CT + Ag (0.001M) exposed for 28 days in SBF.

No trace of silver was detectable on the surfaces of exposed samples probably due to the fact that it was completely released during the incubation period.

As expected, the sample analyzed for comparison does not show traces of Ca and P and, on the contrary, contains a percentage of silver (0.14 at%).

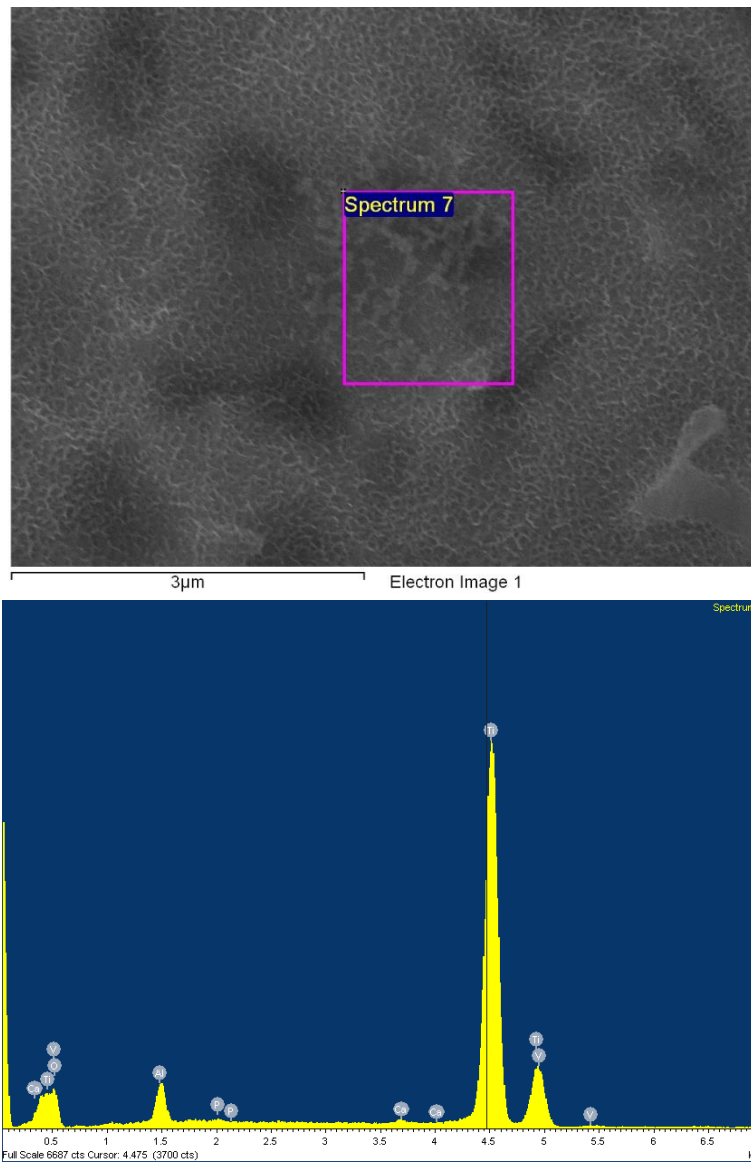


Fig. 67. EDS analysis of Ti6Al4V-CT + Ag (0.001M) exposed for 28 days in SBF.

It can be concluded that the treatments carried out on the Ti6Al4V alloy samples are able to induce inorganic bioactivity resulting in an in vivo biomineralization on the implant.

6.6 Zeta potential measurements

Zeta potential measurements have been conducted on Ti6Al4V-CT + Ag (0.001M) samples in the acid and basic range separately (Fig.68).

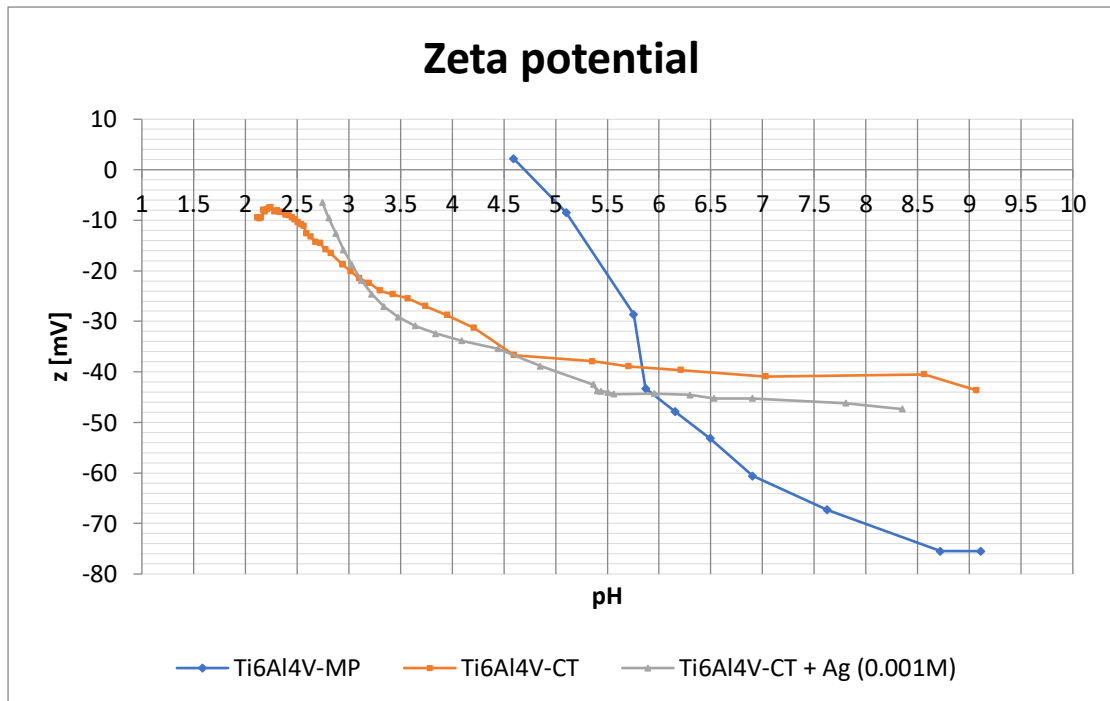


Fig. 68. Zeta potential measurements of Ti6Al4V-CT + Ag 0.001M

From literature, the untreated Ti6Al4V alloy reach the isoelectric point at about $\text{pH}=4.7^{113}$.

As can be seen from the graph, the surface modification through the chemical treatment leads to a displacement of the isoelectric point towards more acidic values ($\text{pH}\approx 2.5$).

Furthermore, the graph of the zeta potential on the treated sample shows, compared to the measurement on the untreated sample (Fig.68), a plateau in the basic range.



The plateau indicates the presence of homogeneous functional groups with acidic behavior on the surface, which, by means of XPS measurements, have been identified as hydroxyl groups (OH) introduced by the surface treatment¹⁰³.

It can be noted that the addition of the antibacterial agent, in this case silver, does not substantially modify the isoelectric point and the surface charge (Fig. 68).

In Table 17 isoelectric point (IEP) and zeta potential at pH=7.4 are shown for each sample.

	IEP	Z (pH=7.4)
Ti6Al4V-MP	≈4.7	≈-66 mV
Ti6Al4V-CT	≈2	≈-41 mV
Ti6Al4V-CT + Ag (0.001M)	≈2.5	≈-46 mV

Table 17. IEP and z potential at pH=7.4 for Ti6Al4V-MP, Ti6Al4V-CT and Ti6Al4V-CT + Ag (0.001M) samples.



7 CONCLUSIONS

The aim of this thesis work was to carry out surface modifications on Ti6Al4V alloy surfaces widely used in the orthopedic and dental fields for parts of prosthetic implants such as hip and knee with the aim of promoting cell adhesion, osseointegration and preventing bacterial adhesion.

To achieve these objectives we focused on two aspects: a controlled oxidation process on the surface with the intent to make the surface chemically and topographically suitable for greater cell adhesion and enrichment of this oxide layer with silver nanoparticles used as an antibacterial agent.

The surface treatment was obtained in two steps: the removal of the native oxide on the material through chemical etching in hydrofluoric acid and a controlled oxidation process in hydrogen peroxide.

The addition of the antibacterial agent on some of the samples took place during the controlled oxidation process by inserting silver nitrate together with gallic acid and polyvinylalcohol (stabilizing and reducing agents) obtaining the formation of silver nanoparticles by reduction of the silver nitrate due to the effect of H_2O_2 .

Surface treatments were carried out at Politecnico di Torino laboratories. On the prepared samples, several tests were carried out including metal ion release tests in physiological solutions based on PBS with variable concentrations of hydrogen peroxide and albumin and surface characterizations by XPS and SEM at the laboratories of the KTH Royal Institute of Technology in Stockholm, and study of inorganic bioactivity through exposure in SBF and measurement of zeta potential at the Polytechnic University of Turin.

The results of the tests carried out showed on the surface of the samples analyzed the presence of a nanostructure free of cracks essential for the



osseointegration process with a certain amount of exposed hydroxyl groups (OH) usable for functionalizations with biomolecules in order to conduct a precise biological response.

Treated surfaces also exhibit an *in vitro* bioactivity behavior, they are characterized by surface deposits of Ca and P, elements essential for the growth of hydroxyapatite.

For what concern the antibacterial effect, the samples functionalized with silver nanoparticles showed an almost total release of the silver in the form of ions after two weeks of incubation and therefore a possible activity against bacterial adhesion and the spread of the infection related to the implant.

Numerous solutions have been proposed in scientific literature.

The most critical problems of these strategies concern the release of the antibacterial agent and its effect in case of infection on the implant surface.

For now, implants based on titanium with antibacterial properties are not commercially available, and the development of surfaces capable of performing antimicrobial activity in an effective but above all prolonged manner and of permanently integrating with the host bone avoiding cytotoxicity problems represents a promising solution.



8 REFERENCES

1. Kulkarni M, A. M., P. S. & A., I. Biomaterial surface modification of titanium and titanium alloys for medical applications. *Nanomedicine*. 111–136 (2014).
2. Turi, G., Santini, S., Zecchinato, G. & Turi, G. LE INFEZIONI DEGLI IMPIANTI ORTOPEDICI.
3. CDC - Nanotechnology - NIOSH Workplace Safety and Health Topic. Available at: <https://www.cdc.gov/niosh/topics/nanotech/default.html>.
4. Maynard, A. & Michelson, E. The nanotechnology consumer products inventory. *Woodrow Wilson Int. Cent. Sch. Washington, DC*, accessed March **23**, (2006).
5. Vance, M. E. *et al.* Nanotechnology in the real world: Redeveloping the nanomaterial consumer products inventory. *Beilstein J. Nanotechnol.* **6**, 1769–1780 (2015).
6. Chernousova, S. & Epple, M. Silver as antibacterial agent: Ion, nanoparticle, and metal. *Angew. Chemie - Int. Ed.* **52**, 1636–1653 (2013).
7. Borgese, F. *Gli elementi della tavola periodica : rinvenimento, proprietà, usi : prontuario chimico, fisico, geologico.* (CISU, 1993).
8. Uso dell'argento: cambiamenti e prospettive. Available at: <https://oro.bullionvault.it/notizie-oro/uso-dellargento-cambiamenti-e-prospettive>.
9. Atiyeh, B. S., Costagliola, M., Hayek, S. N. & Dibo, S. A. Effect of silver on burn wound infection control and healing: Review of the literature. *Burns* **33**, 139–148 (2007).
10. Klasen, H. J. A historical review of the use of silver in the treatment of burns. I. Early uses. *Burns* **26**, 131–138 (2000).
11. Trimestre, I. I. I. ARGENTO: un potente antibatterico naturale! (2012).
12. Wijnhoven, S. W. P. *et al.* Nano-silver - A review of available data and knowledge gaps in human and environmental risk assessment. *Nanotoxicology* **3**, 109–138 (2009).
13. Wong, K. K. Y. & Liu, X. Silver nanoparticles: the real 'silver bullet' in clinical medicine? *Medchemcomm* **1**, 125–131 (2010).
14. Reidy, B., Haase, A., Luch, A., Dawson, K. A. & Lynch, I. Mechanisms of silver nanoparticle release, transformation and toxicity: A critical review of current knowledge and recommendations for future studies and applications. *Materials (Basel)*. **6**, 2295–2350 (2013).
15. Saleh, T. A. & Alaqad, K. Analytical Toxicology Gold and Silver Nanoparticles: Synthesis Methods, Characterization Routes and Applications towards Drugs. *J Env. Anal Toxicol* **6**, (2016).



16. Iravani, S., Korbekandi, H., Mirmohammadi, S. V & Zolfaghari, B. Synthesis of silver nanoparticles: chemical, physical and biological methods. *Res. Pharm. Sci.* **9**, 385–406 (2014).
17. Sharma, V. K., Yngard, R. A. & Lin, Y. Silver nanoparticles: Green synthesis and their antimicrobial activities. *Adv. Colloid Interface Sci.* **145**, 83–96 (2009).
18. Howe, P. D. & Dobson, S. Concise International Chemical Assessment Document 44: Silver and silver compounds: Environmental aspects. *IPCS Concise Int. Chem. Assess. Doc.* (2002). doi:10.1016/j.jconhyd.2010.08.009
19. Ratte, H. T. Bioaccumulation and Toxicity of Silver Compounds: a Review. *Environ. Toxicol. Chem.* **18**, 89 (1999).
20. Batchelor-McAuley, C., Tschulik, K., Neumann, C. C. M., Laborda, E. & Compton, R. G. Why are Silver Nanoparticles More Toxic Than Bulk Silver? Towards Understanding the Dissolution and Toxicity of Silver Nanoparticles. *Int. J. Electrochem. Sci.* **9**, 1132–1138 (2014).
21. Wang, Z., Xia, T. & Liu, S. Mechanisms of nanosilver-induced toxicological effects: more attention should be paid to its sublethal effects. **7**, 1–23 (2017).
22. Bouwmeester, H. *et al.* Review of health safety aspects of nanotechnologies in food production. *Regul. Toxicol. Pharmacol.* **53**, 52–62 (2009).
23. USE OF NANOTECHNOLOGY IN FOOD PROCESSING, PACKAGING AND SAFETY – REVIEW. **10**, 2719–2740 (2010).
24. Benn, T. M. & Westerhoff, P. Nanoparticle silver released into water from commercially available sock fabrics. *Environ. Sci. Technol.* **42**, 4133–4139 (2008).
25. Kulthong, K., Srisung, S., Boonpavanitchakul, K., Kangwansupamonkon, W. & Maniratanachote, R. Determination of silver nanoparticle release from antibacterial fabrics into artificial sweat. *Part. Fibre Toxicol.* **7**, 8 (2010).
26. Geranio, L. & Heuberger, M. The Behavior of Silver Nanotextiles during Washing. **43**, 8113–8118 (2009).
27. Leaper, D. J. Silver dressings: Their role in wound management. *Int. Wound J.* **3**, 282–294 (2006).
28. Brennan, S. A. *et al.* Instructional review: General orthopaedics silver nanoparticles and their orthopaedic applications. *Bone Jt. J.* **97-B**, 582–589 (2015).
29. Kaegi, R. *et al.* Release of silver nanoparticles from outdoor facades. *Environ. Pollut.* **158**, 2900–2905 (2010).
30. Hedberg, J. *et al.* Sequential studies of silver released from silver nanoparticles in aqueous media simulating sweat, laundry detergent solutions and surface water. *Environ. Sci. Technol.* **48**, 7314–7322 (2014).
31. Larese, F. F. *et al.* Human skin penetration of silver nanoparticles through intact and damaged skin. *Toxicology* **255**, 33–37 (2009).
32. Roe, D., Karandikar, B., Bonn-Savage, N., Gibbins, B. & Rouillet, J. baptiste. Antimicrobial surface functionalization of plastic catheters by silver nanoparticles. *J. Antimicrob. Chemother.* **61**, 869–876 (2008).



33. Liu, J., Wang, Z., Liu, F. D., Kane, A. B. & Hurt, R. H. Chemical transformations of nanosilver in biological environments. *ACS Nano* **6**, 9887–9899 (2012).
34. Kittler, S., Greulich, C., Diendorf, J., Köller, M. & Epple, M. Toxicity of silver nanoparticles increases during storage because of slow dissolution under release of silver ions. *Chem. Mater.* **22**, 4548–4554 (2010).
35. Liu, J. & Hurt, R. H. Ion release kinetics and particle persistence in aqueous nano silver colloids. *Environ. Sci. Technol.* **44**, 2169–2175 (2010).
36. Chappell, M. A. *et al.* Simultaneous dispersion-dissolution behavior of concentrated silver nanoparticle suspensions in the presence of model organic solutes. *Chemosphere* **84**, 1108–1116 (2011).
37. Liu, J., Sonshine, D. a, Shervani, S. & Hurt, R. H. Controlled Release of Biologically Active Silver from Nanosilver Surfaces. **4**, 6903–6913 (2010).
38. Stebounova, L. V., Guio, E. & Grassian, V. H. Silver nanoparticles in simulated biological media: A study of aggregation, sedimentation, and dissolution. *J. Nanoparticle Res.* **13**, 233–244 (2011).
39. Damm, C. & Münstedt, H. Kinetic aspects of the silver ion release from antimicrobial polyamide/silver nanocomposites. *Appl. Phys. A Mater. Sci. Process.* **91**, 479–486 (2008).
40. Zhang, W., Yao, Y., Sullivan, N. & Chen, Y. Modeling the primary size effects of citrate-coated silver nanoparticles on their ion release kinetics. *Environ. Sci. Technol.* **45**, 4422–4428 (2011).
41. Stopford, W., Turner, J., Cappellini, D. & Brock, T. Bioaccessibility testing of cobalt compounds. *J. Environ. Monit.* **5**, 675–80 (2003).
42. Drago, L. Infezioni impianto-correlate e biofilm batterico. *LO SCALPELLO-OTODI Educ.* **23**, 153–159 (2009).
43. Campoccia, D., Montanaro, L. & Arciola, C. R. The significance of infection related to orthopedic devices and issues of antibiotic resistance. *Biomaterials* **27**, 2331–2339 (2006).
44. Gold, H. S. & Moellering, R. C. Antimicrobial-Drug Resistance. *N. Engl. J. Med.* **335**, 1445–1453 (1996).
45. Silhavy, T. J., Kahne, D. & Walker, S. The bacterial cell envelope. *Cold Spring Harb. Perspect. Biol.* **2**, 1–16 (2010).
46. Jamal, M. *et al.* Bacterial biofilm and associated infections. *J. Chinese Med. Assoc.* 5–9 (2017). doi:10.1016/j.jcma.2017.07.012
47. Davey, M. E. & O 'toole, G. A. Microbial Biofilms: from Ecology to Molecular Genetics. **64**, 847–867 (2000).
48. Kirmusaoglu, S. Staphylococcal Biofilms: Pathogenicity, Mechanism and Regulation of Biofilm Formation by Quorum-Sensing System and Antibiotic Resistance Mechanisms of Biofilm-Embedded Microorganisms. in *Microbial Biofilms - Importance and Applications* (InTech, 2016). doi:10.5772/62943



49. Feng, Q. L. *et al.* A mechanistic study of the antibacterial effect of silver ions on *Escherichia coli* and *Staphylococcus aureus*. *Journal of Biomedical Materials Research* **52**, 662–668 (2000).
50. Jung, W. K. *et al.* Antibacterial Activity and Mechanism of Action of the Silver Ion in *Staphylococcus aureus* and *Escherichia coli*. *Journal of Microbiology and Biotechnology* **74**, 2171–2178 (2008).
51. Holt, K. B. *et al.* Interaction of Silver (I) Ions with the Respiratory Chain of *Escherichia coli*: An Electrochemical and Scanning Electrochemical Microscopy Study of the Antimicrobial Mechanism of Micromolar Ag⁺. *Journal of Electroanalytical Chemistry* **581**, 13214–13223 (2005). doi:10.1021/bi0508542
52. Li, W.-R. *et al.* Antibacterial effect of silver nanoparticles on *Staphylococcus aureus*. *BioMetals* **24**, 135–141 (2011).
53. Raffi, Hussain, Bhatti, Akhter, Hameed, H. Antibacterial Characterization of Silver Nanoparticles against. *Journal of Nanoparticles* **24**, 192–196 (2008).
54. Elechiguerra, J. L. *et al.* Interaction of silver nanoparticles with HIV-1. *Journal of Nanoparticles* **10**, 1–10 (2005).
55. Lu, L. & Chen, R. Silver nanoparticles inhibit hepatitis B virus replication Original article Silver nanoparticles inhibit hepatitis B virus. (2008).
56. Flores, C. Y. *et al.* Citrate-capped silver nanoparticles showing good bactericidal effect against both planktonic and sessile bacteria and a low cytotoxicity to osteoblastic cells. *ACS Appl. Mater. Interfaces* **5**, 3149–3159 (2013).
57. Asharani, P. V, Low, G., Mun, K., Hande, M. P. & Valiyaveetil, S. Cytotoxicity and Genotoxicity of Silver. *Toxicology Letters* **3**, 279–290 (2009).
58. Arora, S., Jain, J., Rajwade, J. M. & Paknikar, K. M. Interactions of silver nanoparticles with primary mouse fibroblasts and liver cells. *Toxicol. Appl. Pharmacol.* **236**, 310–318 (2009).
59. Marambio-Jones, C. & Hoek, E. M. V. A review of the antibacterial effects of silver nanomaterials and potential implications for human health and the environment. *J. Nanoparticle Res.* **12**, 1531–1551 (2010).
60. Ivask, A. *et al.* Toxicity Mechanisms in *Escherichia coli* Vary for Silver Nanoparticles and Differ from Ionic Silver. *Journal of Nanoparticles* **374–386** (2014). doi:10.1021/nn4044047
61. Pratsinis, S. E. Antibacterial Activity of Nanosilver Ions and Particles. *Journal of Nanoparticles* **5649–5654** (2010). doi:10.1021/es101072s
62. Morones, J. R. *et al.* The bactericidal effect of silver nanoparticles. (2005). doi:10.1088/0957-4484/16/10/059
63. Yang, W., Shen, C., Ji, Q. & An, H. Food storage material silver nanoparticles interfere with DNA replication fidelity and bind with DNA. (2009). doi:10.1088/0957-4484/20/8/085102
64. Sondi, I. & Salopek-sondi, B. Silver nanoparticles as antimicrobial agent: a case study on *E. coli* as a model for Gram-negative bacteria. *Journal of Nanoparticles* **275**, 177–182 (2004).



65. Dibrov, P., Dzioba, J., Gosink, K. K. & Ha, C. C. Chemiosmotic Mechanism of Antimicrobial Activity of Ag⁺ in *Vibrio cholerae*. **46**, 2668–2670 (2002).
66. Liao, S. Y., Read, D. C., Pugh, W. J., Furr, J. R. & Russell, D. Interaction of silver nitrate with readily identifiable groups: relationship to the antibacterial action of silver ions. *Letf. Appl. Microbiol.* **25**, 279–283 (1997).
67. Nelson, D. L., Cox, M. M. & Lehninger, A. L. *I principi di biochimica di Lehninger*. (Zanichelli, 2002).
68. Fosforilazione ossidativa. Available at: <http://www.chimica-online.it/biologia/fosforilazione-ossidativa.htm>. (Accessed: 4th January 2018)
69. Lok, C. *et al.* Proteomic Analysis of the Mode of Antibacterial Action of Silver Nanoparticles research articles. 916–924 (2006). doi:10.1021/pr0504079
70. Carlson, C. *et al.* Unique Cellular Interaction of Silver Nanoparticles : Size-Dependent Generation of Reactive Oxygen Species. 13608–13619 (2008).
71. Manke, A., Wang, L. & Rojanasakul, Y. Mechanisms of Nanoparticle-Induced Oxidative Stress and Toxicity. **2013**, (2013).
72. Turrens, J. F. Mitochondrial formation of reactive oxygen species. *J. Physiol.* **552**, 335–344 (2003).
73. Held, P. An Introduction to Reactive Oxygen Species Measurement of ROS in Cells. *BioTek Instruments* 1–14 (2012). doi:10.1017/CBO9781107415324.004
74. Park, H. *et al.* Silver-ion-mediated reactive oxygen species generation affecting bactericidal activity. *Water Res.* **43**, 1027–1032 (2009).
75. Rahman, M. F. *et al.* Expression of genes related to oxidative stress in the mouse brain after exposure to silver-25 nanoparticles. *Toxicol. Lett.* **187**, 15–21 (2009).
76. Wang, G. *et al.* Antibacterial effects of titanium embedded with silver nanoparticles based on electron-transfer-induced reactive oxygen species. *Biomaterials* **124**, 25–34 (2017).
77. Singh, S., Singh, S. K., Chowdhury, I. & Singh, R. The Open Microbiology Journal Understanding the Mechanism of Bacterial Biofilms Resistance to Antimicrobial Agents. *Open Microbiol. J.* **11**, 53–62 (2017).
78. Sherrard, L. J., Tunney, M. M. & Elborn, J. S. Antimicrobial resistance in the respiratory microbiota of people with cystic fibrosis. www.thelancet.com **384**, (2014).
79. Lok, C.-N. *et al.* Silver nanoparticles: partial oxidation and antibacterial activities. *JBIC J. Biol. Inorg. Chem.* **12**, 527–534 (2007).
80. Pauksch, L. *et al.* Biocompatibility of silver nanoparticles and silver ions in primary human mesenchymal stem cells and osteoblasts. *Acta Biomater.* **10**, 439–449 (2014).
81. Zhang, W. *et al.* Enhanced cytocompatibility of silver-containing biointerface by constructing nitrogen functionalities. *Appl. Surf. Sci.* **349**, 327–332 (2015).
82. Jin, G. *et al.* Synergistic effects of dual Zn/Ag ion implantation in osteogenic activity and antibacterial ability of titanium. *Biomaterials* **35**, 7699–7713 (2014).



83. Bousnaki, M. & Koidis, P. Advances on Biomedical Titanium Surface Interactions. *J. Biomim. Biomater. Tissue Eng.* **19**, 43–64 (2014).
84. Nguyen, V. H. & Lee, B. J. Protein corona: A new approach for nanomedicine design. *Int. J. Nanomedicine* **12**, 3137–3151 (2017).
85. Treuel, L., Docter, D., Maskos, M. & Stauber, R. H. Protein corona - from molecular adsorption to physiological complexity. *Beilstein J. Nanotechnol.* **6**, 857–873 (2015).
86. Wang, K., Zhou, C., Hong, Y. & Zhang, X. A review of protein adsorption on bioceramics. *Interface Focus* **2**, 259–77 (2012).
87. Garland, A., Shen, L. & Zhu, X. Mobile precursor mediated protein adsorption on solid surfaces. *Prog. Surf. Sci.* **87**, 1–22 (2012).
88. Smith, I. O., Baumann, M. J. & McCabe, L. R. Electrostatic interactions as a predictor for osteoblast attachment to biomaterials. *J. Biomed. Mater. Res.* **70A**, 436–441 (2004).
89. Ngankam, A. P., Mao, G. & Van Tassel, P. R. Fibronectin adsorption onto polyelectrolyte multilayer films. *Langmuir* **20**, 3362–70 (2004).
90. Roach, P., Farrar, D. & Perry, C. C. Interpretation of protein adsorption: Surface-induced conformational changes. *J. Am. Chem. Soc.* **127**, 8168–8173 (2005).
91. Green, R. J., Davies, J., Davies, M. C., Roberts, C. J. & Tendler, S. J. B. Surface plasmon resonance for real time in situ analysis of protein adsorption to polymer surfaces. *Biomaterials* **18**, 405–413 (1997).
92. Elwing, H. Protein adsorption and ellipsometry in biomaterial research. *Biomaterials* **19**, 397–406 (1998).
93. Tronic, E. H. Surface Analysis of Adsorbed Proteins: A Multi-Technique Approach to Characterize Surface Structure. (2012).
94. Introduction: Scanning Force Microscopy (SFM) - Soft Matter Physics Division - University of Leipzig. Available at: <http://home.uni-leipzig.de/pwm/web/?section=introduction&page=sfm>. (Accessed: 7th March 2018)
95. Ta, T. C. & McDermott, M. T. Mapping interfacial chemistry induced variations in protein adsorption with scanning force microscopy. *Anal. Chem.* **72**, 2627–2634 (2000).
96. Secondary Ion Mass Spectrometry (SIMS). Available at: <https://www.ifw-dresden.de/institutes/ikm/research-teams-and-topics/micro-and-nanostructures/available-methods/sims/>.
97. Eckhardt, S. *et al.* Nanobio silver: Its interactions with peptides and bacteria, and its uses in medicine. *Chem. Rev.* **113**, 4708–4754 (2013).
98. Kędziora, A. *et al.* Similarities and Differences between Silver Ions and Silver in Nanoforms as Antibacterial Agents. *Int. J. Mol. Sci.* **19**, 444 (2018).
99. Wang, C. *et al.* BSA adsorption on a plasma-deposited silver nanocomposite film controls silver release: A QCM and XPS-based modelling. *Surf. Coatings Technol.* **307**, 1–8 (2016).



100. Wang, X., Herting, G., Odnevall Wallinder, I. & Blomberg, E. Adsorption of bovine serum albumin on silver surfaces enhances the release of silver at pH neutral conditions. *Phys. Chem. Chem. Phys.* **17**, 18524–18534 (2015).
101. Wang, X., Herting, G., Odnevall Wallinder, I. & Blomberg, E. Adsorption of lysozyme on silver and its influence on silver release. *Langmuir* **30**, 13877–13889 (2014).
102. Ferraris, S. *et al.* Surface modification of Ti-6Al-4V alloy for biomineralization and specific biological response: Part I, inorganic modification. *J. Mater. Sci. Mater. Med.* **22**, 533–545 (2011).
103. Ferraris, S. *et al.* Antibacterial and bioactive nanostructured titanium surfaces for bone integration. *Appl. Surf. Sci.* **311**, 279–291 (2014).
104. Sample-Electron Interaction for SEM. Available at: <http://www.nanoscience.com/technology/sem-technology/sample-electron-interaction/>. (Accessed: 16th November 2017)
105. Microscopia elettronica (SEM). Available at: <http://www-2.unipv.it/dottorati/scienzeetecnologie/fisica/XXII ciclo/SEM.pdf>. (Accessed: 16th November 2017)
106. Theodore Peters Jr. Serum Albumin. **37**, 161–245 (1985).
107. Mueller, S., Riedel, H. D. & Stremmel, W. Determination of catalase activity at physiological hydrogen peroxide concentrations. *Anal. Biochem.* **245**, 55–60 (1997).
108. Larsen, A., Stoltenberg, M. & Danscher, G. In vitro liberation of charged gold atoms: autometallographic tracing of gold ions released by macrophages grown on metallic gold surfaces. *Histochem. Cell Biol.* **128**, 1–6 (2007).
109. Kokubo, T. & Takadama, H. How useful is SBF in predicting in vivo bone bioactivity? *Biomaterials* **27**, 2907–2915 (2006).
110. Luxbacher, T. The zeta potential for solid surface analysis. (2014).
111. Yu, F., Addison, O. & Davenport, A. J. A synergistic effect of albumin and H₂O₂ accelerates corrosion of Ti6Al4V. *Acta Biomater.* **26**, 355–365 (2015).
112. Hedberg, Y. S., Žnidaršič, M., Herting, G., Milošević, I. & Odnevall Wallinder, I. Mechanistic insight in the synergistic dissolution of TiAl6V4 by albumin and hydrogen peroxide – importance of albumin-aluminium binding.
113. Roessler, S., Zimmermann, R., Scharnweber, D., Werner, C. & Worch, H. Characterization of oxide layers on Ti6Al4V and titanium by streaming potential and streaming current measurements. *Colloids Surfaces B Biointerfaces* **26**, 387–395 (2002).



9 AKNOWLEDGMENTS

Ringrazio anzitutto la professoressa Silvia Maria Spriano, relatore, e l'ingegnere Sara Ferraris, co-relatore, per l'opportunità datami per conseguire l'esperienza a Stoccolma e per avermi seguito nella stesura di questo elaborato con precisione ed attenzione.

Un ringraziamento particolare va ai colleghi ed agli amici che mi hanno incoraggiato e che mi hanno accompagnato durante tutto il periodo universitario contribuendo a rendere piacevole questo percorso di studi.

Vorrei infine ringraziare la mia famiglia, i miei genitori Giancarlo e Mariangela e mio fratello Umberto Maria per il loro sostegno morale ma soprattutto economico che mi ha permesso di raggiungere questo traguardo.

E infine ringrazio, soprattutto, me stesso per la determinazione e l'impegno, la voglia di sfidarmi, per averci creduto fino alla fine ed esserci riuscito nel migliore dei modi.

"Allora vai senza perdere altro tempo, vai veloce mentre l'ultima luce si spegne, allontanati dal ricordo... ma non dal desiderio. Quello resta, tutto ciò che eravamo e tutto ciò che credevamo da bambini, tutto quello che brillava nei nostri occhi quando eravamo sperduti e il vento soffiava nella notte. Parti e cerca di continuare a sorridere. Trovati un po' di rock and roll alla radio e vai verso tutta la vita che c'è con tutto il coraggio che riesci a trovare e tutta la fiducia che riesci ad alimentare. Sii valoroso, sii coraggioso, resisti. Tutto il resto è buio."

Stephen King



